

Methanol synthesis via hydrogenation of mixed CO/CO<sub>2</sub>  
over Mn modified Cu/ZnO/Al<sub>2</sub>O<sub>3</sub> catalyst



A Thesis Submitted in Partial Fulfillment of the Requirements  
for the Degree of Master of Engineering in Chemical Engineering

Department of Chemical Engineering

FACULTY OF ENGINEERING

Chulalongkorn University

Academic Year 2020

Copyright of Chulalongkorn University

การสังเคราะห์เมทานอลโดยไฮโดรจิเนชันของคาร์บอนมอนอกไซด์ผสมคาร์บอนไดออกไซด์  
บนตัวเร่งปฏิกิริยา Cu/ZnO/Al<sub>2</sub>O<sub>3</sub> ที่ปรับปรุงด้วยแมงกานีส



วิทยานิพนธ์นี้เป็นส่วนหนึ่งของการศึกษาตามหลักสูตรปริญญาวิทยาศาสตรมหาบัณฑิต  
สาขาวิชาวิศวกรรมเคมี ภาควิชาวิศวกรรมเคมี  
คณะวิศวกรรมศาสตร์ จุฬาลงกรณ์มหาวิทยาลัย  
ปีการศึกษา 2563  
ลิขสิทธิ์ของจุฬาลงกรณ์มหาวิทยาลัย

Thesis Title	Methanol synthesis via hydrogenation of mixed CO/CO <sub>2</sub> over Mn modified Cu/ZnO/Al <sub>2</sub> O <sub>3</sub> catalyst
By	Mr. Papawin Tunyasitikun
Field of Study	Chemical Engineering
Thesis Advisor	Professor Dr. BUNJERD JONGSOMJIT, Ph.D.

---

Accepted by the FACULTY OF ENGINEERING, Chulalongkorn University in  
Partial Fulfillment of the Requirement for the Master of Engineering

..... Dean of the FACULTY OF  
ENGINEERING  
(Professor Dr. SUPOT TEACHAVORASINSKUN, D.Eng.)

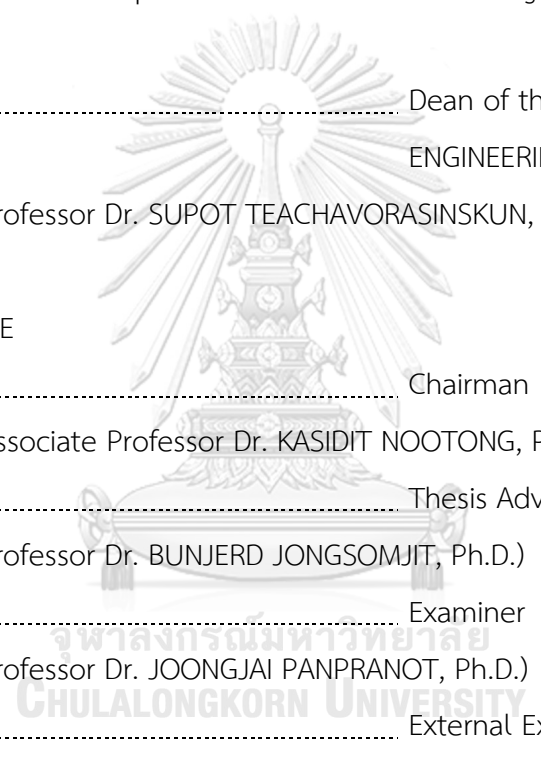
THEESIS COMMITTEE

..... Chairman  
(Associate Professor Dr. KASIDIT NOOTONG, Ph.D.)

..... Thesis Advisor  
(Professor Dr. BUNJERD JONGSOMJIT, Ph.D.)

..... Examiner  
(Professor Dr. JOONGJAI PANPRANOT, Ph.D.)

..... External Examiner  
(Assistant Professor Dr. Sasiradee Jantasee, Ph.D.)



ปภาวิวิท ตูยสิทธิกุล : การสังเคราะห์เมทานอลโดยไฮโดรจิเนชันของคาร์บอนมอนอกไซด์ผสมคาร์บอนไดออกไซด์บนตัวเร่งปฏิกิริยา Cu/ZnO/Al<sub>2</sub>O<sub>3</sub> ที่ปรับปรุงด้วยแมงกานีส. (Methanol synthesis via hydrogenation of mixed CO/CO<sub>2</sub> over Mn modified Cu/ZnO/Al<sub>2</sub>O<sub>3</sub> catalyst) อ.ที่ปรึกษาหลัก : ศ. ดร.บรรเจิด จงสมจิตร

งานศึกษานี้มีวัตถุประสงค์เพื่อศึกษาการสังเคราะห์เมทานอลโดยไฮโดรจิเนชันของคาร์บอนมอนอกไซด์ผสมคาร์บอนไดออกไซด์บนตัวเร่งปฏิกิริยา Cu/ZnO/Al<sub>2</sub>O<sub>3</sub> ที่ปรับปรุงด้วยแมงกานีส ซึ่งใช้วิธีตกตะกอนร่วมในการเตรียมตัวเร่งปฏิกิริยา และศึกษาปริมาณการใช้พลังงานรวมของทั้งระบบในการสังเคราะห์เมทานอล โดยอาศัยการจำลองกระบวนการด้วยซอฟต์แวร์ Aspen Plus V.9 ซึ่งอ้างอิงข้อมูลจากผลการทดลอง สำหรับการปรับปรุงประสิทธิภาพการเร่งปฏิกิริยาของตัวเร่งปฏิกิริยาจะดำเนินการทดสอบด้วยเครื่องปฏิกรณ์ชนิดเบดนิ่งที่มีการไหลต่อเนื่อง ที่อุณหภูมิ 250 องศาเซลเซียส ภายใต้ความดันบรรยากาศและเวลาในการดำเนินการ 5 ชั่วโมง ผ่านปฏิกิริยาไฮโดรจิเนชันของสารป้อนเข้าที่มีองค์ประกอบต่างกันของ CO<sub>2</sub>/H<sub>2</sub>, CO/H<sub>2</sub> และ CO/CO<sub>2</sub>/H<sub>2</sub> และมีค่าความเร็วพื้นที่กาศรายชั่วโมงเท่ากับ 24,000 ml/g<sub>cat</sub>·h การวัดสมบัติเชิงกายภาพและเชิงเคมีของตัวเร่งปฏิกิริยาอาศัยการวิเคราะห์ลักษณะเฉพาะด้วยเทคนิคการวิเคราะห์ประกอบด้วย N<sub>2</sub> adsorption, CO-Chemisorption, SEM-EDX, ICP-MS, XRD, XPS, H<sub>2</sub>-TPR, NH<sub>3</sub>-TPD และ CO<sub>2</sub>-TPD จากผลการทดสอบพบว่าตัวเร่งปฏิกิริยา CZA-Mn มีความสามารถในเร่งปฏิกิริยาที่ดีกว่าตัวเร่งปฏิกิริยา CZA ซึ่งเห็นได้จากค่าปริมาณของผลิตภัณฑ์ที่เกิดขึ้น คือ เมทานอล ต่อหน่วยเวลาต่อหน่วยน้ำหนักของตัวเร่งปฏิกิริยาที่เพิ่มขึ้น ที่สอดคล้องกับผลการวิเคราะห์ลักษณะเฉพาะของตัวเร่งปฏิกิริยา เนื่องจากการเติมแมงกานีสลงบนตัวเร่งปฏิกิริยาจะช่วยทำให้ตำแหน่งของจุดที่ว่างไว้มักกระจายตัวที่ดีขึ้น ช่วยในการแตกตัวของโมเลกุลไฮโดรเจนและเพิ่มการสปีวโอเวอร์ของออกซิเจน นอกเหนือจากนี้ การเติมแมงกานีสลงบนตัวเร่งปฏิกิริยาไม่เพียงแต่ช่วยการรีดักชันของ CuO แต่ยังช่วยทำให้ค่าปริมาณตำแหน่งเบสและเกิดการดูดซับแรงของ CO<sub>2</sub> ที่สูงกว่า และเพิ่มปริมาณของตำแหน่งกรดอ่อน ซึ่งเป็นผลดีต่อค่าการเลือกเกิดของเมทานอล สำหรับพลังงานที่ใช้ในการสังเคราะห์เมทานอล พบว่าการป้อนร่วม CO<sub>2</sub> ในสารตั้งต้นมีความสำคัญต่อปริมาณการใช้พลังงานรวมของทั้งระบบและต่อปริมาณการใช้พลังงานในการผลิตเมทานอล 1 โมล ที่เพิ่มขึ้น จากผลลัพธ์พบว่า สารป้อนเข้า CO/CO<sub>2</sub>/H<sub>2</sub> ที่มีองค์ประกอบ 1:1:2 จะต้องเพิ่มปริมาณการใช้พลังงานในการผลิตเมทานอล 1 โมล ลง 3.6 และ 5.1 เท่าของปฏิกิริยาไฮโดรจิเนชันของคาร์บอนมอนอกไซด์

สาขาวิชา วิศวกรรมเคมี  
ปีการศึกษา 2563

ลายมือชื่อนิสิต .....  
ลายมือชื่อ อ.ที่ปรึกษาหลัก .....

# # 6270151021 : MAJOR CHEMICAL ENGINEERING

KEYWORD: methanol synthesis; hydrogenation; Cu/ZnO/Al<sub>2</sub>O<sub>3</sub>; Manganese; Energy

Papawin Tunyasitikun : Methanol synthesis via hydrogenation of mixed CO/CO<sub>2</sub> over Mn modified Cu/ZnO/Al<sub>2</sub>O<sub>3</sub> catalyst. Advisor: Prof. Dr. BUNJERD JONGSOMJIT, Ph.D.

The purposes of this study are to investigate the methanol synthesis by using mixed CO/CO<sub>2</sub> hydrogenation on Mn modified Cu/ZnO/Al<sub>2</sub>O<sub>3</sub> catalyst which is prepared by the co-precipitation method and to investigate the overall energy consumption of methanol synthesis based on experimental results through the simulation process using Aspen Plus V.9. The improvement of catalytic activity is performed by a continuous fixed bed microreactor at 250°C under atmospheric pressure for 5 hours on the stream through hydrogenation of different feed composition of CO<sub>2</sub>/H<sub>2</sub>, CO/H<sub>2</sub>, and CO/CO<sub>2</sub>/H<sub>2</sub>, and 24000 ml/g<sub>cat</sub>·h of GHSV. The physical and chemical properties of the catalysts are measured by various catalyst characterization techniques including N<sub>2</sub> adsorption, CO-Chemisorption, SEM-EDX, ICP-MS, XRD, XPS, H<sub>2</sub>-TPR, NH<sub>3</sub>-TPD, and CO<sub>2</sub>-TPD. The experimental results indicate that CZA-Mn catalyst has better catalytic activity than CZA catalyst that can be observed from the increase of methanol space time yield that is corresponding with the results of catalyst characterization. Manganese added on the catalyst indicates that active sites have well-dispersion that help to increase the dissociation rate of hydrogen molecules and to improve spillover. Moreover, the addition of manganese on the catalyst not only facilitate the reduction of CuO, but also enhance the number of total basic sites and the strong adsorption of CO<sub>2</sub> due to the shift of moderate basic site to strong basic site and increases the weak acid sites that help to improve the selectivity of methanol. For the overall energy consumption in methanol synthesis investigation, it is found that the amount of CO<sub>2</sub> in the reactant is significant to the overall energy consumption and energy consumption of 1 mol-methanol synthesis. Thus, the results indicate CO/CO<sub>2</sub>/H<sub>2</sub> feed with 1:1:2 composition can increase the energy consumption of 1 mol-methanol synthesis to 3.6 and 5.1 times of CO hydrogenation.

Field of Study: Chemical Engineering

Student's Signature .....

Academic Year: 2020

Advisor's Signature .....

## ACKNOWLEDGEMENTS

I would like to express my special thanks of gratitude to my research supervisor, Professor Dr. Bunjerd Jongsomjit for allowing me to do this research and providing precious guidance from the beginning to the end of this research. I am most grateful for teaching me the methodology and show me how to present the research, and also would like to thank you for your great empathy. I am extremely thankful to my committee: Associate Professor Dr. Kasidit Nootong (Chairman), Professor Dr. Joongjai Panpranot (Examiner), and Assistant Professor Dr. Sasiradee Jantasee (External Examiner) who contribute advice and guidance throughout the research and the Malaysia Thailand Joint Authority, MTJA project that supported me for doing this research. Finally, I would like to thank all staff of the Center of Excellence on Catalysis and Catalytic Reaction Engineering, Chulalongkorn University, and my friends who played a role in the research.

Papawin Tunyasitikun

## TABLE OF CONTENTS

	Page
ABSTRACT (THAI).....	iii
ABSTRACT (ENGLISH).....	iv
ACKNOWLEDGEMENTS .....	v
TABLE OF CONTENTS .....	vi
LIST OF TABLES .....	x
LIST OF FIGURES .....	xi
INTRODUCTION.....	1
1.1 Statement of problem .....	1
1.2 Objectives of research.....	3
1.3 Scopes of research.....	3
1.3.1 Catalyst preparation .....	3
1.3.2 Characterization of catalyst.....	4
1.3.3 Activity Test.....	4
1.3.4 Aspen Plus V.9 simulation.....	4
1.4 Research methodology.....	5
1.5 Research plan .....	7
BACKGROUND AND LITERATURE REVIEW.....	8
2.1 The reaction of methanol synthesis via hydrogenation .....	8
2.2 The reaction of methane reforming.....	9
2.3 Methanol.....	10
2.4 Catalyst components .....	12

2.5 Cu, Zn, Al, Mn precursor and NaHCO <sub>3</sub> .....	14
2.6 Catalyst preparation .....	17
2.7 Literature reviews.....	18
EXPERIMENT.....	37
3.1 Catalysts preparation.....	37
3.2 Catalysts characterizations .....	37
3.2.1 X-ray diffraction (XRD).....	38
3.2.2 Scanning Electron Microscope (SEM).....	38
3.2.3 Energy-dispersive X-ray spectroscopy (EDX).....	38
3.2.4 N <sub>2</sub> physisorption .....	39
3.2.5 Temperature-programmed reduction (TPR).....	39
3.2.6 Temperature-programmed desorption of carbon dioxide (CO <sub>2</sub> -TPD).....	39
3.2.7 Temperature-programmed desorption of ammonia (NH <sub>3</sub> -TPD).....	39
3.2.8 X-ray Photoelectron spectroscopy (XPS).....	40
3.2.9 CO-Chemisorption (CO-Chem) .....	40
3.2.10 Inductive Coupled Plasma Spectrometer Mass Spectrometer (ICP-MS). 41	
3.3 Activity test.....	42
3.4 Simulation.....	44
RESULTS AND DISCUSSION.....	49
4.1 Catalyst characterization.....	49
4.2 Catalyst performance .....	63
4.3 Energy consumption in methanol synthesis .....	66
CONCLUSIONS AND RECOMMENDATION.....	69
Recommendations.....	70



APPENDIX.....	71
APPENDIX.A CALCULATION OF CATALYST PERFORMANCE .....	71
A.1 CO <sub>2</sub> conversion.....	71
A.2 CO conversion .....	71
A.3 Methanol selectivity.....	71
A.4 Space time yield .....	71
A.5 Catalytic properties of CZA and CZA-Mn catalysts.....	75
APPENDIX.B CALCULATION OF CRYSTALLITE SIZE.....	77
B1. The Scherrer equation.....	77
APPENDIX.C CALBRATION .....	78
C.1 CO calibration.....	78
C.2 CO <sub>2</sub> calibration .....	78
C.3 CH <sub>3</sub> OH calibration .....	79
APPENDIX.D X-RAY PHOTOELECTRON SPECTROSCOPY .....	80
D.1 Chemical species of CZA catalyst.....	80
D.2 Chemical species of CZA-Mn catalyst.....	83
APPENDIX.E CALCULATING VOLUME CHEMISORBED .....	86
E.1 Calculation volume chemisorbed in CO-Chemisorption .....	86
APPENDIX.F THERMGRAVIMETRIC ANALYSIS.....	89
F.1 TGA curves for CO <sub>2</sub> hydrogenation.....	89
F.2 TGA curves for CO hydrogenation.....	90
F.3 TGA curves for CO/CO <sub>2</sub> hydrogenation.....	91
APPENDIX.G DISCUSSION OF SIMULATION RESULTS .....	92

G.1 Effect of CO <sub>2</sub> utilization in reforming of methane and methanol synthesis. .....	92
APPENDIX.H CALCULATION OF THE HEAT REQUIREMENT FOR THE REACTOR. ....	99
H.1 Calculate the heat requirement for the reactor.....	99
REFERENCES .....	105
VITA.....	110



## LIST OF TABLES

	<b>Page</b>
Table 1 Information of Cupric Nitrate Trihydrate AR/ACS. [6].....	14
Table 2 Information of Zinc Nitrate Hexahydrate. [6].....	15
Table 3 Information of Aluminum Nitrate Nonahydrate. [7].....	15
Table 4 Information of Manganese(II) Nitrate Tetrahydrate. [7].....	16
Table 5 Information of Sodium Hydrogen Carbonate. [6].....	16
Table 6 Condition of TCD detector.....	43
Table 7 Condition of FID detector.....	43
Table 8 Textural properties and Reducibility result.....	50
Table 9 Element distribution of CZA and CZA-Mn catalysts.....	54
Table 10 XPS spectra of Cu, Zn, and Al species of CZA and CZA-Mn catalysts.....	59
Table 11 The amounts of acid sites of CZA and CZA-Mn catalysts. ....	61
Table 12 The amounts of basic sites of CZA and CZA-Mn catalysts.....	62
Table 13 The overall energy consumption for hydrogenation with different feeds gas. .....	68

## LIST OF FIGURES

	Page
Figure 1 World methanol demand according to use. [4].....	11
Figure 2 Catalyst components and their function. [5].....	12
Figure 3 The Schematic of methanol synthesis. ....	42
Figure 4 The simulation of methane steam reforming in Aspen Plus using RPlug model block. ....	46
Figure 5 The simulation of methane steam reforming in Aspen Plus using RStoic model block. ....	47
Figure 6 The simulation of bi-reforming of methane in Aspen Plus using RStoic model block.....	47
Figure 7 The simulation of CO hydrogenation in Aspen Plus using RStoic model block. .....	47
Figure 8 The simulation of CO and CO <sub>2</sub> hydrogenation in Aspen Plus using RStoic model block. ....	48
Figure 9 The N <sub>2</sub> adsorption-desorption isotherm at 77K, 1 atm of CZA and CZA-Mn catalysts after calcination. ....	49
Figure 10 The SEM-EDX images of CZA catalyst.....	52
Figure 11 The SEM-EDX images of CZA-Mn catalyst.....	53
Figure 12 XRD pattern of CZA and CZA-Mn catalysts after calcination. [21] .....	56
Figure 13 XPS spectra of CZA and CZA-Mn catalysts.....	57
Figure 14 XPS signals of CZA and CZA-Mn catalysts. (a) XPS of Cu species, b) XPS of Zn species and c) XPS of Al species.....	58
Figure 15 H <sub>2</sub> -TPR profiles of CZA and CZA-Mn catalysts.....	60
Figure 16 NH <sub>3</sub> -TPD profiles of CZA and CZA-Mn catalysts.....	61

Figure 17 CO <sub>2</sub> -TPD profiles of CZA and CZA-Mn catalysts.....	62
Figure 18 Catalytic activity of CZA catalyst for hydrogenation to methanol with different feeds gas.....	63
Figure 19 Catalytic activity of CZA-Mn catalyst for hydrogenation to methanol with different feeds gas.....	65
Figure 20 Catalytic activity of CZA and CZA-Mn catalyst for CO <sub>2</sub> and CO/CO <sub>2</sub> hydrogenation to methanol.....	66
Figure 21 The energy consumption to produce 1 mol of methanol for hydrogenation with different feeds gas.....	67



# CHAPTER 1

## INTRODUCTION

### 1.1 Statement of problem

Climate change refers to the changing climate as a result of direct and indirect effect from production and consumption activities by human life that cause the amount of greenhouse gases in the atmosphere and accumulate more than it should have been that lead the earth to retain more heat in the atmosphere. Because of this, the world is abnormally warming. The phenomenon that makes the world warming is called greenhouse effect.

Since the production of methanol is inadequate. Therefore, methanol must be imported and employ reforming process to produce industrial methanol. With fossilized natural gas that causing global warming problems, syngas is an alternative that using biomass as raw material. Methanol is the tenth of most important organic chemical raw material and fuel, which is applied to many fields. It was found that around two-third of the methanol used in industry is obtained from the hydrogenation reaction of  $\text{CO}_2$  and the around one-third of methanol is synthesized from hydrogenation reaction of  $\text{CO}$ .

At this moment in the world, we have really big problem of natural resources such as fossil fuels and also  $\text{CO}_2$ . We have unclosed carbon cycle so we are taking a lot of energies from fossil fuel for example coal, oil, natural gas and we are just burning them and using for transport or taking electric energy out of it and again at the end of the day what we have is  $\text{CO}_2$  which is accumulated in the atmosphere. At this moment conversion of this atmospheric  $\text{CO}_2$  into fossil fuel is not actually done. In order to have to elemental carbon management, we need to close this carbon cycle from  $\text{CO}_2$  into possibly fuel and among all the chemicals which can be used as fuel. It was thought that methanol can be the liable one because methanol is fundamental chemical in chemical industry for example on the production of a solvent in plastics, pharmaceuticals, formaldehyde, acetic acid, etc. In addition, methanol can be used as fuel and this is very important. We can drive car with

methanol or blend with gasoline or we can actually use it as it is in fuel cell and this is very important. We can use methanol as C1 feedstock so we can also produce olefins, which are very fundamental chemicals. So, that is the reason why we decided to work on CO<sub>2</sub> conversion especially hydrogenation to methanol.

Heterogeneous catalyst is a catalyst in a different phase to the reactants. The importance of catalysts in industry is because catalysts are hugely important in the chemical industry. The catalysts provide an alternative reaction pathway and require lower activation energy. Therefore, the energy demands of process will be decreased. The process requires less energy. This is beneficial for chemical industry and environment because it is decreased the demand of fossil fuels and decrease the greenhouse gas emission which have been generated in producing energy to drive these reactions. More molecules have an energy in excess of this new lower activation energy, so the rate of reaction increases. The catalyst would be cheaper than the large amount of energy required to increase temperature of the reaction. This is extending an economic benefits of using catalyst. Industrial methanol is produced from Cu/ZnO/Al<sub>2</sub>O<sub>3</sub> catalyst by using CO<sub>2</sub>, CO and H<sub>2</sub> mixture. The active site on the industrial catalyst has been identified as a copper, zinc decorated step surface. This zinc decorated catalyst has been shown to be more active towards methanol synthesis than copper alone. Cu/ZnO/Al<sub>2</sub>O<sub>3</sub> catalyst is chosen to produce methanol as Cu/ZnO/Al<sub>2</sub>O<sub>3</sub> catalyst prepared by conventional co-precipitation methods. It exhibits high activity in the methanol synthesis from syngas. Cu-ZnO exhibits a poor activity for CO<sub>2</sub> conversion and methanol formation and Cu-based catalyst supported on ZnO-Al<sub>2</sub>O<sub>3</sub> mixed oxides exhibits a high catalytic activity for methanol synthesis from CO<sub>2</sub>. In fact, Cu species (Cu<sup>+</sup>, Cu<sup>0</sup>) are the active site for hydrogenation reaction of methanol. ZnO is used as dispersant for Cu and a hydrogen reservoir. It also activates CO<sub>2</sub> and produces catalytical active site through Cu-ZnO interactions. For Al<sub>2</sub>O<sub>3</sub>, it is used for improving its catalytic performance and improve the dispersion of Cu-ZnO and their catalytic activity and nano-sized Al<sub>2</sub>O<sub>3</sub> that can even increase the selectivity of the reaction through its microporous structure and Al is used as a structural promoter. Interestingly, we have found that CO<sub>2</sub>, CO and H<sub>2</sub> can easily adsorb on the copper-base catalyst which is an important

step to conversion of CO<sub>2</sub>. Utilizing CO<sub>2</sub> by converting it into valuable chemicals and fuels such as methanol would enable the Earth's plants once again balance the carbon cycle.

In this research, the first part is to study about methanol synthesis via hydrogenation of mixed CO/CO<sub>2</sub> over Mn modified Cu/ZnO/Al<sub>2</sub>O<sub>3</sub> catalyst including CO, CO<sub>2</sub>, and CO/CO<sub>2</sub> hydrogenations. The second part is to study about the operating condition of the reactor for methane steam reforming, bi-reforming, CO, and CO/CO<sub>2</sub> hydrogenation from relevant researches. These examples are further used to be a guideline for a process simulation for studying the overall energy consumption in methanol synthesis based on experimental results, together with the simulation program, Aspen Plus V.9, which is used to calculate the overall energy consumption in each process and energy required to produce one mole of the product. An expected benefit is this data can be utilized to observe the energy consumption comparing between these three simulations, CO, CO<sub>2</sub>, and CO/CO<sub>2</sub> hydrogenations.

## 1.2 Objectives of research

1.2.1 To investigate methanol synthesis via hydrogenation of mixed CO/CO<sub>2</sub> over Mn modified Cu/ZnO/Al<sub>2</sub>O<sub>3</sub> catalyst.

1.2.2 To investigate the overall energy consumption in methanol synthesis based on experimental results through the simulation process using Aspen Plus V.9.

## 1.3 Scopes of research

### 1.3.1 Catalyst preparation

1.3.1.1 Preparation of CZA (60:30:10 wt.%) by co-precipitation with pH=8.

1.3.1.2 Preparation of CZA-Mn (60:30:10 wt.%, Mn=0.1 wt.%) by co-precipitation with pH=8.



### 1.3.2 Characterization of catalyst

1.3.2.1 X-ray diffraction (XRD)

1.3.2.2 Scanning electron microscopy (SEM)

1.3.2.3 Energy-dispersive X-ray spectroscopy (EDX)

1.3.2.4 N<sub>2</sub> physisorption

1.3.2.5 Temperature-programmed reduction (TPR)

1.3.2.6 Temperature-programmed desorption of carbon dioxide  
(CO<sub>2</sub>-TPD)

1.3.2.7 Temperature-programmed desorption of ammonia (NH<sub>3</sub>-TPD)

1.3.2.8 X-ray photoelectron spectroscopy (XPS)

1.3.2.9 CO-Chemisorption (CO-Chem)

1.3.2.10 Inductively coupled plasma mass spectrometry (ICP-MS)

### 1.3.3 Activity Test

1.3.3.1 Settling the condition by feeding reactants of CO:H<sub>2</sub> = 1:2, CO<sub>2</sub>:H<sub>2</sub> = 1:3, CO:CO<sub>2</sub>:H<sub>2</sub> = 1:1:2, T = 250°C for CZA catalysts, P = 1 atm, 5 h.

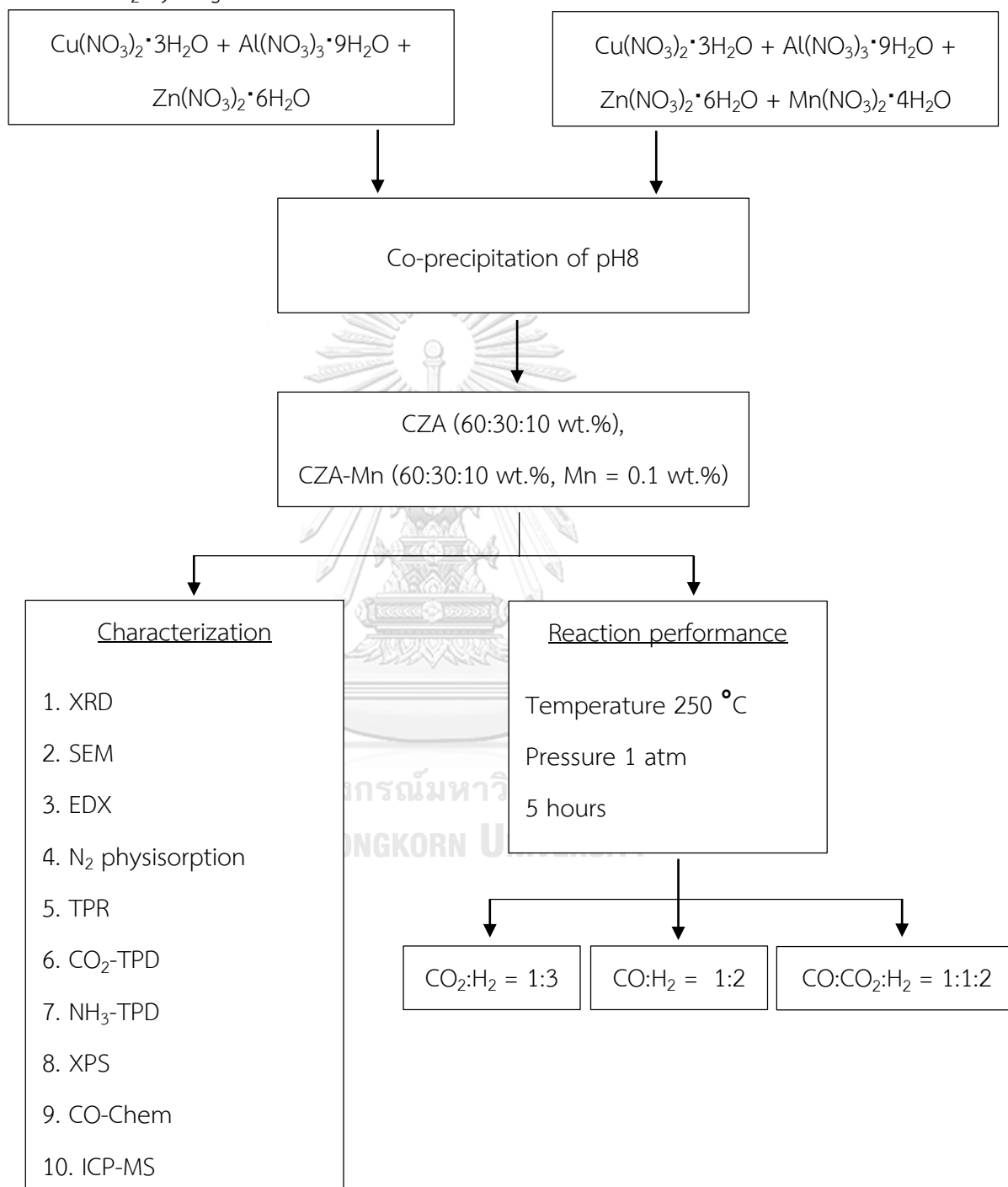
1.3.3.2 Analysis of data by Space time yield of CH<sub>3</sub>OH, CO<sub>2</sub> conversion, CO conversion, CO selectivity and CH<sub>3</sub>OH selectivity measured by gas chromatograph (GC).

### 1.3.4 Aspen Plus V.9 simulation

1.3.4.1 Studying the operating condition of the reactor for methane steam reforming, bi-reforming, CO and CO/CO<sub>2</sub> hydrogenation from relevant researches as a guideline for a process simulation with experimental results obtained through the simulation process using Aspen Plus V.9.

## 1.4 Research methodology

Part 1: The effect of Mn on CZA catalyst in methanol synthesis via CO, CO<sub>2</sub>, and CO/CO<sub>2</sub> hydrogenation.



## Part 2: Simulation

Study about the reactions from relevant researches.

1. Methane steam reforming
2. Bi-reforming of methane
3. CO hydrogenation
4. CO/CO<sub>2</sub> hydrogenation

Simulation by Aspen plus V.9.

1. Components-Specifications
2. Property Specifications, Methods
3. Feed Stream Specifications
4. Unit Operation Block Specifications
5. Run

Simulation by Aspen plus V.9 based on experimental results using the same procedure.

1. CO hydrogenation
2. CO<sub>2</sub> hydrogenation
3. CO/CO<sub>2</sub> hydrogenation

## 1.5 Research plan

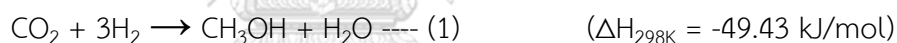
Topic	2019		2020	
	Semester 1	Semester 2	Semester 1	Semester 2
1. Literature review				
2. Simulation by Aspen Plus V.9				
3. Conference paper writing				
4. Preparation of CZA, CZA-Mn				
5. Thesis-proposal writing				
6. Characterization of CZA, CZA-Mn				
7. Test reaction of CZA, CZA-Mn				
8. Thesis writing				

## CHAPTER 2

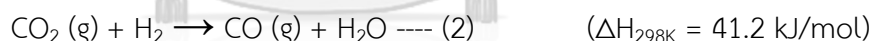
### BACKGROUND AND LITERATURE REVIEW

#### 2.1 The reaction of methanol synthesis via hydrogenation

Hydrogenation produces many advantage chemicals, and its employment is increasing spectacularly, particularly in the petroleum refining industry. The cost of hydrogen is a major factor in restricting growth. Hydrogenation is a chemical reaction between molecular hydrogen ( $H_2$ ) and another compounds or element. Hydrogen gas is produced from hydrocarbons by the process known as steam reforming. Two types of reaction pathways have been identified in the literature for the hydrogenation from  $CO_2$  to methanol. First, it is consisted in the direct hydrogenation of  $CO_2$  to methanol. Second,  $CO_2$  is firstly converted to CO (through the RWGS reaction), then to methanol. Generally, methanol synthesis by  $CO_2$  hydrogenation over CuO/ZnO based catalysts implicates three competitive reactions. The first reaction is the direct synthesis of methanol from  $CO_2$ :



The second one is the inter-conversion between  $CO_2$  and CO (RWGS reaction):



The third one is the synthesis of methanol from CO:



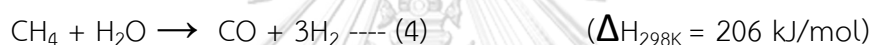
For the reaction performed at 250 °C. It is clear that at low pressure, carbon monoxide is the main product. On the other hand, at high pressure, CO is transformed to methanol. Therefore, carbon monoxide and methanol are produced from  $CO_2$  by parallel reactions.

Hydrogenations are generally executed in the presence of a catalyst and under high temperature and pressure. Combination of noble metals, nickel, copper, and various metal oxide are the common catalysts. This raw material is synthesized by catalytic hydrogenation of  $CO_2$  and CO over Cu/ZnO/ $Al_2O_3$  ternary catalysts at 50–100 bar and 250–300°C. It has been estimated that around 2/3 for the production

of methanol in industrial conditions is obtained from the hydrogenation of CO<sub>2</sub> and the rest is synthesized from hydrogenation of CO. [1]

## 2.2 The reaction of methane reforming

Steam reforming or steam methane reforming is the general and cost-effective method for hydrogen production, and it is provided for 50% of the world's hydrogen production and the chemical synthesis for syngas or synthesis gas production that actually made by reacting methane (CH<sub>4</sub>) or natural gas with water. It is usually in the form of a catalyst like nickel to make the reaction go faster even though the temperature is ridiculously high anyways like 800-850°C and pressure ranging between 25 and 40 atm. These two molecules or the mixed feed react and the product will be hydrogen gas and carbon monoxides by the following reactions:



The first reaction is the reforming reaction, and the second is the water gas shift reaction as a little bonus step because this action carbon monoxide can further react with water to produce one extra hydrogen. Both reactions produce hydrogen. The net reaction is highly endothermic, requiring specific heat. The combined steam and CO<sub>2</sub> reforming of methane, CO<sub>2</sub> can be converted into higher value products, shortened as CSCRM (see Eq. (6)), also known as bi-reforming reaction of methane.



CSCRM has recently occurred as a promising technique since it can generate a green and sustainable energy source from biogas, a non-fossil fuel resource mainly consists of methane, carbon dioxide and water. However, the bibliographic knowledge about CSCRM reaction is little-known as reported in literature due to the complexity of this reaction involving multiple main reactions, namely, SRM and DRM as well as several parallel reactions. [2]

## 2.3 Methanol

The first the homologous series of alcohols is methanol ( $\text{CH}_3\text{OH}$ ). Methanol is the simple of all alcohols. Methanol is found in combined state in oil of wintergreen as methyl salicylate and in clove oil as methyl benzoate. It is prepared by the action of water gas and hydrogen. Customarily, methanol was made from destructive distillation of wood and the product was known as wood alcohol. Methanol is also known as methyl alcohol. Methanol is consisting of hydrogen, oxygen, and a single carbon atom. It has the highest hydrogen to carbon ratio of any liquid fuel. These chemical properties contribute to methanol sustainability as a petrochemical feedstock and fuel. Methanol is commonly produced from natural gas. Increasingly, methanol is produced from renewable feedstock such as renewable energy, carbon ( $\text{CO}_2$ ) capture, municipal waste and agricultural waste. Methanol is produced from such feedstock which create circular economics where what is normally deemed waste is used to produce methanol which is a useful and higher value product such processes effectively promote sustainability by creating value from waste and diversifying how waste is managed. Methanol is used to produce a wide range of extensive products such as material for constructing houses, paints, plastics, car parts and medical equipment such as personal protective equipment. When produced from renewable feedstock, renewable methanol becomes a sustainable, net carbon-neutral fuel compliant with climate goal. Upon combustion methanol compounds and physical properties results in significantly lower emission. Specifically, the absence of carbon and carbon bonds in methanol molecules is key to the negligible emission of soot or particulate matter and the oxygen atom contribute to a fuller and cleaner combustion making methanol an environment-friendly fuel that contributes to better air quality.

Commercially, methanol is produced from syngas, which is prepared from natural gas or coal, which contains  $\text{CO}$  and  $\text{H}_2$  along with a small amount of  $\text{CO}_2$ . Methanol is currently produced from syngas using copper-based catalysts. [3]

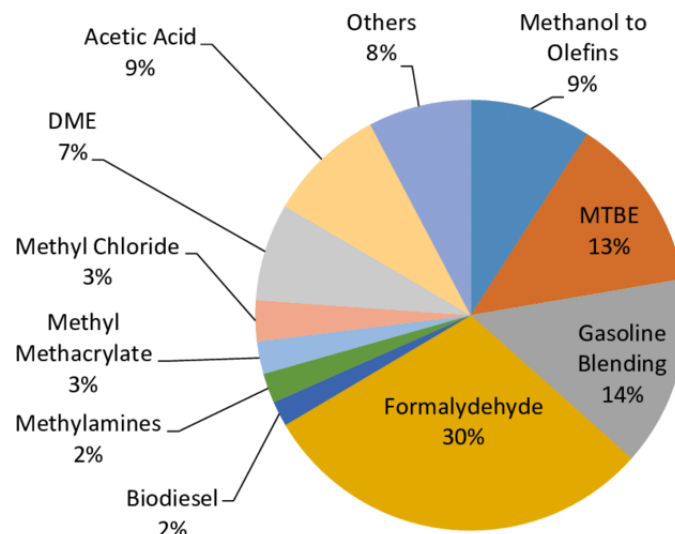


**Figure 1** World methanol demand according to use. [4]

#### Uses of methanol

- Formaldehyde resins used in wood products such as particle board.
- Acetic acid used in making Polyethylene Terephthalate plastic bottles and polyester fibers.
- A solvent and an antifreeze in pipelines and windshield washer fluid.
- Denatured ethanol is used as fuel.
- As a solvent for varnishes, paints and polishes.
- Used in making dyes, drugs and perfumes.
- As a motor fuel along with petrol.
- Transportation fuel for passenger vehicles and trucks.
- Hydrogen carrier for fuel cell vehicles, stationary fuel cell power plants, and portable fuel cell devices such as cellular phones.
- Additive to remove harmful nitrates from wastewater treatment plant effluent by accelerating bacterial degradation.

#### Physical properties

- Molar mass is 32.04 g/mol.
- Colorless liquid, possesses a strong alcoholic odor.
- Volatile, boiling point is 64.7°C , melting point is -97.6°C.



- Lighter than water, density is  $0.792 \text{ g/cm}^3$ .
- Neutral compound.
- Miscible with water in all proportions. Heat is evolved on mixing.
- Burns with a bluish flame.
- Highly poisonous in nature.

## 2.4 Catalyst components

In general, catalyst components consist of 3 parts. Active phase, Support/Carrier and Promoters and Inhibitors.

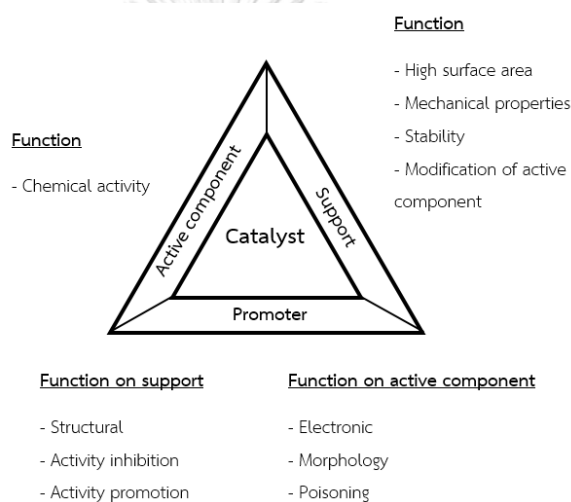


**Figure 2** Catalyst components and their function. [5]

Each component has different responsibility, and each substance can be classified to one component or more than one component. All catalyst is not necessary to consist of all 3 components, but active phase is needed for all of them. Catalyst which has only active phase such as metal catalysts or oxide catalysts. Catalyst which has active phase and support are classified to Supported Oxide Catalysts and Supported Metal Catalysts. Catalyst which has promoter are called Promoted Catalysts. For  $\text{Cu/ZnO/Al}_2\text{O}_3$  catalyst : Cu-active phase,  $\text{Al}_2\text{O}_3$ -support, ZnO-promoter.

Active phase is the active site for reaction. In general, active site are dispersed on porosity of supported catalyst in form of nanoparticle with diameter of 1-50 nm. Specific surface area of these particle is consisted of active site (Atom or Particle) which can catalyze various reaction. Example of active phase substance are Metal,

Metal Oxide and metal Sulfide. Selection of Active phase component is the first procedure for catalyst design. The factor which used to classify active phase is Conductivity. Those are metal, semiconductor and insulator and 3 types of active phase can also classify to be metals and metals components which are in the form of oxide, sulfide, nitrite, and carbene. Without active site, reaction will not occur.

Support is a porous material which have high specific surface area such as alumina, silica, activated carbons, etc. If there is no support for metal catalyst which is active site, it will be crystalized. Support will increase dispersion of active phase and if metal amount is decreased, the dispersion of active phase will increase, and it will be affected specific surface area per metal weight. Moreover, support must have high Strength and high heat resistance properties. Therefore, Heat and stability of support have to be improved to increase active site and supported catalyst's efficiency.

The purpose of preparation for catalyst which consist of support is to separate crystal of active site. Crystallization of active phase will be occurred when particle of catalyst dispersed on support. Transportation of active site depends on interaction between catalyst and support. If it has weak interaction, Transportation of active site will have high efficiency and can be crystallized easily with high temperature than temperature that cause coalesce. On the other hand, if it has strong interaction, the chemical compound between catalyst and support will be occurred. Catalytic activity will be reduced. Generally, interaction between catalyst and support should not be extremely strong or weak.

Promoters is used to support active phase and support by changing morphological or electron properties or increasing mechanical properties and reaction resistance with feeding substance and heat resistance. Therefore, promoters will increase radioactivity and/or stability of catalyst. Generally, promoter will be added in small amount (1-5 wt.%) for support and maintain substance or specific surface area and increase radioactivity of catalyst. Promoters can be metal or metal

oxide such as alkaline metal ( $\text{Na}_2\text{CO}_3$ ,  $\text{MgO}$ ) and rare earth metal oxide ( $\text{CeO}_2$ ,  $\text{La}_2\text{O}_3$ ).

## 2.5 Cu, Zn, Al, Mn precursor and $\text{NaHCO}_3$

**Table 1** Information of Cupric Nitrate Trihydrate AR/ACS. [6]

CUPRIC NITRATE TRIHYDRATE AR/ACS	
Purity	99.5%
Molecular formula	$\text{Cu}(\text{NO}_3)_2 \cdot 3\text{H}_2\text{O}$
Molecular weight [g/mol]	241.60
Shelf life	60 months
Physical state at 20°C	Solid
Colour	Blue crystalline
Odour	Odorless
pH value	3 - 4
Melting point [°C]	115°C
Boiling point [°C]	170°C
Density [g/cm <sup>3</sup> ]	2.05
Solubility in water [% weight]	138g/100cc H <sub>2</sub> O at 20°C

**Table 2** Information of Zinc Nitrate Hexahydrate. [6]

ZINC NITRATE HEXAHYDRATE	
Purity	98%
Molecular formula	$\text{Zn}(\text{NO}_3)_2 \cdot 6\text{H}_2\text{O}$
Molecular weight [g/mol]	297.48
Shelf life	60 months
Physical state at 20°C	Solid
Colour	Colorless crystals
Odour	Slight nitric acid odor
pH value	3.5 – 5.4
Melting point [°C]	36°C
Density [g/cm <sup>3</sup> ]	2.07
Solubility in water [% weight]	200g/100cc H <sub>2</sub> O at 20°C

**Table 3** Information of Aluminum Nitrate Nonahydrate. [7]

ALUMINUM NITRATE NONAHYDRATE	
Purity	98%
Molecular formula	$\text{Al}(\text{NO}_3)_3 \cdot 9\text{H}_2\text{O}$
Molecular weight [g/mol]	375.13
Shelf life	60 months
Physical state at 20°C	Solid
Colour	White crystals
pH value	2.5 – 3.5
Melting point [°C]	73°C
Boiling point [°C]	135°C
Density [g/cm <sup>3</sup> ]	2.07
Solubility in water [% weight]	64g/100cc H <sub>2</sub> O at 25°C

**Table 4** Information of Manganese(II) Nitrate Tetrahydrate. [7]

MANGANESE(II) NITRATE TETRAHYDRATE	
Purity	97%
Molecular formula	$\text{Mn}(\text{NO}_3)_2 \cdot 4\text{H}_2\text{O}$
Molecular weight [g/mol]	251.01
Shelf life	60 months
Physical state at 20°C	Solid
Colour	Pink-White crystals
pH value	3
Melting point [°C]	37°C
Boiling point [°C]	135°C
Density [g/cm <sup>3</sup> ]	2.13
Solubility in water [% weight]	380g/100cc H <sub>2</sub> O at 25°C

**Table 5** Information of Sodium Hydrogen Carbonate. [6]

SODIUM HYDROGEN CARBONATE	
Purity	99.7%
Molecular formula	$\text{NaHCO}_3$
Molecular weight [g/mol]	84.01
Shelf life	60 months
Physical state at 20°C	Solid
Colour	White crystals
pH value	8 - 8.5
Melting point [°C]	300°C
Boiling point [°C]	135°C
Density [g/cm <sup>3</sup> ]	2.16
Solubility in water [% weight]	9g/100cc H <sub>2</sub> O at 20°C

## 2.6 Catalyst preparation

Catalyst preparation is the important procedure because it will be affected to substance properties, chemical properties and state of catalyst and specific properties of active site which are dispersed on supported catalyst. Therefore, catalyst preparation is the determination for active site for each catalyst.

Precipitation is the one of oxide catalyst preparation that use for preparing catalyst which consist of active phase and support. Oxide catalyst from this method will have high specific surface area and porosity. On the other hand, these oxide catalysts are used to be supported oxide catalyst.

Coprecipitation is the method that metals are precipitated with supported oxide catalyst or reactant of supported oxide catalyst. Therefore, coprecipitation is the method for preparing metal or oxide catalyst on supported metal/oxide catalyst and bulk catalyst such as  $\text{Al}_2\text{O}_3$ ,  $\text{SiO}_2$ ,  $\text{ZrO}_2$ ,  $\text{TiO}_2$ . Moreover, coprecipitation will cause intimate contact between 2 or more metals which will be appropriate for hydrotalcite substance preparation such as  $\text{Ni}_6\text{Al}_2(\text{OH})_{16}\text{CO}_3$  and  $\text{Ni}_5\text{Al}_2(\text{OH})_{16}\text{CO}_3$ , or per oxide substance such as  $\text{NiO-Al}_2\text{O}_3$ ,  $\text{SiO}_2\text{-Al}_2\text{O}_3$ .

## 2.7 Literature reviews

CO <sub>2</sub> hydrogenation to methanol			
No	Published year	Catalyst, Reactor type And Reaction condition	Significant results
1	2015	<p><b>Catalyst :</b> Cu/ZnO/Al<sub>2</sub>O<sub>3</sub></p> <ul style="list-style-type: none"> <li>- Carbonate co-precipitation.</li> <li>- Cu/Zn/Al composition of 60:25:15.</li> <li>- 6 CZA catalysts with using citric acid, oxalic acid or urea.</li> <li>- Calcination at 450 °C for 4 h.</li> </ul> <p><b>Reactor type :</b> fixed-bed reactor.</p> <p><b>Reaction condition :</b></p> <ul style="list-style-type: none"> <li>- 240 °C, 3.0 MPa, 3600 h<sup>-1</sup></li> <li>- Molar feed composition of CO<sub>2</sub>/H<sub>2</sub> = 1:3.</li> <li>- Reduced in H<sub>2</sub> flow at 270 °C, 1 atm for 1 h.</li> </ul>	<p>Combustion temperature decreases caused by increasing of the quantity of citric acid. The increasing citric acid in catalyst preparation (Citric acid gives the highest activity) will increase the conversion of CO<sub>2</sub> and STY<sub>MeOH</sub>. The activity of catalyst was not only related to the active metal surface area but also the interaction between copper-oxide components.</p>
2	2011	<p><b>Catalyst :</b> Cu/ZnO/Al<sub>2</sub>O<sub>3</sub></p> <ul style="list-style-type: none"> <li>- Co-precipitation.</li> </ul>	<p>The activity of CZA-1 was much higher than that of CZA-2 that used CO<sub>2</sub> assisted aging</p>

		<ul style="list-style-type: none"> <li>- Cu:Zn:Al = 6:3:1, molar ratio.</li> <li>- Calcination at 350 °C for 6 h.</li> <li>- A referenced catalyst without CO<sub>2</sub> assisted aging was named CZA-2.</li> </ul> <p><b>Reactor type :</b> fixed-bed micro-reactor</p> <p><b>Reaction condition :</b></p> <ul style="list-style-type: none"> <li>- SV = 6000 h<sup>-1</sup>, P = 5 MPa, CO<sub>2</sub>:H<sub>2</sub>:N<sub>2</sub> = 25:75:1.</li> <li>- Reduced in 5% H<sub>2</sub> in N<sub>2</sub> flow at 300°C, 1 atm for 6 h.</li> </ul>	<p>for preparation. The aging-modified catalyst had a larger surface area, larger pore volume, higher catalytic activity, and smaller crystallite size. The obtained result found that at 240 °C gave the highest space time yield 254 g/(L·h) for and CZA-1 and 155 g/(L·h) for CZA-2.</p>	
3	2015	<p><b>Catalyst :</b> Cu/Y-Al<sub>2</sub>O<sub>3</sub> modified by ZnO, ZrO<sub>2</sub> and MgO</p> <ul style="list-style-type: none"> <li>- Impregnation.</li> <li>- Calcination at 600 °C for 6 h.</li> </ul> <p><b>Reactor type :</b> fixed-bed reactor</p> <p><b>Reaction condition :</b></p> <ul style="list-style-type: none"> <li>- 1400-5000 h<sup>-1</sup>, 230-310 °C , 6-32 atm,</li> <li>- H<sub>2</sub>:CO<sub>2</sub> = 3:1.</li> <li>- Reduced in 80 ml/min H<sub>2</sub> flow at desired</li> </ul>	<p>For Cu-ZnO-ZrO<sub>2</sub>-MgO/Al<sub>2</sub>O<sub>3</sub> catalyst. It was found that the methanol production could be enhanced with the higher reaction temperature thought the RWGs and methanation reactions. The high GHSV and high pressure were beneficial to the increased on the STY of CH<sub>3</sub>OH .</p> <p>ZnO, ZrO<sub>2</sub> and MgO's simultaneous modification used to improve the Cu dispersion and the amount of metallic copper surface area,</p>	[10]



		<p>temperature, 1 atm for 6 h.</p>	<p>improved to the metallic copper formed with a small crystallite size.</p>	
4	2016	<p><b>Catalyst</b> : Cu/ZnO/Al<sub>2</sub>O<sub>3</sub>/ZrO<sub>2</sub></p> <ul style="list-style-type: none"> <li>- Co-precipitation.</li> <li>- The addition of different weight percentages of binder alumina sol from 0 to 20 wt. %.</li> <li>- Cu/Zn/Al/Zr molar ratio of 2:1:1.2:0.9.</li> <li>- Calcination at 773 K for 5 h.</li> </ul> <p><b>Reactor type</b> : fixed-bed reactor.</p> <p><b>Reaction condition</b> :</p> <ul style="list-style-type: none"> <li>- 523 K, 5.0 MPa and</li> <li>WHSV = 4000 mL g<sub>cat</sub><sup>-1</sup> h<sup>-1</sup></li> <li>- H<sub>2</sub>/CO<sub>2</sub>/N<sub>2</sub> = 73:24:3</li> </ul>	<p>For the fixed-bed reactor, the activity is decreased with the added of alumina sol that caused by the decrease of Copper surface area and interaction with Cu-ZnO. With increasing alumina sol would cause the CH<sub>3</sub>OH selectivity decreased, because the decrease of the proportion between strongly basic sites and total basic sites.</p>	[11]
5	2019	<p><b>Catalyst</b> : CuZnAlZr</p> <ul style="list-style-type: none"> <li>- Co-precipitation.</li> <li>- Formaldehyde (FA) as precursor.</li> <li>- Calcination at 350–650 °C for 5 h.</li> </ul> <p><b>Reactor type</b> : fixed-bed reactor.</p>	<p>The dispersed metallic copper species with low temperature reduction caused a weak interaction of support oxides during calcination in N<sub>2</sub>.</p> <p>FA pre-activation could increased more</p>	[12]

		<p><b>Reaction condition :</b></p> <ul style="list-style-type: none"> <li>- 250 °C , 30 atm and GHSV = 4000 h<sup>-1</sup></li> <li>- H<sub>2</sub>/CO<sub>2</sub> = 3:1</li> <li>- reduced in 30 mL/min H<sub>2</sub> flow at 350 °C, 1 atm for 1 h.</li> </ul>	<p>crystallized ZnO, that presented a strong synergistic effect with Cu for CO<sub>2</sub> hydrogenation to methanol. It was found that CuZnAlZr catalyst from FA pre-activation gave the STY<sub>MeOH</sub> more than conventional methanol catalyst for 25%.</p>	
6	2019	<p><b>Catalyst :</b> CuO/ZnO/Al<sub>2</sub>O<sub>3</sub></p> <ul style="list-style-type: none"> <li>- Co-precipitation.</li> <li>- Zr-modified.</li> <li>- Calcination at 500 °C for 5 h.</li> </ul> <p><b>Reactor type :</b> fixed-bed reactor</p> <p><b>Reaction condition :</b></p> <ul style="list-style-type: none"> <li>- 200-260 °C , 2.76 MPa and GHSV = 823 h<sup>-1</sup></li> <li>- 6 mL/min CO<sub>2</sub>, 18 mL/min H<sub>2</sub></li> <li>- Reduced in 20 mL/min H<sub>2</sub> flow at 250 °C, 1 atm for 10 h.</li> </ul>	<p>An atomic ratio of Cu/Zn/Zr/Al are 4:2:1:0.5, the optimized catalyst composition. The stability test showed that the CZZA catalyst had higher stability during hydrogenation reaction and the max. methanol yield of 12.4 % which were much higher as compared to CZA.</p>	[13]
7	2018	<p><b>Catalyst :</b> Cu/ZnO/Al<sub>2</sub>O<sub>3</sub></p> <ul style="list-style-type: none"> <li>- Co-precipitation.</li> <li>- Calcination at 300 °C for 3 h.</li> <li>- Considered two conditions, namely</li> </ul>	<p>The unwashed method showed higher performance for methanol production than another method. The lower precipitation temperature and unwashed by water was</p>	[14]

		<p>washed and unwashed filtration.</p> <p><b>Reactor type :</b> fixed-bed reactor</p> <p><b>Reaction condition :</b></p> <ul style="list-style-type: none"> <li>- 160-220 °C, 7 bar and GHSV = 1950 h<sup>-1</sup></li> <li>- H/CO<sub>2</sub> = 9:1</li> </ul>	<p>favourable for higher Copper dispersion, higher methanol synthesis activity and a amorphous Cu crystal.</p>	
8	2020	<p><b>Catalyst :</b> CuO/ZnO/Al<sub>2</sub>O<sub>3</sub></p> <ul style="list-style-type: none"> <li>- Co-precipitation.</li> <li>- Different In<sub>2</sub>O<sub>3</sub> and Al<sub>2</sub>O<sub>3</sub> contents.</li> <li>- Calcination at 320 °C for 3 h..</li> </ul> <p><b>Reactor type :</b> fixed-bed reactor</p> <p><b>Reaction condition :</b></p> <ul style="list-style-type: none"> <li>- 250 °C, 50 atm and GHSV = 15000 h<sup>-1</sup></li> <li>- CO<sub>2</sub>/H<sub>2</sub> = 20:80</li> <li>- Reduced in diluted H<sub>2</sub> (5% in N<sub>2</sub>) flow at 295 °C, 1 atm for 14 h.</li> </ul>	<p>With H<sub>2</sub>/CO<sub>2</sub> substrate, the sample with higher amount of In<sub>2</sub>O<sub>3</sub> exhibited higher stability. Moreover, In<sub>2</sub>O<sub>3</sub> could directly converted CO<sub>2</sub> to methanol but the CO<sub>2</sub> conversion to methanol was low because of a strong basicity.</p> <p>The increasing of Pd into the catalyst could improve the methanol synthesis for CO<sub>2</sub> hydrogenation.</p>	[1]
9	2014	<p><b>Catalyst :</b> CuO/ZnO/Al<sub>2</sub>O<sub>3</sub></p> <ul style="list-style-type: none"> <li>- Co-precipitation.</li> <li>- The mole ratio is 6:3:1.</li> <li>- Graphene nanosheet (GNS) modified by</li> </ul>	<p>With additional GNS into the CZA catalyst could enhance the catalyst performance for methanol production. The 10 wt.% GNS modified CZA catalyst gave a STY of methanol 92.5% which</p>	[15]

		<p>high energy ball milling.</p> <ul style="list-style-type: none"> <li>- Calcination at 350 °C for 6 h.</li> </ul> <p><b>Reactor type</b> : fixed bed microreactor.</p> <p><b>Reaction condition</b> :</p> <ul style="list-style-type: none"> <li>- 250 °C , 3 MPa and GHSV = 12000 h<sup>-1</sup>.</li> <li>- Reactant gas H<sub>2</sub>/CO<sub>2</sub>/N<sub>2</sub> = 69:23:8.</li> <li>- Reduced in diluted H<sub>2</sub> (5% in N<sub>2</sub>) flow at 280 °C, 1 atm for 6 h.</li> </ul>	<p>higher than that on the CZA catalyst without GNS.</p> <p>However, the smaller particle CuO and ZnO higher, the improved catalytic performance was attributed to the outstanding promotion of GNS</p>	
10	2017	<p><b>Catalyst</b> : Cu/ZnO based</p> <ul style="list-style-type: none"> <li>- Impregnation.</li> <li>- Various supports such as Al<sub>2</sub>O<sub>3</sub>, Al<sub>2</sub>O<sub>3</sub>-ZrO<sub>2</sub>, SBA-15 and Al-modified SBA-15.</li> <li>- Calcination at 350 °C for 4 h.</li> </ul> <p><b>Reactor type</b> : fixed bed micro-reactor</p> <p><b>Reaction condition</b> :</p> <ul style="list-style-type: none"> <li>- 210 °C , 22.5 bar.</li> <li>- CO<sub>2</sub>/H<sub>2</sub> = 1:3.</li> <li>- Reduced in diluted H<sub>2</sub> (5% in N<sub>2</sub>) flow at 250 °C for 4 h. under atmospheric pressure.</li> </ul>	<p>The Cu/ZnO catalyst on SBA-15 support had the largest copper surface area and dispersion, smallest crystallite size and it is easily reduced which resulted in the highest catalytic activity and 13.96% CO<sub>2</sub> conversion and methanol selectivity of 91.32%. This oxide support affected the catalytic performance and selectivity of each product.</p>	[16]

11	2019	<p><b>Catalyst :</b> CuO/ZnO/Al<sub>2</sub>O<sub>3</sub></p> <ul style="list-style-type: none"> <li>- Co-precipitation.</li> <li>- Cu/Zn/Al weight ratio of 60:30:10.</li> <li>- Calcination at 350 °C for 12 h.</li> </ul> <p><b>Reactor type :</b> fixed bed micro-reactor</p> <p><b>Reaction condition :</b></p> <ul style="list-style-type: none"> <li>- 170-270 °C , 1-75 bar.</li> <li>- CO<sub>2</sub>/H<sub>2</sub> = 1:3.</li> <li>- reduced in 1.3 L/h. H<sub>2</sub> flow at 350 °C, 1 atm for 8 h.</li> </ul>	<p>Methanol selectivity and CO<sub>2</sub> conversion strongly depend on pressure, reaction temperature, flow rate and the catalyst composition. High flow-rate and high pressure increase the methanol formation. Methanol is directly produced from CO<sub>2</sub> whatever the pressure, while carbon monoxide can be produced by the decomposition of the formate at low pressure or directly from CO<sub>2</sub> reduction.</p>	[17]
----	------	---	--	------

CO hydrogenation to methanol			
No	Published year	Catalyst, Reactor type And Reaction condition	Significant results
1	2016	<p><b>Catalyst :</b> Cu/ZnO/Al<sub>2</sub>O<sub>3</sub></p> <ul style="list-style-type: none"> <li>- Co-precipitation.</li> <li>- Co-modified catalysts with different Na loadings by wet impregnation.</li> <li>- Calcination at 350 °C for 3 h..</li> <li>- Co(20.0%):Cu(48.0%):Zn(21.6%):Al(10.4%)</li> </ul> <p><b>Reactor type :</b> fixed-bed reactor</p> <p><b>Reaction condition :</b></p> <ul style="list-style-type: none"> <li>- 280 °C , 60 bar and GHSV = 9600 h<sup>-1</sup>.</li> <li>- CO:H<sub>2</sub>:N<sub>2</sub> = 40:40:20 (H<sub>2</sub>/CO = 1:1).</li> <li>- Reduced in dilute H<sub>2</sub> (H<sub>2</sub>/N<sub>2</sub> = 0.25). flow at 350 °C, 1 atm for 15 h.</li> </ul>	<p>Catalysts exhibited strong initial deactivation because of coking of isolated metallic Co surface site favoring HC formation. Alcohols increased with low Na loading (≤0.6 wt.%) and the first 10 h time of stream showing improved the formation of Cu-Co surface alloy, active sites for higher alcohol synthesis (HAS).</p> <p>Catalysts presented high Na loading (≥0.8 wt.%) could produce the stabilizing amorphous oxide matrix to failed led to drastic sintering of Cu<sup>0</sup> particles and increasing carbidizing of metallic Co forming bulk Co<sub>2</sub>C.</p> <p>Generating of addition active sites for HAS with closely contact between Co<sup>0</sup> and Co<sub>2</sub>C that was known as facilitate molecular CO</p>
			Reference [18]

			adsorption.	
2	2015	<p><b>Catalyst :</b> Cu/ZnO/Al<sub>2</sub>O<sub>3</sub></p> <ul style="list-style-type: none"> <li>- Co-precipitation.</li> <li>- Co-modified catalysts.</li> <li>- Calcination at 350 °C for 3 h.</li> </ul> <p><b>Reactor type :</b> fixed-bed reactor</p> <p><b>Reaction condition :</b></p> <ul style="list-style-type: none"> <li>- 280 °C, 60 bar and GHSV = 9600 h<sup>-1</sup></li> <li>- CO:H<sub>2</sub>:N<sub>2</sub> = 40:40:20 (H<sub>2</sub>/CO = 1:1)</li> <li>- Reduced in dilute H<sub>2</sub> (H<sub>2</sub>/N<sub>2</sub> = 0.25). flow at 350 °C, 1 atm for 15 h.</li> </ul>	<p>An increasing of Cu/Co ratio that caused by the higher formation of alcohols and Cu/Co ratio 2.5 was recognized to optimum composition in term of activity and selectivity. A major enrichment of Zn in the catalyst surface came from the conditions during activation and HAS. The distribution of product shifted favorably towards higher alcohols with increasing time on stream as an extended close interface contact between the metallic copper.</p>	[19]
3	2015	<p><b>Catalyst :</b> Cu/Zn/Al</p> <ul style="list-style-type: none"> <li>- A complete liquid-phase method.</li> <li>- Various triethanolamine (TEA) contents.</li> <li>- Calcination at 250 °C for 8 h.</li> </ul> <p><b>Reactor type :</b> a continuous-flow, slurry reactor</p> <p><b>Reaction condition :</b></p>	<p>TEA decreased the amount of weak acid and increased the Cu component on the catalyst surface and caused the interaction among Cu, Zn and Al changed. Besides, it made the catalysts easier to reduce. A suitable quantity of TEA appropriate for the HAS and the best catalytic activity when the molar quantity</p>	[20]

		<ul style="list-style-type: none"> <li>- 250-290 °C , 4.5 MPa</li> <li>- H<sub>2</sub>/CO = 2:1.</li> <li>- Feed flow rate of 150 mL/min.</li> <li>- Maximum reduction temperature in the range of 460–530 K.</li> </ul>	<p>of TEA was equal to Al.</p>	
4	2013	<p><b>Catalyst :</b> Cu/Zn/Al</p> <ul style="list-style-type: none"> <li>- Co-precipitation.</li> <li>- Three samples molar content of 60:30:10, 45:45:10 and 33:33:33.</li> <li>- K promoted and substituting Zn and/or Al by Mn and/or Cr.</li> <li>- Calcination at 350 °C for 4 h.</li> </ul> <p><b>Reactor type :</b> fixed-bed reactor</p> <p><b>Reaction condition :</b></p> <ul style="list-style-type: none"> <li>- 300-320 °C , 40 bar</li> <li>- W/F ratio of 0.74 g s/cm<sup>3</sup></li> <li>- H<sub>2</sub>/CO = 2:1.</li> <li>- Reduced in H<sub>2</sub> flow at 350 °C, 1 atm for 3 h.</li> </ul>	<p>Low Al component (K-Cu<sub>45</sub>Zn<sub>45</sub>Al<sub>10</sub>) and Cu/Zn atomic ratio of 1:1 revealed the optimum performance in terms of selectivity and activity to produce higher alcohols. High Al component, advocate methanol synthesis at the expense of higher alcohols. Al reduced the basicity on the catalyst.</p> <p>The lower exposed copper surface that causes by large CuO crystals were formed as a result in reducing activity by 50% of replacement of Zn and/or Al by Mn and/or Cr. The most perceptible changes were indicated for the catalyst, where a 50% increased in HAS was measured.</p>	[21]



5	2016	<p><b>Catalyst :</b> Cu/Zn/Al/Zr</p> <ul style="list-style-type: none"> <li>- Complete liquid-phase</li> <li>- Al/Zr atomic ratios of 4:1, 2:1</li> <li>- Calcination at 300 °C for 8 h.</li> </ul> <p><b>Reactor type :</b> a continuous-flow, slurry reactor</p> <p><b>Reaction condition :</b></p> <ul style="list-style-type: none"> <li>- 523 K, 4.5MPa</li> <li>- Feed flowrate of 150mL/min.</li> <li>- Reduced in H<sub>2</sub>/N<sub>2</sub> (75 mL/min, V(H<sub>2</sub>)/V(N<sub>2</sub>)=1:4) flow at 280 °C, 1 atm for 8 h.</li> </ul>	<p>The increasing of Zr/Al atomic ratio, the catalytic performance and stability would be also increased. Zr was useful to improve the stability of the catalysts and Al initiated the formation of higher alcohols. For improving the dispersion of copper and made the catalyst easier to reduce, use Zr and this also decreased the number of weak acid sites and advocated the stability of porous structure.</p> <p>The number of weak acidic sites caused the higher alcohols formation and when they decreased might lead to the deactivation of catalyst.</p>	[22]
---	------	--	---	------

CO/CO <sub>2</sub> hydrogenation to methanol				
No	Published year	Catalyst, Reactor type And Reaction condition	Significant results	Reference
1	2009	<p><b>Catalyst :</b> Cu/ZnO/Al<sub>2</sub>O<sub>3</sub></p> <ul style="list-style-type: none"> <li>- Co-precipitation.</li> <li>- Modified by adding small amount of Mn, Mg, Zr, Cr, Ba, W and Ce oxides.</li> <li>- Calcination at 350 °C for 3 h</li> </ul> <p><b>Reactor type :</b> fixed-bed reactor</p> <p><b>Reaction condition :</b></p> <ul style="list-style-type: none"> <li>- 240 °C , 5 MPa and GHSV = 12400 h<sup>-1</sup></li> <li>- CO/CO<sub>2</sub>/H<sub>2</sub> = 1:1:14.5</li> <li>- reduced in diluted H<sub>2</sub> (3% in N<sub>2</sub>) flow at 240 °C, 1 atm for 15 h.</li> </ul>	<p>Mn and Zr promote catalysts had high activity for methanol production from synthesis gas. The added Zr increased the reduction temperature of Cu<sup>2+</sup> ions, and improved Cu dispersion on the catalyst surface. Addition of Zr could increase Cu dispersion, surface area on catalyst surface. Mn and Zr promoters, their synergetic effect made the CZA-Mn-Zr catalyst most stable.</p> <p>Significant increasing in bulk and surface properties of the catalyst and CuO reduction would be easier is accompanied by increasing STY of methanol for CZA/MnO.</p>	[3]
2	2012	<p><b>Catalyst :</b> Cu/ZnO/Al<sub>2</sub>O<sub>3</sub></p> <ul style="list-style-type: none"> <li>- Co-precipitation.</li> </ul>	<p>For improving the catalyst activity and stability, small quantity of SiO<sub>2</sub> and the oxide</p>	[23]

		<p>- Adding small amount of colloidal silica (0.6 wt.%) and Mn, Ga and Zr oxides.</p> <p>- Calcination at 350 °C for 3.5 h.</p> <p><b>Reactor type :</b> fixed-bed reactor</p> <p><b>Reaction condition :</b></p> <ul style="list-style-type: none"> <li>- 240 °C, 4.5 MPa and GHSV = 15000 h<sup>-1</sup>.</li> <li>- CO/CO<sub>2</sub>/H<sub>2</sub> = 1:1.38:16.5.</li> <li>- reduced in diluted H<sub>2</sub> (5% in N<sub>2</sub>) flow at 295 °C, 1 atm for 14 h.</li> </ul>	<p>additives are introduced. With adding silica would increase the BET surface, the dispersion of Cu, and pore volume, shown by higher Cu surface area. Good interaction of CuO and ZnO was the favor of AP method of catalyst preparation. Stability and the crystallite size of catalyst which was affected to SiO<sub>2</sub> was higher than CZAS catalyst and in Ga<sub>2</sub>O<sub>3</sub>-modified catalyst and ZrO<sub>2</sub>-modified catalyst.</p>	
3	2020	<p><b>Catalyst :</b> CuO/ZnO/Al<sub>2</sub>O<sub>3</sub></p> <ul style="list-style-type: none"> <li>- Co-precipitation.</li> <li>- Different In<sub>2</sub>O<sub>3</sub> and Al<sub>2</sub>O<sub>3</sub> contents.</li> <li>- Calcination at 320 °C for 3 h.</li> </ul> <p><b>Reactor type :</b> fixed-bed reactor</p> <p><b>Reaction condition :</b></p> <ul style="list-style-type: none"> <li>- 250 °C, 50 atm and GHSV = 15000 h<sup>-1</sup>.</li> <li>- CO/CO<sub>2</sub>/H<sub>2</sub> = 10:10:80.</li> <li>- Reduced in diluted H<sub>2</sub> (5% in N<sub>2</sub>) flow at</li> </ul>	<p>Addition of indium increased the higher oxygen vacancies and also increased the BET area and Cu surface, whereas decreased the Cu crystallite. This result showed that methanol synthesis in catalysts containing In<sub>2</sub>O<sub>3</sub> decreased. Also, the increased in In<sub>2</sub>O<sub>3</sub> component, the methanol production rate decrease.</p> <p>The drastic drop-in catalytic performance</p>	[1]

		<p>295 °C, 1 atm for 14 h.</p>	<p>in H<sub>2</sub>/CO/CO<sub>2</sub> feed caused by the In<sub>2</sub>O<sub>3</sub> influenced the adsorption of CO<sub>2</sub> and made it stronger which in turn.</p>	
4	2007	<p><b>Catalyst</b> : Cu/ZnO/Al<sub>2</sub>O<sub>3</sub></p> <ul style="list-style-type: none"> <li>- Co-impregnation.</li> <li>- 2-butanol promoting.</li> <li>- Dried for 12 h. at 393 K.</li> </ul> <p><b>Reactor type</b> : semi-batch reactor</p> <p><b>Reaction condition</b> :</p> <ul style="list-style-type: none"> <li>- 443 K; P, 5.0 MPa.</li> <li>- Solvent, 2-butanol 40 ml.</li> <li>- Feed gas, 20 ml/min.</li> </ul> <p>CO/CO<sub>2</sub>/H<sub>2</sub>/Ar=32.4:5.07:59.51:3.02.</p> <ul style="list-style-type: none"> <li>- Reduced in diluted H<sub>2</sub> (5% in N<sub>2</sub>) flow at 493 K, 1 atm for 10 h.</li> </ul>	<p>In presence of the CuO/ZnO which make the performance of the catalysts increased for reaction temperature. For methanol production, the active site of the CZA catalysts were the Cu<sup>0</sup> and the Cu-Zn site as special site.</p>	[24]
5	2018	<p><b>Catalyst</b> : Cu/ZnO/Al<sub>2</sub>O<sub>3</sub></p> <ul style="list-style-type: none"> <li>- Co-precipitation.</li> <li>- Al-containing precursors</li> <li>- Calcination at 350 °C for 4 h.</li> </ul>	<p>The Cu replacement by Zn in malachite lattice, was leading to various performance of the obtained catalyst could be affected by Al-containing precursor. The catalyst which contain</p>	[25]

		<p><b>Reactor type :</b> fixed-bed reactor</p> <p><b>Reaction condition :</b></p> <ul style="list-style-type: none"> <li>- 230 °C, 5 MPa and GHSV = 10000 h<sup>-1</sup>.</li> <li>- CO/CO<sub>2</sub>/H<sub>2</sub>/N<sub>2</sub> = 13:2:80:5.</li> <li>- Reduced in diluted H<sub>2</sub> (5% in N<sub>2</sub>) flow at 230 °C, 1 atm.</li> </ul>	<p>Al in form of Al(OH)<sub>3</sub> performed high Cu substitution in the co-precipitated zinc malachite, and showed higher catalytic activity compared to its counterparts. Combination of Al with the active component of Cu/ZnO in the methanol production catalyst, Al(OH)<sub>3</sub> was an excellent Al-containing precursor.</p>	
6	2018	<p><b>Catalyst :</b> CuO/ZnO/Al<sub>2</sub>O<sub>3</sub></p> <ul style="list-style-type: none"> <li>- Co-precipitation</li> <li>- 16 series catalysts in four different groups with various compositions.</li> <li>- Calcination at 320 °C for 3 h.</li> </ul> <p><b>Reactor type :</b> fixed-bed reactor</p> <p><b>Reaction condition :</b></p> <ul style="list-style-type: none"> <li>- 250 °C, 5 MPa</li> <li>- CO/CO<sub>2</sub>/H<sub>2</sub> = 9.94:8.95:81.11.</li> <li>- Reduced in diluted H<sub>2</sub> (5% in N<sub>2</sub>) flow at 240 °C, 1 atm for 12 h.</li> </ul>	<p>CuO/ZnO=2.7 and CuO/Al<sub>2</sub>O<sub>3</sub>=9 are the most active catalyst. The smallest Cu crystallite size and the highest BET and Cu surface area were observed for the sample with a CuO/Al<sub>2</sub>O<sub>3</sub>=9. The best productivity and selectivity is CuO/ZnO=1.8. It was found that some interwoven nano-twin was formed at CuO/ZnO=1.8, that enhance the methanol productivity and the catalytic stability. Moreover, the lowest Cu surface area and the largest Cu crystal size was noticed on the sample with CuO/ZnO = 1.8.</p>	[26]

This study aims to use Cu/ZnO/Al<sub>2</sub>O<sub>3</sub> catalyst for the catalytic synthesis of methanol from CO hydrogenation, CO<sub>2</sub> hydrogenation and CO/CO<sub>2</sub> hydrogenation. The relevant research of this study consist of 2 parts from a different source

1. Research publications include catalyst components and the weight/mole ratio of Cu/Zn/Al, modifiers and methods.
2. Research and experimental from Kamonlak and Phapatchaya to Continue studying. See details the following.

#### 2.7.1 Cu

Most of literature reviews had exhibited that the species of Cu (Cu<sub>2</sub>O or metallic Cu particles) on the CZA catalysts were the sites of active or the catalytic active center for hydrogenation for methanol. [12], [10] The metallic Cu surface area and basicity were main limiting factor for the catalytic activity of the CZA catalysts. The performance of catalyst increased linearly with S<sub>Cu</sub> and the quantity of basic sites. [27] The yield of CH<sub>3</sub>OH increased with the increase of the Cu surface area. As a matter of fact, there were not a direct variation. The result exposed that the performance of CZA catalyst were related to Cu surface area and the interaction between Copper-oxide components. [8] CO<sub>2</sub> conversion was directly proportional to the active sites of Cu<sup>0</sup>. [17]

#### 2.7.2 Zn

Zn which is a promoter modification led to the well-dispersed Cu and increasing the metallic copper surface area, improved to the metallic copper formed with a small size particle, enhanced the catalytic activity of CZA catalyst in methanol production. [10] The catalyst sample with high Zn component demonstrated a high catalytic activity along with good thermo-stability. [25] The main function which ascribed to the ZnO was helped to the well-dispersed CuO, therefore was providing high amount of metallic copper expose to the feeds reaction. [28] ZnO could be used as a dispersant for copper and a hydrogen reservoir [12], ZnO was role to provide active sites for H<sub>2</sub> spillover, and a poison scavenger. It also activated CO<sub>2</sub> and produces catalytically active sites through Cu-ZnO interactions. [10]

### 2.7.3 Al

$\text{Al}_2\text{O}_3$  which is modifiers and a structural promoter was introduced into Cu-ZnO system to improve catalytic activity. [12], [13] Addition of Al had been reported to improve the BET surface area or the specific surface area and copper dispersion of catalyst, leading to a remarkable increasing in catalyst activity, and especially the stability and improved the synergistic effect between Cu-Zn in methanol synthesis. [25], [23] Methanol selectivity decreased with the Al loading increased. On the other hand, for methanol, the yield of CO and CO selectivity increased with the increasing of reaction temperature. The increasing trend in CO selectivity and yield were resulted from increased Al loading. [13]

### 2.7.4 Ratio of Cu/Zn/Al

Study of the influence of CuO/ZnO weight ratios, textural properties and catalytic performance of different CuO/ZnO/ $\text{Al}_2\text{O}_3$  catalysts including (C1) : 10:80:10, (C2) : 40:50:10, (C3) : 50:40:10, (C4) : 60:30:10, (C5) : 70:20:10. CuO/ZnO/ $\text{Al}_2\text{O}_3$  catalyst which a Cu/Zn/Al weight ratio of 60:30:10, exhibit the highest  $\text{CO}_2$  conversion and methanol selectivity. Methanol selectivity increases with the metallic copper surface area for the samples containing 10-60% of copper, while it decreases when the copper content exceeded 60%. It can be explained by the positive synergetic effect obtained by the contact between copper and zinc oxides. [17] Most of relevant research also found that using of the mole ratio is 60:30:10 [15], [10], [28] are the same or close to. Cu/Zn/Al atomic ratio of 60:25:15 [8], 66% CuO, 24% ZnO, and 10%  $\text{Al}_2\text{O}_3$  by weight. [23], molar Cu:Zn:Al ratio of 60:27:13. [19]

### 2.7.5 Modifiers

Different promoters had noticeable effect on Cu particle size, specific surface area, catalytic activity, and stability of CZA catalyst in hydrogenation for methanol. The obtained modifiers from the literature view include Mn, Zr, Cr, Mg, V, Ce, Ti, Ga, W, Ba and Pd. [15], [3] For [23] the effect of Fe and Pd could act to restrained copper sintering along with the oxidation of copper surface to enhanced the stability of CZA catalyst. Zr acted to structural promoter, could preclude the aggregation of copper and zinc, and improved the dispersion of copper, whereby enhancing the structural of catalyst. Zr modified catalysts had shown Zr loading did not significantly affect

CO<sub>2</sub> conversion. [13], [22] For A-Zr catalyst, the interaction between Cu-Zr ion had occurred during the reduction. This interaction is the inverse of Cu reduction and caused the change of CuO to Cu<sup>0</sup>. As a result, the reduction of copper became slower and more difficult. This effect resulted in smaller copper crystallite size or well-dispersed copper on the catalyst surface. It looked like increasing Zr could be improve stability of the catalyst. [3] For the A-Mn catalyst, the result predicted that the interaction between CuO-MnO had a lower reduction temperature or the added of MnO enhanced the reducibility of CuO. Whereas, the reduction temperature for the CuO which was not interacted with MnO was still about the same temperature. It seems to adding Mn could enhance the activity of catalyst and when promoted Mn and Zr to CZA catalyst, the total surface area increased. When these two promoters were added together, the specific surface area is more than 65% increasing. [3]

#### 2.7.6 Method

The conventional co-precipitation method is commonly used in the preparation of Cu-ZnO catalyst which is reference from the literature review. From 22 literature reviews, there are 19 papers that using the co-precipitation method. The rest using other methods. Ultrasound-assisted, sol-gel and solid-state [27], the impregnation method [10], co-impregnation method [24], complete liquid-phase technology [22]. The co-precipitation [14]. Lower precipitation temperature while preparing the catalyst was favorable for obtaining higher Copper dispersion, smaller Copper particle, and higher methanol production activity. Kuo et al. showed that Cu, Zn, and Al ion were appropriate for precipitation at 70 °C but cautioned that although preparing a catalyst at a high temperature was advantageous for precipitation, catalytic performance was low. The selection of preparation method was important for obtaining excellent catalyst for methanol synthesis. The preparation method could impact the size of the crystallite size, the dispersion of metals on the catalyst surface, and the interaction between active species-support and others which were related to the catalytic activity of catalyst. [12], [23] The preparation method affected on the average Cu crystallite size, the interactions of metals, the exposed copper phases surface area, the ratio of metallic copper/oxidized copper. [27]



### 2.7.7 Previous research

For studying the effect of increasing pH value in CZA catalyst preparation. It was found that the example from XRD found slight crystallite size of CuO and ZnO resulting to have higher dispersion of CuO based. BET surface was found that CZA-PH9 had the lowest surface area. The main active site of Cu is reported in form of Cu<sup>0</sup> and the CZA-PH8 showed the highest reducibility among other catalysts. CZA-PH8 and CZA-PH9 showed high number of basic sites which can enhanced the adsorption of CO<sub>2</sub> gas by carbonate group on surface. NH<sub>3</sub>-TPD was examined, and high acidity was indicated that it affected to decrease of activity of CZA catalyst. XPS exposed that Cu<sup>2+</sup> species was mainly in all CZA catalysts. Next, study the effect of Mn, Zr, and Si promoters on CZA-PH8 catalyst. From XRD patterns were found that the modification of Zr, Mn, and Si could decrease crystallite size to 3.43-4.42. The Mn and Zr have a good dispersion of CuO, ZnO and leading to low agglomeration. Mn promoter was found to show the highest surface area. It had relation with high CuO, ZnO dispersion in XRD part and Mn promoter improve Cu<sup>0</sup> dispersion as measured by H<sub>2</sub>-Chemisorption. The shifting of moderate acidity site became to weak acid is an important property for not promoting H<sub>2</sub> saturation to undesirable H<sub>2</sub>O product. This phenomenon was appeared with Mn promotion. This reason introduced basicity of Mn promotion. Reaction test showed a good activity by Mn promoter. It can improve CZA-PH8 expressing the highest CO<sub>2</sub> conversion and methanol yield at 4.70% and 0.46%, respectively. [29]

## CHAPTER 3

### EXPERIMENT

#### 3.1 Catalysts preparation

Preparation of the catalyst is considered to be very important as this affects the physical and chemical properties of the catalyst and state of catalyst which is characteristics of active site that are dispersed on support. Catalyst preparation is the core for the design of optimal active sites of the catalyst.

3.1.1 CuO/ZnO/Al<sub>2</sub>O<sub>3</sub> catalyst (weight ratio of Cu:Zn:Al = 60:30:10) was prepared by co-precipitation method. The mixed aqueous solution of the copper (II) and zinc and aluminum nitrate precursors Cu(NO<sub>3</sub>)<sub>2</sub>·3H<sub>2</sub>O (99.5% purity), Zn(NO<sub>3</sub>)<sub>2</sub>·6H<sub>2</sub>O (98% purity) and Al(NO<sub>3</sub>)<sub>3</sub>·9H<sub>2</sub>O (98% purity) were dissolved in DI water. Sodium hydrogen carbonate NaHCO<sub>3</sub> was dropped into the mixed aqueous solution or precursor solution for adjusting pH and the pH was kept constant at 8 under stirring the temperature was maintained at 80°C for 120 min. Finally, the precipitate was washed with DI water by centrifuge and dried overnight in air at 110°C, then, followed by calcination in air at 300°C for 3 h.

3.1.2 CuO/ZnO/Al<sub>2</sub>O<sub>3</sub>-Mn catalyst with 0.1 wt.% of Mn and the same composition (weight ratio of Cu:Zn:Al = 60:30:10) was prepared by co-precipitation method. DI water dissolved metal precursors including copper (II) and zinc, aluminum and manganese(II) nitrate precursors Cu(NO<sub>3</sub>)<sub>2</sub>·3H<sub>2</sub>O (99.5% purity), Zn(NO<sub>3</sub>)<sub>2</sub>·6H<sub>2</sub>O (98% purity), Al(NO<sub>3</sub>)<sub>3</sub>·9H<sub>2</sub>O (98% purity) and Mn(NO<sub>3</sub>)<sub>2</sub>·4H<sub>2</sub>O (97% purity). Then, the step of co-precipitation method is similar to 3.1.1.

#### 3.2 Catalysts characterizations

The objective of the characterizations of the catalyst are as following

1. To comprehend the relationship between physical properties, chemical properties and catalytic properties which means finding the relationship between the structure and function of the catalyst.
2. To measure the physical properties and chemical properties such as pore size, surface area and etc. for designing the reactor,

simulation and appropriate process. 3. To ensure the confidence of quality control by using the catalyst that may change physical properties and chemical properties of the catalyst during catalyst activation and reaction. 4. To discover the cause of the catalyst deactivation and design the catalyst regeneration step and choose the catalyst properties that minimize cause of the catalyst deactivation.

### 3.2.1 X-ray diffraction (XRD)

A sample is placed into the center of an instrument and illuminated with a beam of X-ray. The signal coming from the sample is recorded and graphed, where peaks are observed related to the atomic structure of the sample. X-ray diffraction is extensively used in material characterization. The material characterization is necessary to identify both the elements present as well as the structure in order to fully define the material unlike other characterization methods. X-ray diffraction can provide determination of the elemental composition of the material composition of the material as well as the crystalline structure of the samples which is defined by the atomic arrangement. For the crystal size of the CuO particles from the X-ray patterns can calculate by using the Scherrer equation.

### 3.2.2 Scanning Electron Microscope (SEM)

Scanning Electron Microscope is used for analyze the element distributions in different part of sample. It basically uses electrons to see objects to take the image of the material shape, material as the agglomeration of metal species, particle size and using morphological studies on catalyst surface. Morphology means how it looks like the surface structure, the texture, the pore, pore size, etc., in which the physical dispersion of CZA catalysts could be referred to the surface structure.

### 3.2.3 Energy-dispersive X-ray spectroscopy (EDX)

Energy-dispersive X-ray spectroscopy is a chemical technique employed in conjunction with SEM and use to identify the element, to analyze the element distributions in synthesise structure or different part of samples and to determine the metal contents of each material or the precursors and catalysts.

### 3.2.4 N<sub>2</sub> physisorption

The N<sub>2</sub> physisorption was used to find the specific surface area of a porous material with the size of the pore by Brunauer-Emmett-Teller (BET) analysis. Adsorption-Desorption curves are reported on the adsorption isotherm graph. The first part of the adsorption curve is used to calculate the specific surface area which can be calculated from section of isotherm (generally  $P/P_0 = 0.05-0.35$ ) by BET equation. The linearization of the BET equation is represented in BET surface area plot graph where a function of adsorbed volume is reported in function of relative pressure from the slope and intercept which used to calculate the adsorbed volume and the specific area in m<sup>2</sup>/g of sample. Also, the adsorption curve is possible used to calculate the pore size distribution.

### 3.2.5 Temperature-programmed reduction (TPR)

Temperature-programmed reduction (TPR) was used to analyze the optimal reduction temperature of Cu oxides to metal that improve its dispersion on support of catalyst. This technique of H<sub>2</sub>-TPR exhibits the catalyst reducibility or the reduction behavior. To determine temperature of reduction as following, 0.05 g. of catalyst was preheated to 300°C and 1 hour. The reducing was conducted with 10% H<sub>2</sub>/Ar between 30–500°C.

### 3.2.6 Temperature-programmed desorption of carbon dioxide (CO<sub>2</sub>-TPD)

The technique of the basicity of the samples was measured Temperature-programmed desorption of carbon dioxide illustrate the basicity property of the surface. To determine the basic site as following. The 0.07 g. catalyst was loaded and pretreated with carrier flow 25 mL/min at 250°C for 30 min and adsorbed CO<sub>2</sub> at 30°C in 1 hour. Next step, the desorbed of CO<sub>2</sub> was heated to 500°C by heating rate of 10°C /min.

### 3.2.7 Temperature-programmed desorption of ammonia (NH<sub>3</sub>-TPD)

The technique of the acidity of the samples was measured Temperature-programmed desorption of ammonia illustrate the acidic property of the surface and

gives formation regarding number of active adsorption site and nature of adsorption site. To determine the acid site as following, the 0.07 g. of catalyst was loaded and pretreated with He as carrier flow 25 mL/min at 250°C for 30 min and adsorbed NH<sub>3</sub> analysis gas at 30°C in 1 hour. Finally, the desorbed of NH<sub>3</sub> was heated to 500°C by heating rate of 10°C /min.

### 3.2.8 X-ray Photoelectron spectroscopy (XPS)

X-ray Photoelectron spectroscopy (XPS) was characterize the surface properties of catalyst and provides the elemental information, chemical state or oxidation state and depth resolution achievable. Cu, Zn, Al, O, C species was detected between intensity and binding energy eV. CZA catalyst was determined in 0-1200 eV.

### 3.2.9 CO-Chemisorption (CO-Chem)

The active metal of catalyst and disperse of active site of CZA catalysts was obtained by using CO-Chemisorption which had the similarity method with TPR. The catalyst must be reduced from metal oxide to active metal for H<sub>2</sub> adsorption and cooled down to 40°C and then purging in the flow of He for 30 min. The chemisorption analysis was conducted by passing of the pulses of CO gas (80  $\mu$ L each time) which were dosed over catalyst sample through an injection port. For the active metal surface area (per gram of metal) and metal dispersion of the CuO particles can calculate by using the following equation.

$$MSA_S (m^2/g_{cat}) = S_f \times \frac{V_{ads}}{V_g} \times N_A \times \sigma_m \times \frac{m^2}{10^{18}nm^2} \quad (7)$$

Where

$S_f$  = stoichiometry factor

$V_{ads}$  = volume adsorbed, (cm<sup>3</sup>/g)

$V_g$  = molar volume of gas at STP , 22414 (cm<sup>3</sup>/mol)

$N_A$  = Avogadro's number, 6.023x10<sup>23</sup> (molecules/mol)

$\sigma_m$  = cross-sectional area of active metal atom, (nm<sup>2</sup>)

$$D (\%) = S_f \times \frac{V_{\text{ads}}}{V_g} \times \frac{m.w.}{\%M} \times 100\% \times 100\% \quad (8)$$

Where

$S_f$  = stoichiometry factor

$V_{\text{ads}}$  = volume adsorbed, (cm<sup>3</sup>/g)

$V_g$  = molar volume of gas at STP , 22414 (cm<sup>3</sup>/mol)

$m.w.$  = molecular weight of the metal, (a.m.u.)

$\%M$  = % metal, (%)

### 3.2.10 Inductive Coupled Plasma Spectrometer Mass Spectrometer (ICP-MS)

The actual quantity of elemental compositions of the calcined catalysts including Cu, Zn, Al, and Mn in bulk of the CZA catalysts at ppt to ppm levels was determined by inductively coupled plasma spectrometry mass spectrometer (ICP-MS) which could distinguish different of element species and measure all element in single analysis after the catalysts were dissolved with HCl as atomizer.

### 3.3 Activity test

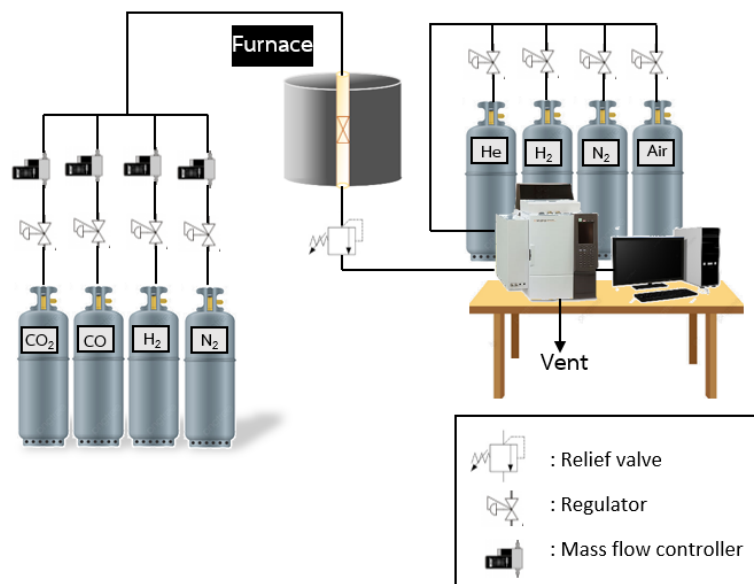


**Figure 3** The Schematic of methanol synthesis.

Start from loading of CZA, CZA-Mn 0.1 g. each catalyst into the reactor with quartz wool. The catalytic tests have been performed in a fix-bed microreactor. The reactor geometries with 12 mm. of outer diameter, 10 mm. of inner diameter and 50 cm. of length. Prior to reaction, the catalyst was pretreated by N<sub>2</sub> for removal of moisture at 250 °C and 30 min. Secondly, the fresh catalyst was reduced in 20% H<sub>2</sub> balance N<sub>2</sub> (50 ml/min) at 300 °C under atmospheric pressure. After the reduction step, the reactor was cooled to reaction temperature 250 °C at 1 atm. and was fed with the reactant gas mixture for CO, CO<sub>2</sub>, and CO/CO<sub>2</sub> hydrogenation (CO/H<sub>2</sub> = 1:2, CO<sub>2</sub>/H<sub>2</sub> = 1:3, CO/CO<sub>2</sub>/H<sub>2</sub> = 1:1:2 respectively). The catalyst was tested for methanol synthesis by time on stream in 5 hours. The analysis gas was detected by multi-detector TCD and FID GC-2014. as shown in **Table 6** and **Table 7**.

**Table 6** Condition of TCD detector.

Gas Chromatograph	Shimadzu GC 2014
GC type	Multi-detector
Detector 1	TCD
Pack-bed reactor	Shincarbon
Carrier gas	Helium gas
Injector temperature	170 °C
Column temperature (Link FID)	Initial 150 °C Hold 240 °C Cool down 150 °C
Detector temperature	150 °C
Time analysis	15 min

**Table 7** Condition of FID detector.

Gas Chromatograph	Shimadzu GC 2014
GC type	Multi-detector
Detector 2	FID
Capillary column	Rtx-5
Carrier gas	Nitrogen gas Hydrogen gas Air zero gas
Injector temperature	170 °C
Column temperature (Link TCD)	Initial 150 °C Hold 240 °C Cool down 150 °C
Detector temperature	150 °C
Time analysis	1 min



### 3.4 Simulation

Simulation with Aspen plus V.9 software.

3.4.1 Identify elements and compounds that employ in the process such as methane, water, carbon monoxide, hydrogen, carbon dioxide and methanol.

3.4.2 Consider selecting a thermodynamic model. In this work uses Redlich-Kwong-Soave-Boston-Mathias (RKS-BM) because all elements and compounds as covalent compounds are non-polar and slightly polar that suitable for hydrocarbon production processes such as gas and petrochemical processes with having to admit that there is no any equation of state that can be used very well with all kind of fluids in any case or condition.

3.4.3 The reactor used in the simulation is RStoic which know the stoichiometry of various reaction, conversion or extent of reaction without needing to know reaction rate known as chemical kinetics. That suitable for simulations reaction or sequential reaction.

3.4.4 Define all equipment used in this process and connect the next line to each device in the process.

3.4.5 Specify the components, the feed rate of each component, temperature and pressure of the feed line, and the operating condition of reactor in each process according to results of a relevant researches for methane steam reforming, bi-reforming, CO and CO/CO<sub>2</sub> hydrogenation, respectively. For CO hydrogenation and CO/CO<sub>2</sub> hydrogenation will use the same relevant research for simulation.

3.4.5.1 M. Nazari and S.M. Alavi. 2019. An investigation of the simultaneous presence of Cu and Zn in different Ni/Al<sub>2</sub>O<sub>3</sub> catalyst loads using Taguchi design of experiment in steam reforming of methane. [30]

- The methane steam reforming reaction :  $\text{CH}_4 + \text{H}_2\text{O} \leftrightarrow \text{CO} + 3\text{H}_2$
- The water gas shift reaction :  $\text{CO} + \text{H}_2\text{O} \leftrightarrow \text{CO}_2 + \text{H}_2$
- The operation condition : temperature = 700°C, pressure = 1 atm.
- The ratio of water to methane = 4:1,

The feed rate of methane = 0.0002719 mol/min

- Results : CH<sub>4</sub> conversion = 99, H<sub>2</sub> yield = 331, CO selectivity = 30

3.4.5.2 N. Kumar, A. Roy, Z. Wang, E.M. L'Abbate, D. Haynes, D. Shekhawat and J.J. Spivey. 2016. Bi-reforming of methane on Ni-based pyrochlore catalyst. [31]

- The bi-reforming of methane reaction :  $3\text{CH}_4 + \text{CO}_2 + 2\text{H}_2\text{O} \leftrightarrow 4\text{CO} + 8\text{H}_2$

- The operation condition : temperature = 950°C, pressure = 1 atm.

- Mol% : CO<sub>2</sub> = 16 , CH<sub>4</sub> = 51 , H<sub>2</sub>O = 33

- Results : CH<sub>4</sub> conversion = 96.6, CO<sub>2</sub> conversion = 99.1,

CO selectivity = 124.36, CO yield = 99.5

3.4.5.3 William L. Luyben. 2010. Design and Control of a Methanol Reactor/Column Process. [32]

- The CO hydrogenation reaction :  $\text{CO} + 2\text{H}_2 \leftrightarrow \text{CH}_3\text{OH}$

- The CO<sub>2</sub> hydrogenation reaction :  $\text{CO}_2 + 3\text{H}_2 \leftrightarrow \text{CH}_3\text{OH} + \text{H}_2\text{O}$

- The operation condition: temperature = 254°C, pressure = 42 atm.

- The feed rate of CO = 785 kg/h, The feed rate of CO<sub>2</sub> = 2630 kg/h.,

The feed rate of H<sub>2</sub> = 7616 kg/h.

- Results : CO<sub>2</sub> conversion = 96, CO<sub>2</sub> conversion = 96, H<sub>2</sub> conversion = 98.6,

The methanol in the distillate product = 3278 kmol/h

These examples are further used to be a guideline and to ensure that the simulation from Aspen Plus V.9 is reliable for investigating the energy consumption for methanol as shown in 3.4.8.

3.4.6 Order to run program then compare the results in each process from simulation by aspen plus software such as yield with the results from relevant research. If found that the results is similar then look at the next result of energy.

3.4.7 Simulation of the methane steam reforming using reactor as RPlug with reference to the size of reactor, catalyst specifications, LHHW-type equations (Langmuir-Hinshelwood-Hougen-Watson), shown in (9), (10).

$$R_{MSR} = \frac{k_1 K_1 \left[ K_1 \frac{P_{CH_4} P_{CO}}{P_{H_2}^{2.5}} - P_{H_2}^{0.5} P_{CO} \right]}{\left[ 1 + K_{CO} P_{CO} + K_{H_2} P_{H_2} + K_{CH_4} P_{CH_4} + \frac{K_{H_2O} P_{H_2O}}{P_{H_2}} \right]^2} \quad (9)$$

$$R_{WGS} = \frac{k_0 P_{CO} P_{H_2O} \left[ 1 - \frac{P_{CO_2} P_{H_2}}{P_{CO} P_{H_2O} K_e} \right]}{\left[ 1 + K_{CO} P_{CO} + K_{H_2O} P_{H_2O} + K_{CO_2} P_{CO_2} + K_{H_2} P_{H_2} \right]^2} \quad (10)$$

And kinetic parameters from relevant research, [33] for filling kinetic factor, driving force expression and adsorption expression [34] at operating condition: temperature = 700°C, pressure = 1 atm (**Fig. 4**) to use as information to verify that the results from the simulation using RStoic can be accepted and then double check the heat of reaction obtained from simulation with experiment for more accurate.

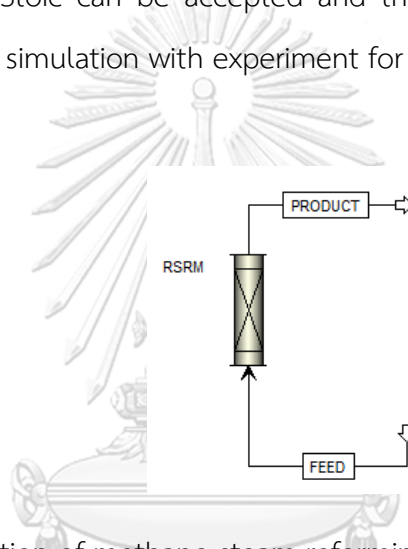


**Figure 4** The simulation of methane steam reforming in Aspen Plus using RPlug model block.

For the results of energy used to compare between process with CO<sub>2</sub> to be used as a co-reactant and process without CO<sub>2</sub>. To do so, it must be set basic the amount of feed flow rate into the reactor in the same flow rate. Therefore, it must be set basic the amount of feed flow rate into the reactor in the same flow rate in both processes consist of the reforming process and methanol synthesis. However, the results from the simulation, such as yield, of the process must be equal to the actual results from the experiment before adjusting the values.

There are 4 processes for simulation in this study which conclude 1. Methane steam reforming 2. Bi-reforming of methane 3. CO hydrogenation 4. CO/CO<sub>2</sub> hydrogenation. Shown in **Fig. 5-8**

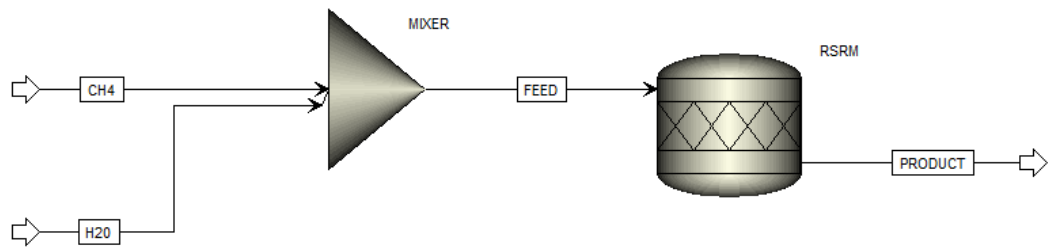


**Figure 5** The simulation of methane steam reforming in Aspen Plus using RStoic model block.

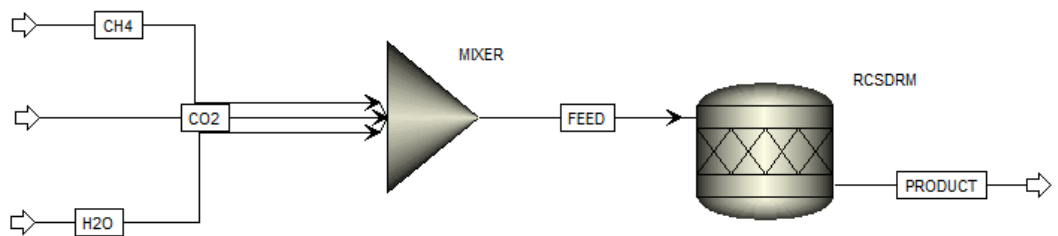


**Figure 6** The simulation of bi-reforming of methane in Aspen Plus using RStoic model block.

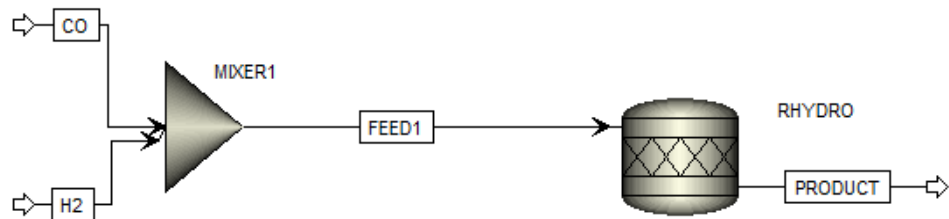


**Figure 7** The simulation of CO hydrogenation in Aspen Plus using RStoic model block.

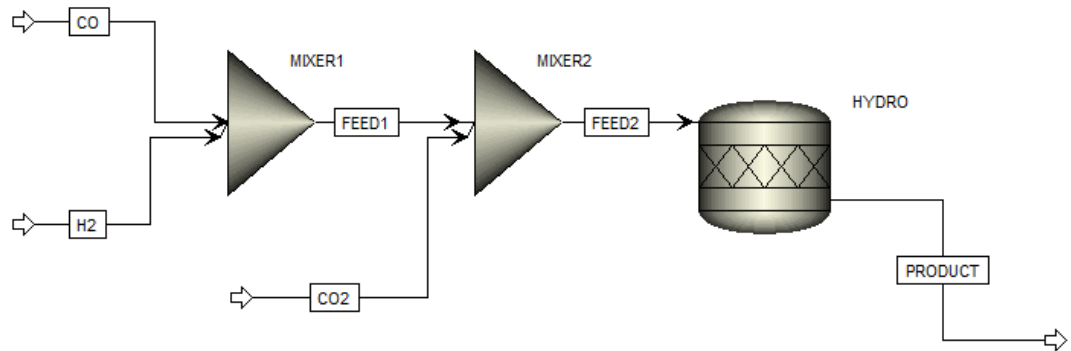


**Figure 8** The simulation of CO and CO<sub>2</sub> hydrogenation in Aspen Plus using RStoic model block.

3.4.8 For the simulation of CO, CO<sub>2</sub> and CO/CO<sub>2</sub> hydrogenation, the procedures as 3.4.1-3.4.6 are repeated by using the experimental results to determine mass and energy in each process.

## CHAPTER 4

### RESULTS AND DISCUSSION

#### 4.1 Catalyst characterization

The fundamental characteristics of heterogeneous catalysts are generally structuring with pores. Thus, porous structures, shapes, surface area, and pore size distribution are important properties in catalysis. The internal surface area is determined by using The  $N_2$  physisorption technique or BET based on the adsorption and condensation of  $N_2$  at the boiling point of liquid  $N_2$  of 77K at 1 atm. The adsorption of adsorbate is the category of physical adsorption (physisorption) or Van Der Waals adsorption that is an interaction between of atom adsorbed on a solid surface and molecules of adsorbate without a form of chemical bonding. Pore size distribution of CZA and CZA-Mn catalysts are shown in **Fig. 9**.

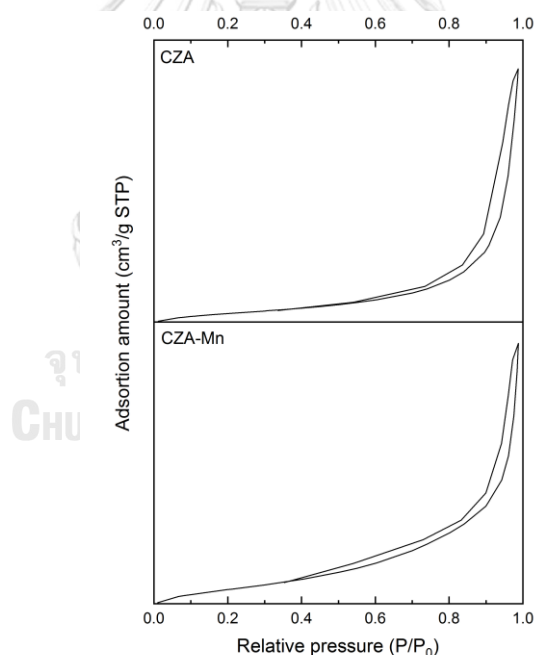


**Figure 9** The  $N_2$  adsorption-desorption isotherm at 77K, 1 atm of CZA and CZA-Mn catalysts after calcination.

The  $N_2$  adsorption-desorption isotherm plots reveal the presence of microporosity (2-50 nm) and two catalysts have the type IV isotherm indicating that capillary condensation of  $N_2$  can occur in this porous structure. In addition, these

isotherms show the type H3 hysteresis loop, which is unlimited adsorption with a high ratio of  $P/P_0$ . [35] On the surface with pore,  $N_2$  can diffuse inside. If  $N_2$  which adsorbed in the pore was known, it can be converted to pore volume and surface area. If the adsorbed molecular size of  $N_2$  which occupies an area of cross-sectional area  $0.162 \text{ nm}^2$ , the specific surface area is calculated by using Brunauer–Emmett–Teller, BET method with isotherm graph at a relative pressure ( $P/P_0$ ) in the range of 0.05-0.30. For the cumulative pore volume and radius of a pore, they are calculated by Barrett-Joyner-Halenda, BJH method with isotherm graph at a relative pressure ( $P/P_0$ ) in the range of 0.99 and the quantitative measurement of the surface area of CZA and CZA-Mn catalysts is shown in **Table 8**.

**Table 8** Textural properties and Reducibility result.

Samples	$S_{\text{BET}}^{\text{a}}$ ( $\text{m}^2/\text{g}$ )	$V_{\text{p}}^{\text{b}}$ ( $\text{cm}^3/\text{g}$ )	$D_{\text{BJH}}^{\text{c}}$ (nm)	$S_{\text{Cu}}$ ( $\text{m}^2/\text{g}$ )	$D_{\text{Cu}}$ (%)	d (nm)	Reducibility ( $^{\circ}\text{C}$ )	
							TR <sub>1</sub>	TR <sub>2</sub>
CZA	55	0.26	15.2	8.2	1.3	6.5	221.5	-
CZA-Mn	58	0.22	10.8	9.2	1.5	7.8	211.0	239.3

<sup>a</sup> Determined from BET method

<sup>b,c</sup> Determined from BJH desorption method

It is found that the Mn-modified CZA catalyst does not change the textural property significantly. CZA-Mn has higher BET surface area, pore volume and pore size are smaller than CZA catalyst. Determination of surface area is important because usual reaction occurred at the catalyst surface. Therefore, high surface area indicates well dispersion of the active site. If a catalyst has high surface area, pore size will be small because even though a high amount of pore is good, but very small pore can lead to a low diffusion capacity of reactant or product through the pore. Therefore, the pore structure and surface area have to be optimized.

CO-chemisorption technique was used for measuring the dispersion of active sites which can give information for well-dispersed catalyst by measuring the amount of active metal surface area (per gram of metal) and % metal dispersion as shown in **Table 8**. It is found that the Mn-modified CZA catalyst improves the dispersion of CuO species. Well-dispersed catalyst has occurred when active phases are monolayer dispersion on a support surface, or it has to be very tiny. A selective adsorbate is used for indicating active phase concentration, but it is not adsorbed on the support surface. This technique is effective with a heterogeneous catalyst because chemical adsorption is the physical adherence or bonding of ions and molecules (adsorbate) through the surface of another molecule. Adsorbent on the surface cannot be moved dependently and it has monolayer coverage. Therefore, we can calculate the amount of active site position from adsorbed gas measurement. Calculation of surface area used for activating the reaction is important for catalyst characterization. According to common principle, the active site of catalyst is directly proportional to the active site concentration which is ready for activating the reaction. The concentration of active metal sites is a function of metal loading and dispersion of active phase.  $D_{Cu}$  value is defined as the ratio of atom or molecule of the active site on the surface which ready for reaction activation.



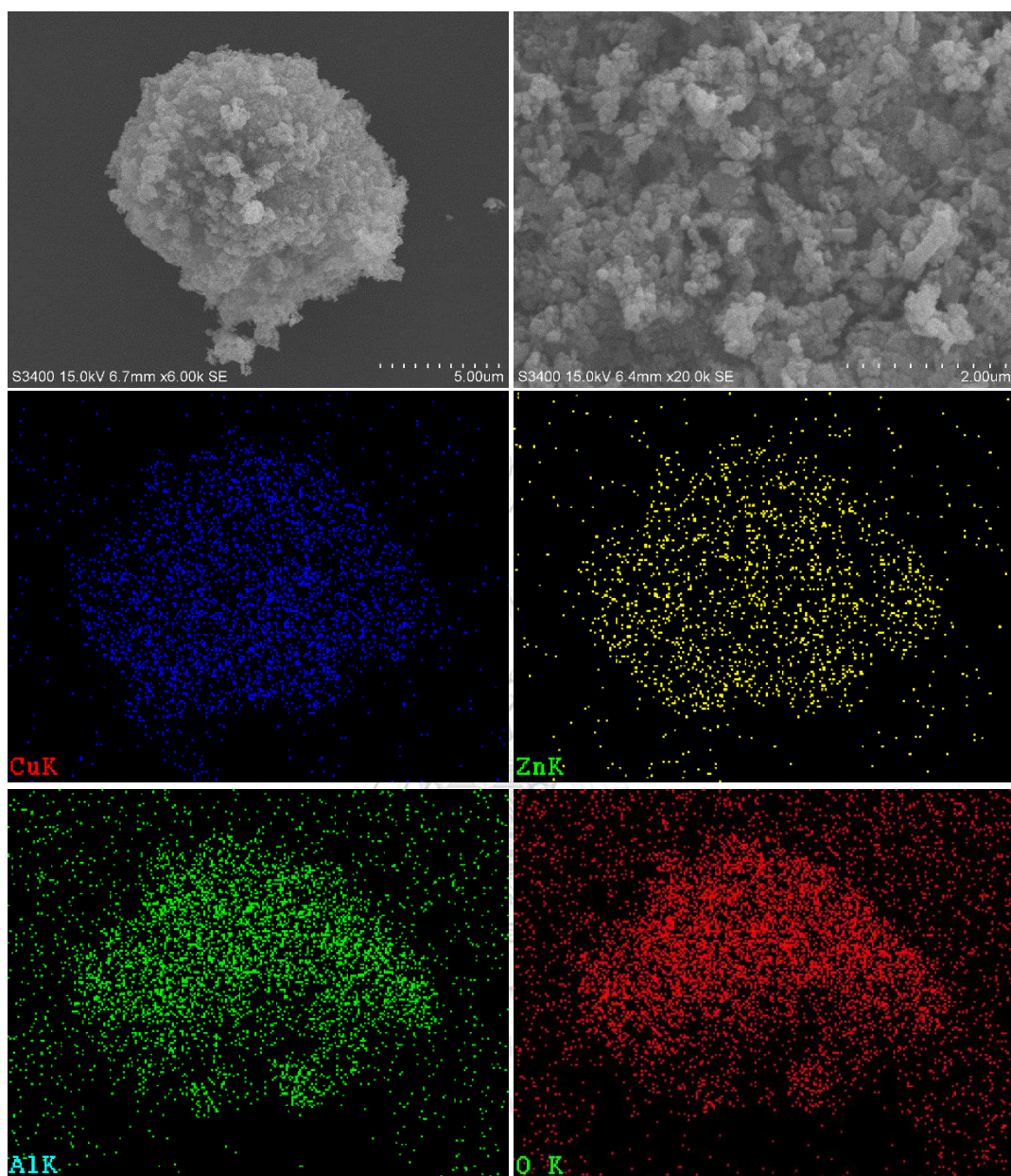


Figure 10 The SEM-EDX images of CZA catalyst.

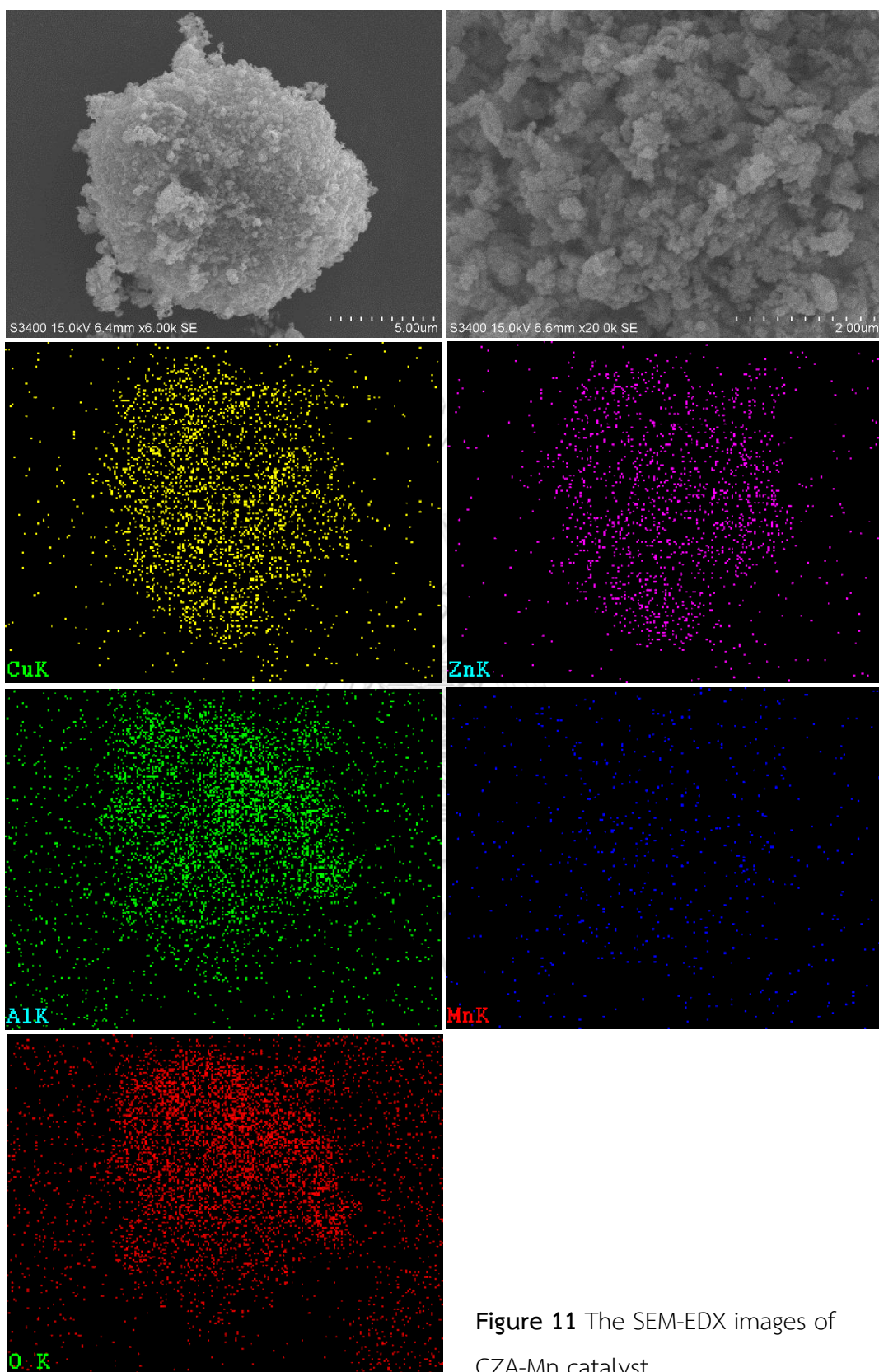


Figure 11 The SEM-EDX images of CZA-Mn catalyst.

The scanning electron microscope (SEM) was a common technique for studying the different surface morphology of two catalysts. The SEM images are shown in **Fig. 10** and **Fig. 11** indicating that the microstructure of granular catalysts are observed between the two CZA catalysts. The Mn-modified CZA catalyst also maintained its overall morphological characteristics or does not change the morphology significantly. SEM can be used with the EDX, which enables highly local resolved elemental analysis of the surfaces. Because of its excellent spatial resolution, it can show a detail of surface analysis at high imaging magnifications. The EDX images are also shown in **Fig. 10** and **Fig. 11** revealing that two catalysts are well-dispersed according to all elements distributed on the catalyst surface. The energy dispersive X-ray spectrometry, EDX and inductively coupled plasma mass spectrometry, ICP-MS can be used for determining the composition of any portion or analyze the catalyst elemental distribution. All values are summarized in **table 9** which present in percent weight of all elements. It was found that ICP-MS gave the actual metal composition, which was close to the expected composition of the catalyst, more than the EDX. This is due to the analysis of ICP-MS is for elemental in bulk catalyst, whereas the EDX is performed for elemental analysis in near surface layer of the catalysts.

**Table 9** Element distribution of CZA and CZA-Mn catalysts.

Elements	CZA			CZA-Mn		
	Wt% (Expect)	EDX (Wt%)	ICP-MS (Wt%)	Wt% (Expect)	EDX (Wt%)	ICP-MS (Wt%)
Cu	60.0	54.1	57.4	60.0	51.5	58.4
Zn	30.0	33.6	33.3	30.0	36.1	31.9
Al	10.0	12.3	9.3	10.0	10.9	9.7
Mn	-	-	-	0.1	1.5	0.1

Catalyst characterization analysis based on the basic properties of catalyst can classify into 3 types. Those are physical property, mechanical property, and chemical property. According to the catalyst characterization analysis above, it analyzes physical properties which are particle/crystallite size, surface area, pore volume, pore size, the concentration of active metal sites, and dispersion of active sites except for the EDX, ICP-MS and CO-Chemisorption which uses for analyzing the chemical composition that is a chemical property. For catalyst characterization analysis in case of the chemical properties, they consist of chemical structure, chemical composition, oxidation state, reduction behavior, acidity, and basicity. For this literature, the mechanical property is not included.

Study of structural properties of catalysts by using X-ray diffraction spectroscopy (XRD) is the oldest technique and most common technique for catalyst characterization. The XRD application of catalytic studying is used for indicating crystalline phases in the catalyst. For indicating phase composition of catalyst, it shows a diffraction pattern that is compared as a fingerprint for the specific character of each phase. In common, heterogeneous catalyst consists of many phases which cannot be identified. Catalyst phase can be identified by pattern comparison with diffraction pattern of a pure phase or the reference pattern database such as powder diffraction file, PDF and there is a program for phase identification of samples by comparing diffraction pattern with all possible pattern in all databases.

The preparation of CZA and CZA-Mn catalysts is based on the co-precipitation method for CO/CO<sub>2</sub> hydrogenation reaction. In this literature, XRD is used for active site and promoter phase identification.

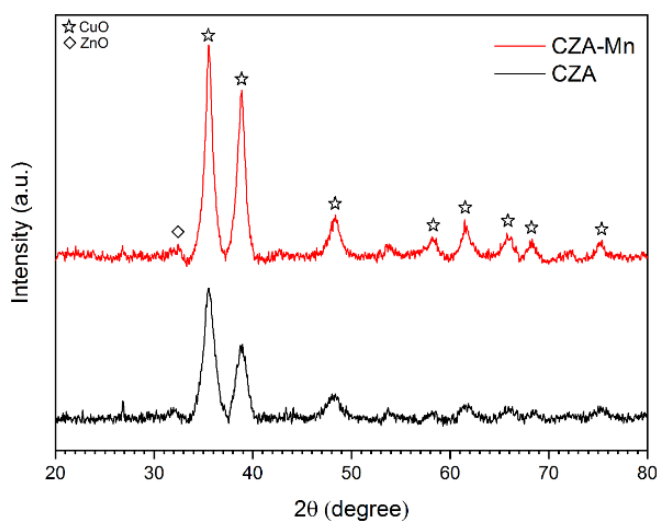


**Figure 12** XRD pattern of CZA and CZA-Mn catalysts after calcination. [21]

The XRD patterns of CZA and CZA-Mn catalysts after calcination at 300°C are shown in **Fig. 12** indicating the characteristic diffraction peaks consistent with the Bragg angles  $2\theta$  peaks of CuO phase over those catalysts at  $2\theta$  of 35.5°, 38.8°, 48.5°, 58.1°, 61.6°, 65.9°, 68.3°, and 75.2°. [17] Moreover, the peaks of CuO are visible as strong intensity peaks due to the highest copper loading amount (around 60 wt%) and the diffraction peak at  $2\theta$  of 31.9° [17] is attributed to ZnO phase. Meanwhile, absence of Al<sub>2</sub>O<sub>3</sub> features is found as a separate phase or disappearance of diffraction peaks with the broad reflections. [19] Generally, the diffraction peak characteristic of alumina appears at  $2\theta$  of 66.5° and 68.2°. [17] It is possible because a poorly crystallized aluminum existed in an amorphous state/character of the oxide precursors refers to a high dispersion and the particle sizes are too small or the relatively low calcination temperature. In fact, Al<sub>2</sub>O<sub>3</sub> acts as a structural spacer and in higher Al contents, catalysts tend to be more amorphous. [26] Generally, the addition of low Mn content at 0.1 wt% leads to a concern that XRD cannot show its unique diffraction pattern because XRD has limitations. Provided that material is present the amount greater than ~1 wt%. of the sample for mixed materials or sufficiently crystalline to diffract X-rays (crystallites larger than 3-5 nm). Generally, the peaks in the XRD pattern of manganese appeared at  $2\theta$  around 35.0°, 40.7°, 58.8°, 70.3°, and 73.9°. [36]

With the added Mn-modified CZA catalyst, the intensity of diffraction peaks is stronger and sharper than that with the sample without Mn suggesting higher CuO

crystallinity and larger CuO crystallite sizes. The obtained average particle/crystallite size of CuO nanoparticles in catalyst samples was calculated from the width at half maximum from XRD patterns by Scherrer equation, as recorded in **Table 8**. It can be seen that CZA-Mn catalyst exhibited relatively large CuO crystals compared with CZA catalyst. The crystallite size of CuO increased slightly from 6.5 nm to 7.8 nm. [3]

For X-ray photoelectron spectroscopy, it provides the information of the chemical composition and oxidation state of each element of catalyst samples. For catalysts studied in this literature, the components include Cu, Zn, Al, Mn, O, and C. Carbon will appear in hydrocarbon contaminant. A peak position will be determined by comparing binding energy and XPS data Tables and reference data because binding energy is the specific characteristic of each element. Therefore, XPS spectra can be used for the catalyst characterization.

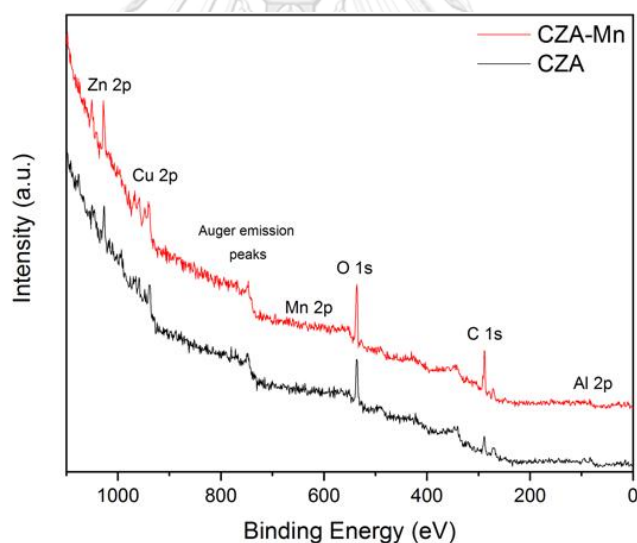


**Figure 13** XPS spectra of CZA and CZA-Mn catalysts.

From **Fig. 13**, it shows that photoelectron peaks for all elements, which are expected to have an Auger electron peak also occurred that is reducing ion bombardment by the release of Auger electron in the complex compound. The binding energy period occurred in a range of low to 250 eV peak for Al2p. It will be unresolved because it has a low separate value due to using a high energy scanning period. Moreover, the peak of C1s which cannot be identified specific properties of the complex compound

because the surface is not clean by sputtering or oxidation in XPS machine which C-peak always occurs. Hydrocarbon compound which may be adsorbed is because of pump oil or atmosphere.

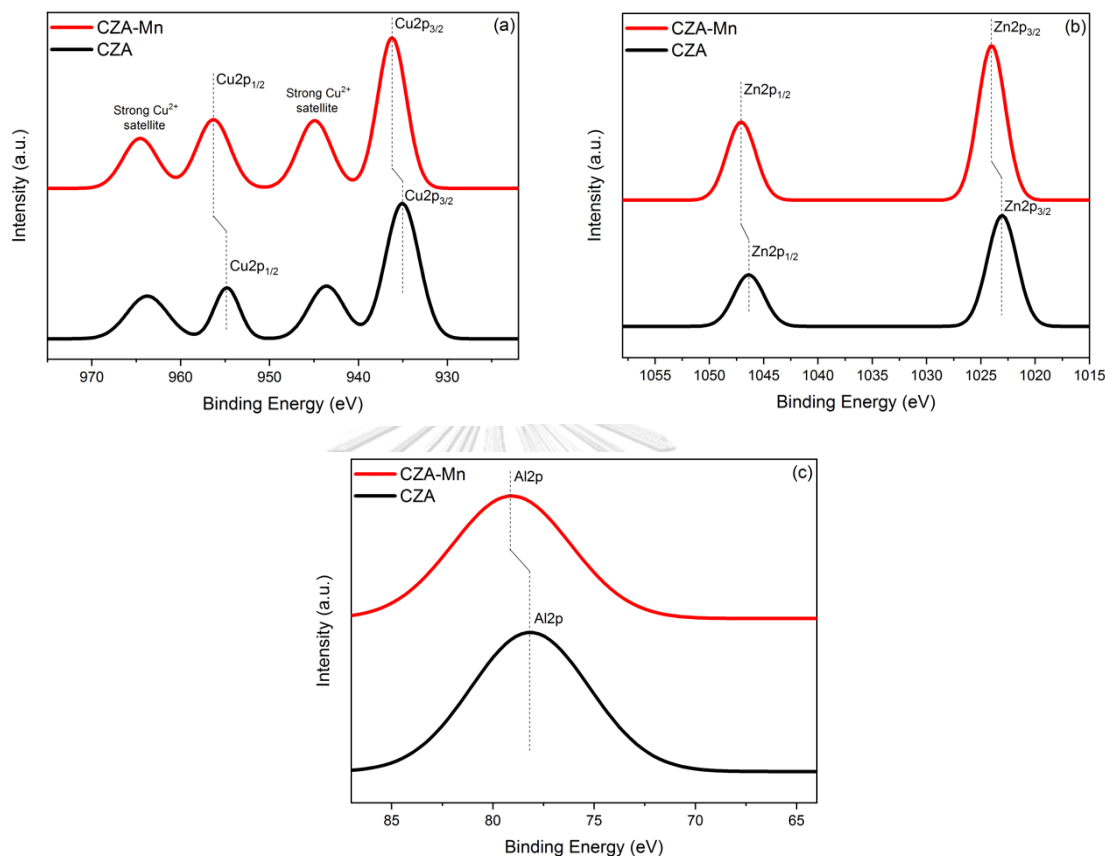


**Figure 14** XPS signals of CZA and CZA-Mn catalysts. (a) XPS of Cu species, b) XPS of Zn species and c) XPS of Al species

In the XPS spectra, the metal composition of Cu, Zn, and Al for two typical fresh catalysts are presented in **Fig. 14** and **Table 10**, the binding energy of  $\text{Cu}2p_{3/2}$  and  $\text{Cu}2p_{1/2}$  peaks are located around 935.4-936.2 eV and 954.8-956.3 eV, corresponding to copper species existing in the state of  $\text{Cu}^{2+}$  ions in oxide form (mostly CuO) which mainly acts as the active phase for mixed  $\text{CO}/\text{CO}_2$  hydrogenation reaction to methanol. Moreover, The XPS characterization also shows the intensity of the shake-up satellite at 943.6-944.9 eV and 963.8-964.5 eV attributed to  $\text{Cu}2p_{3/2}$  and  $\text{Cu}2p_{1/2}$ , respectively. It confirms that the presence of  $\text{Cu}^{2+}$  is only evident on the



catalyst surface. The satellite peaks are attributed to CuO charge transfer between metal and surrounding ligand. [37] The binding energy of Zn2p<sub>3/2</sub> and Zn2p<sub>1/2</sub> peaks are located around 1023.0-1024.0 eV and 1046.4-1047.1 eV indicating to the oxidation state of Zn<sup>2+</sup> in the form of ZnO on the surface of both catalysts. In addition, the XPS peaks at 78.1-79.1 eV are an indication of the presence of Al2p that can be assigned to the chemical state of Al<sup>3+</sup> in Al<sub>2</sub>O<sub>3</sub>.

However, it can be seen that all of the peaks related to Cu, Zn, and Al composition of Mn-modified CZA catalyst shift to the higher binding energy. The possible reason is the increasing binding energy due to an increase in oxidation state but in this case, there is no change of the oxidation state. The increasing binding energy can be related to the increasing electronegativity due to the added Mn-modified CZA catalyst.

**Table 10** XPS spectra of Cu, Zn, and Al species of CZA and CZA-Mn catalysts.

Samples	Binding energy (eV)				
	Cu <sup>2+</sup>		Zn <sup>2+</sup>		Al <sup>3+</sup>
	Cu2p <sub>3/2</sub>	Cu2p <sub>1/2</sub>	Zn2p <sub>3/2</sub>	Zn2p <sub>1/2</sub>	Al2p
CZA	935.4	954.8	1023.0	1046.4	78.1
CZA-Mn	936.2	956.3	1024.0	1047.1	79.1

The temperature-programmed reduction (TPR) is commonly used for monitoring the reduction behavior of the catalysts to determine what temperature should be used for catalyst activation.



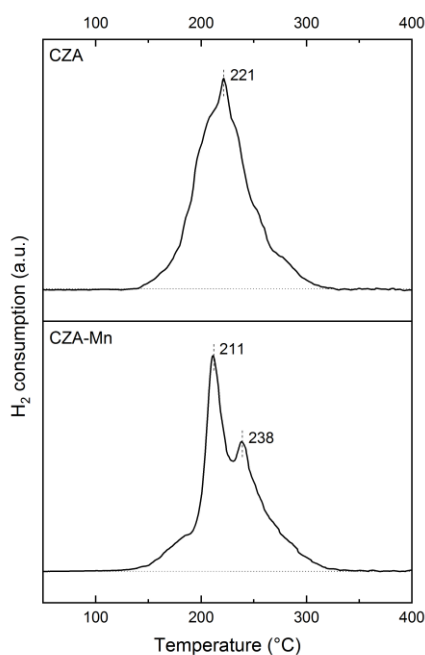


**Figure 15** H<sub>2</sub>-TPR profiles of CZA and CZA-Mn catalysts.

The TPR profiles/patterns of two catalysts are given in **Fig. 15**, two catalysts display an onset temperature at 120°C and the reduction temperature in the range between 210 and 240°C. However, these can also be referred as “the H<sub>2</sub> consumption”. It indicates only Cu<sup>2+</sup> species in CuO that is reduced below 300°C while the reduction of Zn, Al, and Mn in oxide form is impossible at these temperatures. The pure CZA catalyst shows the main sharp reduction peak (221°C) characteristics but CZA-Mn exhibits another small shoulder peak (238°C) while the TPR profile of the main peak (211°C) is stronger or shaper and more symmetrical. [9] These results suggested that the modification of this promoter with the added amount of Mn can facilitate the reduction of CuO. The position of the main reduction peak shifts to lower temperature from 221 to 211°C. It is affected to highly dispersion of Cu oxide species and is assigned to CuO exposed in support oxide structure due to interaction between CuO/Al<sub>2</sub>O<sub>3</sub>. The higher temperature shoulder peak is attributed to the stronger interaction between metal and support or the reduction of CuO in bigger nanoparticles which show higher CuO crystallinity and larger CuO average crystallite sizes with the Mn-modified. These results are in good agreement with those results obtained by XRD analysis measurement.

The NH<sub>3</sub>-TPD technique is performed to evaluate the surface acid properties of the catalysts. The acidity can be divided into three regions of the acid site with a

different range of  $\text{NH}_3$  desorption temperatures. As presented in **Fig. 16**, it shows regions of the weak acid sites (below  $300^\circ\text{C}$ ), the moderate acid sites ( $300\text{--}500^\circ\text{C}$ ), and the strong acid sites (above  $500^\circ\text{C}$ ).

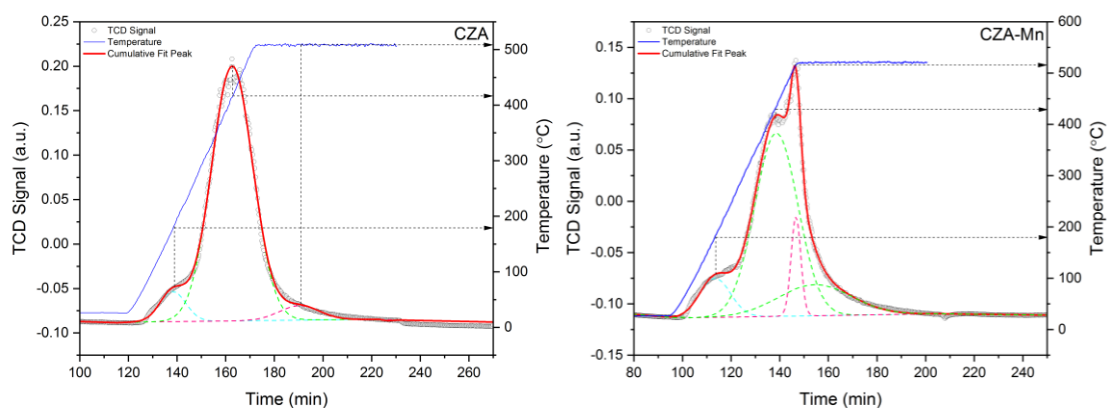


**Figure 16**  $\text{NH}_3$ -TPD profiles of CZA and CZA-Mn catalysts.

The weak acid sites were ascribed mainly occurred by  $\text{ZnO}$ . Besides, the moderate and strong acid sites were attributed to the interaction between  $\text{ZnO}$  and  $\text{Al}_2\text{O}_3$ , which referred to the Bronsted acid sites and Lewis acid sites, respectively. [38] The information about the acidity of the pre-reduce catalysts surfaces are shown in **table 11**.

**Table 11** The amounts of acid sites of CZA and CZA-Mn catalysts.

Samples	Number of acid sites ( $\mu\text{mol/g.cat}$ )			Number of total acid sites ( $\mu\text{mol/g.cat}$ )
	Weak	Moderate	Strong	
CZA	178.76	2240.27	137.01	2556.03
CZA-Mn	234.61	1987.07	170.47	2392.15

It can be ascribed to the moderate acid site that is dominant for two catalysts. For  $\text{CO}/\text{CO}_2$  hydrogenation reaction to methanol, many researchers proposed that the presence of the high intensity of the weak acid sites could improve the adsorption of  $\text{CO}/\text{CO}_2$  molecules and desorption of product as methanol. [16] This study reveals that the number of total acid sites of CZA is slightly higher than CZA-Mn. Moreover, the addition of Mn may be beneficial or promote the formation of methanol and

improve the catalytic performance related to the selectivity of product with the number of weak acid sites increased.

The information about the basicity of the pre-reduced catalyst is provided by CO<sub>2</sub>-TPD technique. As shown in **Fig. 17** and **table 12**,

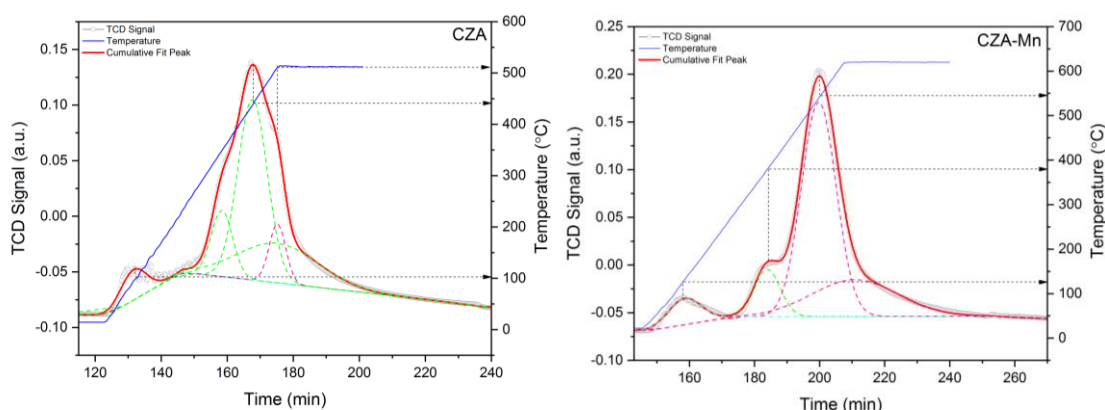


**Figure 17** CO<sub>2</sub>-TPD profiles of CZA and CZA-Mn catalysts.

Three regions in the desorption curves or the CO<sub>2</sub>-TPD profiles are assigned to the weak basic sites (below 300 °C) that were ascribed the CO/CO<sub>2</sub> adsorbed on surface OH groups saturating coordination vacancy (e.g. alumina), the moderate basic sites (300-500 °C) were related to the coordination of metal-oxygen bond as metal-oxide pairs, where metals are Zn, Al or Mn, and the strong basic sites (above 500 °C) were attributed to unsaturated O<sup>2-</sup> ions.

**Table 12** The amounts of basic sites of CZA and CZA-Mn catalysts.

Samples	Number of basic sites (μmol/g.cat)			Number of total basic sites (μmol/g.cat)
	Weak	Moderate	Strong	
CZA	168.43	715.80	244.07	1128.30
CZA-Mn	89.79	106.30	1054.54	1250.63

It is found that Lewis basic sites are dominant in the catalyst synthesis. For CO/CO<sub>2</sub> hydrogenation reaction to methanol, many researchers proposed that the distribution of basic sites was influenced importantly by the selectivity of CH<sub>3</sub>OH, and it increased linearly with the increase of the proportion of strong basic sites to the total basic sites. [11] This study shows a large amount of moderate basic sites, which

are observed on CZA catalyst, whereas the addition of Mn increases the number of total basic sites and can be ascribed to the strong basic site that was dominant for CZA-Mn catalyst. Moreover, it is found that the number of strong basic sites is about 4.3 times as high as that of the CZA catalyst, which is in good agreement with the selectivity of methanol.

## 4.2 Catalyst performance

In this study, the catalyst activity testing is performed at a GHSV of 24,000 ml/gcat/h in a fixed amount of total feed gas flow rate at 40 ml/min under different feed composition of  $\text{CO}_2/\text{H}_2 = 1:3$ ,  $\text{CO}/\text{H}_2 = 1:2$ , and  $\text{CO}/\text{CO}_2/\text{H}_2 = 1:1:2$  over 0.1 gram of copper/zinc-based catalysts prepared by co-precipitation method which are used for methanol synthesis via CO,  $\text{CO}_2$ , and  $\text{CO}/\text{CO}_2$  hydrogenation. The temperature of the reactor is kept constant at  $250^\circ\text{C}$  with atmospheric pressure. By reason of the target product is methanol, thus this study will be focused on the productivity, space time yield of methanol with different feeds gas which is tested for 5 hours on stream for CZA catalyst as shown in **Fig. 18**.

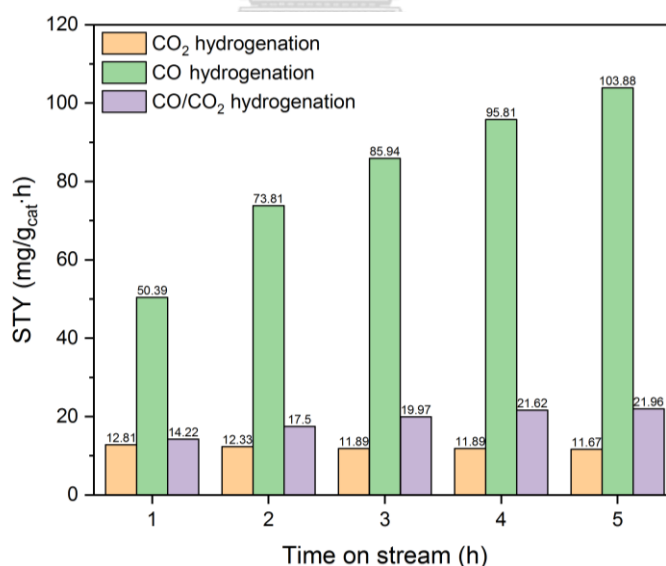


**Figure 18** Catalytic activity of CZA catalyst for hydrogenation to methanol with different feeds gas.

It is found that the productivity of methanol increased for the CO hydrogenation with increasing time on stream. This tends to increase steadily and the obtained result is similar to production with mixed  $\text{CO}/\text{CO}_2$  reactant co-feeds. The

hydrogenation of CO to methanol always produces the highest STY of methanol during the hydrogenation testing due to methanol is only product that can be obtained. The lowest methanol formation is produced from CO<sub>2</sub> hydrogenation and the methanol production slightly decreases because of the deactivation of the catalyst during 5-hour test period. In general, industrial methanol production by CO, CO<sub>2</sub>, and CO/CO<sub>2</sub> hydrogenation reaction was operated at high pressure (50-100 atm). In this study, CO is the major product observed for CO<sub>2</sub> hydrogenation. In parallel from methanol production, the reverse water gas shift (RWGs) is another main reaction in the CO<sub>2</sub> hydrogenation process, which has low CO<sub>2</sub> conversion and methanol selectivity at low pressure over the CZA catalysts. It can be concluded that methanol and CO are produced at the same intermediate species. For hydrogenation to methanol with different feed reaction, it seems to occur in different active sites of the catalyst surface for adsorption and dissociation of CO<sub>2</sub>, CO and H<sub>2</sub>. As known, CO hydrogenation proceeds through oxidized Cu sites, the surface was majorly covered by Cu<sup>+</sup>, and while the metallic Cu covered the surface is the main source of methanol which was CO<sub>2</sub>. On the other hand, CO<sub>2</sub> oxidized the surface metallic Cu to Cu<sup>+</sup> and CO and H<sub>2</sub> was easily reduce Cu<sup>+</sup> to metallic Cu. Likewise, H<sub>2</sub>O and CO<sub>2</sub> stabilized the Cu<sup>+</sup>. [1] It can be also found that the creation of the Cu-Zn active site by formation of the Cu-Zn alloy on the Cu surface, which is related to the role of ZnO was also ascribed to the stabilization of Cu<sup>+</sup>. [21] Therefore, amount of methanol which is synthesized from CO or CO<sub>2</sub> depended on the ratio of Cu<sup>+</sup>/Cu. In addition, higher CO<sub>2</sub> amount in the feed restrains the methanol production. With comparison of the activity in CO<sub>2</sub> hydrogenation and CO/CO<sub>2</sub> mixed feed, it shows more decrease in activity in CO<sub>2</sub>/H<sub>2</sub> feed compared to CO/CO<sub>2</sub>/H<sub>2</sub> feed. In fact, CO<sub>2</sub>/H<sub>2</sub> feed has more oxidizing properties than CO/CO<sub>2</sub>/H<sub>2</sub> feed because there is no CO to recover active copper sites and Cu<sup>+</sup>/Cu<sup>0</sup> cycles are disrupted. Therefore, the CO hydrogenation is decreased. [1] Next, the results of effect of Mn content in CZA-Mn catalyst on methanol synthesis under the same condition and time on stream are shown in **Fig. 19**.

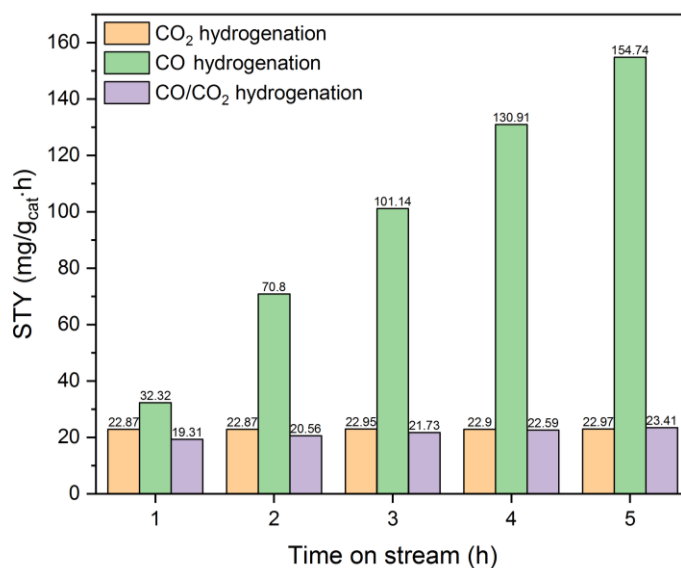


**Figure 19** Catalytic activity of CZA-Mn catalyst for hydrogenation to methanol with different feeds gas.

It is shown that adding Mn-modified on CZA catalyst can increase catalyst performance having higher quantity of methanol production in different feed mixture. Moreover, it can also improve the selectivity to methanol. Tendency for methanol production is CO hydrogenation > CO/CO<sub>2</sub> hydrogenation > CO<sub>2</sub> hydrogenation which is similar to methanol production by using CZA catalyst. From the results of catalyst characterization, it confirms that adding Mn promoter can increase catalytic activity by increasing of Cu dispersion obtained from CO-chemisorption technique suggesting that the specific activity with the metallic copper surface area increased. Meanwhile, another important factor is basicity or the nature or number of basic sites by CO<sub>2</sub>-TPD technique. It is found that the strong basic site, strong CO<sub>2</sub> adsorption, which is dominated for CZA-Mn catalyst is in a good agreement with the selectivity of methanol. Generally, the intermediate species were adsorbed on strongly basic sites preferred to be hydrogenated into methanol but it should be known that strong adsorption of CO<sub>2</sub> was not sufficient and stronger adsorption, dissociative adsorption and finally spill-over of hydrogen species on the surface were necessary. It is found that when adding Mn-modification, the position of the main reduction peak shifts to lower temperature from H<sub>2</sub>-TPR results indicating well-disperse of CuO species. Therefore, it does not only help to accelerate the dissociation of hydrogen and improves spillover effect, but also likely generates

oxygen vacancies. Due to strong basic sites prefer to be hydrogenated into methanol. Therefore, acidity or the nature or number of acid sites relate to the high selectivity of methanol with the number of weak acid sites increase which is related to  $\text{NH}_3$ -TPD results showing that the amount of weak basic sites of CZA-Mn is more than CZA. Next, the results of effect of  $\text{CO}_2/\text{H}_2$  and  $\text{CO}/\text{CO}_2/\text{H}_2$  in hydrogenation to methanol over CZA-Mn are shown in **Fig. 20**.

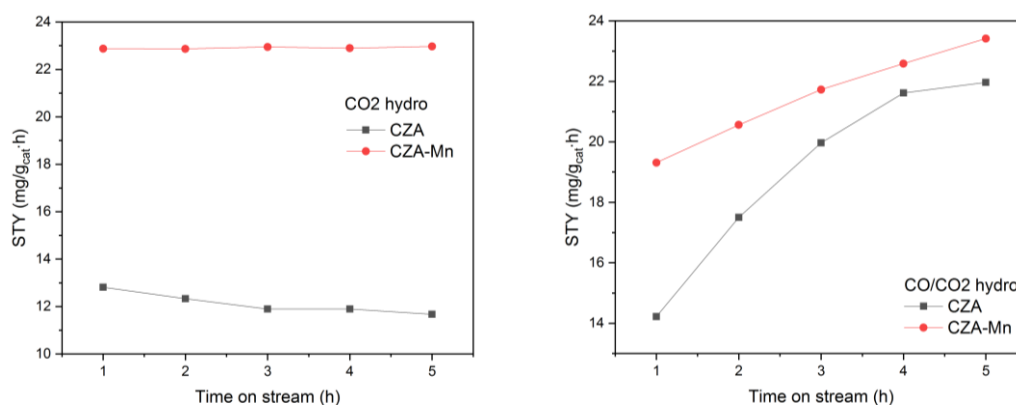


**Figure 20** Catalytic activity of CZA and CZA-Mn catalyst for  $\text{CO}_2$  and  $\text{CO}/\text{CO}_2$  hydrogenation to methanol.

However, the increasing of Mn-promoter occurs to the hydrogenation of  $\text{CO}_2$  become dominant. It is found that CZA-Mn in  $\text{CO}_2/\text{H}_2$  feed is more stable and have reached the steady-state period with a faster rate than the observed rate in the  $\text{CO}/\text{CO}_2/\text{H}_2$  feed. Probably in the latter feed, strong adsorption of  $\text{CO}_2$  on the reduced copper decreases the CO hydrogenation gradually and reaches steady-state period later than  $\text{CO}_2/\text{H}_2$  feed. [1]

### 4.3 Energy consumption in methanol synthesis

The overall energy consumption and energy consumption to produce 1 mol of methanol in methanol synthesis in hydrogenation with different reactant feed gas containing  $\text{CO}_2/\text{H}_2$ ,  $\text{CO}/\text{H}_2$ ,  $\text{CO}/\text{CO}_2/\text{H}_2$  are evaluated by Aspen Plus V9 simulation. At first, it starts by specify the components, the feed rate of each component, temperature and pressure of the feed line, and the operating condition of reactor in each process according to results of a relevant researches for methane steam

reforming, bi-reforming, CO and CO/CO<sub>2</sub> hydrogenation, respectively. As shown in APPENDIX.G for using as guideline or example for simulation, it can be applied to catalyst performance testing. In this study, it uses Redlich-Kwong-Soave-Boston-Mathias (RKS-BM) model. The reactor used in the simulation is RStoic.

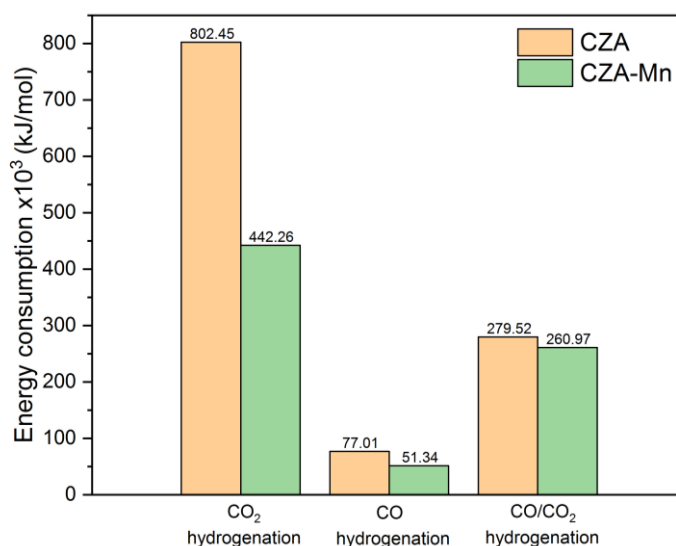


**Figure 21** The energy consumption to produce 1 mol of methanol for hydrogenation with different feeds gas.

From **Fig. 21**, it is shown that tendency for using energy consumption to produce 1 mol of methanol is in the order of CO<sub>2</sub> hydrogenation > CO/CO<sub>2</sub> hydrogenation > CO hydrogenation. It is found that adding Mn promoter can decrease energy consumption for 1 mol of methanol production for 44.8%, 33.3% and 6.6% for CO<sub>2</sub>, CO and CO/CO<sub>2</sub> hydrogenation, respectively. Moreover, the CO/CO<sub>2</sub> feed with composition feed of 1:1 through hydrogenation reaction increases energy consumption for 1 mol of methanol production for 3.6 and 5.1 times of energy consumption for hydrogenation of CO using CZA and CZA-Mn, respectively. Therefore, using CO<sub>2</sub> as co-reactant or reactant, the overall energy consumption and energy consumption for 1 mol methanol production will be increased. The purpose of using CO<sub>2</sub> to be another reactant or co-feed is practical with the trade off in the higher energy consumption due to the temperature dependence of the heat capacity which is used to calculate gases properties, generally the use of the ideal gas heat capacity rather than the actual heat capacity. The ideal gas heat capacity of



each gas is different depending on the function of temperature (without pressure). The ideal gas heat capacity is increased toward an upper limit. Even though the ideal gas heat capacity can be applied for real gases correctly and accurately especially in low pressure. In this study, it indicated that energy of system depends on the enthalpy change of the products as they are heated from 298.15 K (25°C) to 523.15 K (250°C) and also depends on the amount of the species in the products stream such as CO<sub>2</sub> hydrogenation with feed ratio of CO<sub>2</sub> to H<sub>2</sub> = 1:3 as shown in APPENDIX.H. H<sub>2</sub> which is used as reactant is applied in the small amount, remaining high. Therefore, energy which is used for heating will be also high. Moreover, the ratio between the heat capacities of gases in the ideal-gas state of CO<sub>2</sub> and CO is 1.69. If heat is supplied to the reactor, products will reach a temperature of 523.15 K (250°C) from 298.15 K (25°C). The overall energy consumption is shown in **Table 13**.

**Table 13** The overall energy consumption for hydrogenation with different feeds gas.

Samples	Total energy consumption, x10 <sup>-6</sup> kW		
	CO <sub>2</sub> hydrogenation	CO hydrogenation	CO/CO <sub>2</sub> hydrogenation
CZA	4.82	4.47	4.63
CZA-Mn	4.96	4.43	4.59

It is shown that energy consumption is inversely proportional to quantity of methanol synthesis. In common, heat of reaction for hydrogenation is always exothermic reaction, referred to reaction in which heat was given from the system to the surrounding. Products were more stable than reactant. Exothermic reaction shows as negative value as the same with heat duty value in APPENDIX.G (table G.9) but this study is found that heat duty is (+) positive because there is low methanol production which has low CO<sub>2</sub> and CO conversion in all processes. Heat duty with (+) positive sign may indicate that if the requirement for methanol production following the experiment of catalyst performance under operating condition at 250°C under atmospheric pressure. The temperature has to be maintained and ideally, heater, as utility, should be equipped to enable all the important parameters to be monitored and controlled because it is endothermic process.

## CHAPTER 5

### CONCLUSIONS AND RECOMMENDATION

The methanol synthesis in hydrogenation with different feed composition of  $\text{CO}_2/\text{H}_2$ ,  $\text{CO}/\text{H}_2$ , and  $\text{CO}/\text{CO}_2/\text{H}_2$  over  $\text{Cu}/\text{ZnO}/\text{Al}_2\text{O}_3$  catalysts at  $250^\circ\text{C}$  under atmospheric pressure and the effect of addition manganese in catalytic performance are investigated. According to the result for catalytic activity, adding manganese as modifier increases catalytic activity for methanol synthesis as observed by increasing of methanol STY that is corresponding with the results of catalyst characterization. For physical properties, manganese added on the catalyst can improve dispersion of CuO species, which can facilitate the dissociation of hydrogen and improve spillover. For chemical properties, adding manganese not only facilitate the reduction of CuO, but also enhance the number of total basic sites and the strong adsorption of  $\text{CO}_2$  due to the shift of moderate basic site to strong basic site and increases the weak acid sites that help to improve the selectivity of methanol.

The overall energy consumption and energy consumption of 1 mole of methanol production in the hydrogenation processes are investigated with Aspen plus V.9 software. The simulation results have shown that overall energy consumption and energy consumption for 1 mol methanol production is increased by applied  $\text{CO}_2$  as co-reactant or reactant through hydrogenation reaction. Tendency of methanol production is  $\text{CO}_2$  hydrogenation >  $\text{CO}/\text{CO}_2$  hydrogenation >  $\text{CO}$  hydrogenation, which is opposite with methanol production quantity. Therefore, the results indicate that energy consumption after adding manganese as modifier for 1 mol of methanol production decreases by 44.8%, 33.3% and 6.6% for  $\text{CO}_2$ ,  $\text{CO}$  and  $\text{CO}/\text{CO}_2$  hydrogenation, respectively. Furthermore,  $\text{CO}/\text{CO}_2/\text{H}_2$  feed with 1:1:2 composition can increase the energy consumption of 1 mol-methanol synthesis to 3.6 and 5.1 times of  $\text{CO}$  hydrogenation.

### Recommendations

(1) Effect of feed composition of CO/CO<sub>2</sub>/H<sub>2</sub> can be studied by various composition of reactant feed for finding optimal feed which can produce the highest methanol quantity.

(2) Stability of catalysts can be studied by increasing time of reaction to be longer for studying deactivation of catalyst by TPO technique.

(3) Mn content can be studied for CZA catalyst for increasing of catalyst activity.

(4) Behaviors of spent catalysts can be studied for investigating change in basic properties of catalyst after hydrogenation process.

(5) For keeping reduce catalyst & spent catalyst, they should not be touched by air and using them for catalyst characterization analysis immediately because Cu have high oxidation properties.



## APPENDIX

### APPENDIX.A CALCULATION OF CATALYST PERFORMANCE

A.1 CO<sub>2</sub> conversion

$$\text{CO}_2 \text{ conversion (mol\%)} = \frac{\text{CO}_{2,in}}{\text{CO}_{2,in} - \text{CO}_{2,out}} \times 100$$

A.2 CO conversion

$$\text{CO conversion (mol\%)} = \frac{\text{CO}_{in}}{\text{CO}_{in} - \text{CO}_{out}} \times 100$$

A.3 Methanol selectivity

$$S_{\text{MeOH}} \text{ (mol\%)} = \frac{\text{mole of Methanol}}{\text{All product}} \times 100$$

A.4 Space time yield

$$\text{STY (mg/g}_{\text{cat}}\text{h)} = \frac{\text{weight of produced alcohol}}{\text{catalyst weight} \times \text{time}}$$

**Table A.4.1** Space time yield of methanol and CO on CZA catalyst of CO<sub>2</sub> hydrogenation.

Time (h)	STY of methanol (mg/g <sub>cat</sub> h)	STY of CO (mg/g <sub>cat</sub> h)
0	-	-
1	12.81	4828.02
2	12.33	4796.68
3	11.89	4701.01
4	11.89	4651.85
5	11.67	4673.54

**Table A.4.2** Space time yield of methanol and CO on CZA-Mn catalyst of CO<sub>2</sub> hydrogenation.

Time (h)	STY of methanol (mg/g <sub>cat</sub> h)	STY of CO (mg/g <sub>cat</sub> h)
0	-	-
1	22.87	8300.50
2	22.87	8034.70
3	22.95	7951.61
4	22.90	7927.34
5	22.97	7885.38

**Table A.4.3** Space time yield of methanol on CZA catalyst of CO hydrogenation.

Time (h)	STY of methanol (mg/g <sub>cat</sub> h)
0	-
1	50.39
2	73.81
3	85.94
4	95.81
5	103.88

**Table A.4.4** Space time yield of methanol on CZA-Mn catalyst of CO hydrogenation.

Time (h)	STY of mathanol (mg/g <sub>cat</sub> h)
0	-
1	32.32
2	70.80
3	101.14
4	130.91
5	154.74

**Table A.4.5** Space time yield of methanol on CZA catalyst of CO/CO<sub>2</sub> hydrogenation.

Time (h)	STY of Methanol (mg/g <sub>cat</sub> h)
0	-
1	14.22
2	17.50
3	19.97
4	21.62
5	21.96

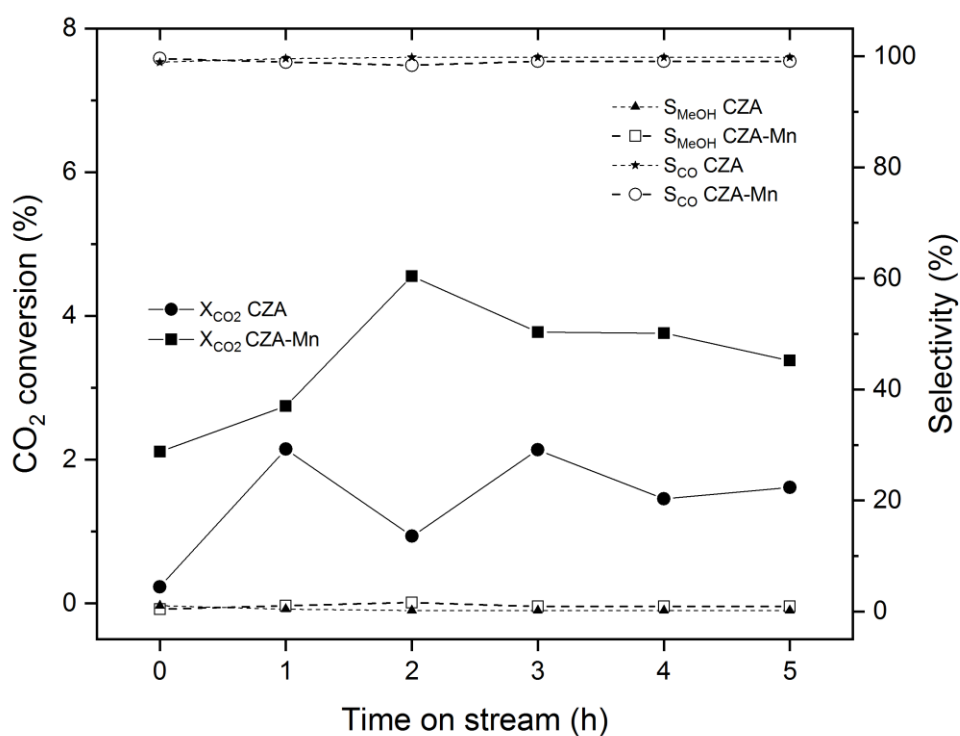
**Table A.4.6** Space time yield of methanol on CZA-Mn catalyst of CO/CO<sub>2</sub> hydrogenation.

Time (h)	STY of Methanol (mg/g <sub>cat</sub> h)
0	-
1	19.31
2	20.56
3	21.73
4	22.59
5	23.41

## A.5 Catalytic properties of CZA and CZA-Mn catalysts

**Table A.5.1** CO and CO<sub>2</sub> conversion and product selectivity obtained from CZA and CZA-Mn catalysts for the hydrogenation at 5 h-reaction time.

Catalyst	CO <sub>2</sub> hydrogenation			CO hydrogenation	
	CO <sub>2</sub> conversion (mol%)	CO Selectivity (mol%)	Methanol Selectivity (mol%)	CO conversion (mol%)	Methanol Selectivity (mol%)
CZA	1.6	99	1	1.6	100.0
CZA-Mn	3.4	98	2	2.5	100.0

**Figure A.5.1** Catalytic properties of CZA and CZA-Mn catalysts at 250°C, 1 atm for CO<sub>2</sub> hydrogenation.



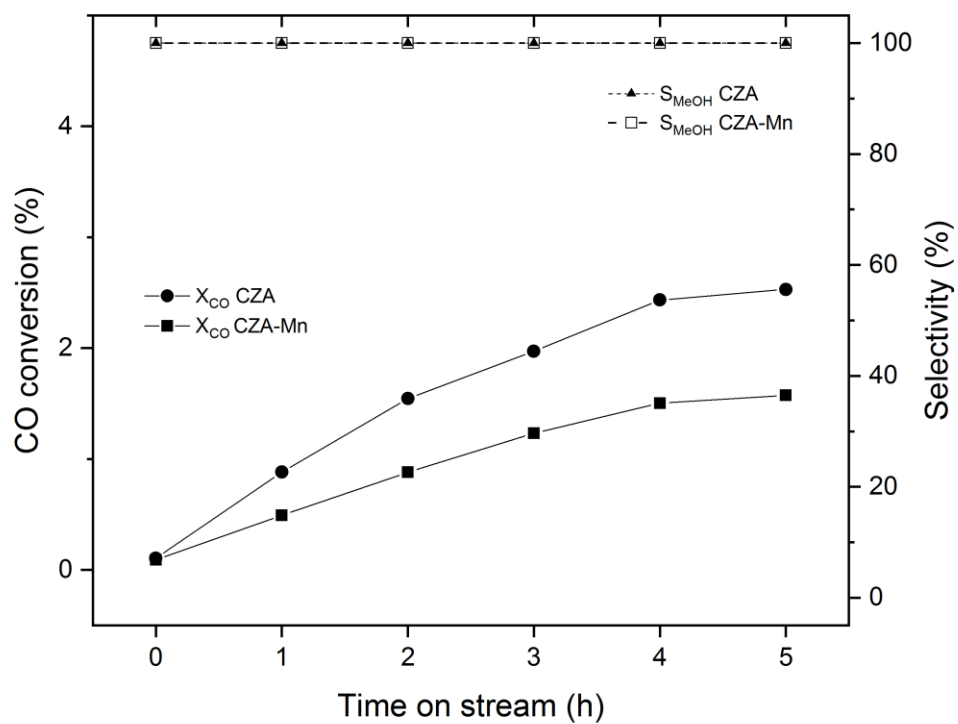


Figure A.5.2 Catalytic properties of CZA and CZA-Mn catalysts at 250°C, 1 atm for CO hydrogenation.



## APPENDIX.B CALCULATION OF CRYSTALLITE SIZE

## B1. The Scherrer equation

$$D = \frac{K\lambda}{\beta \cos\theta}$$

Where

D = Volume average crystallite size, (Å)

K = a constant, (0.9)

$\lambda$  = X-ray wavelength, CuK $\alpha$  radiation, ( $\lambda$  = 1.5406 Å)

$\beta$  = the peak width, (radian)

$\theta$  = the angle between the beam and the normal on the reflection plane,  
(degree)



## APPENDIX.C CALBRATION

## C.1 CO calibration

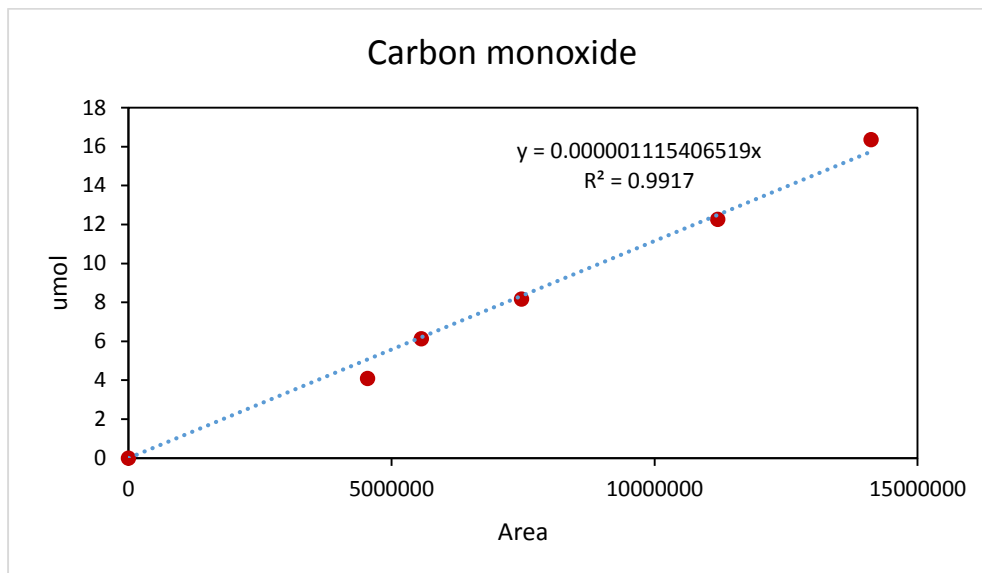
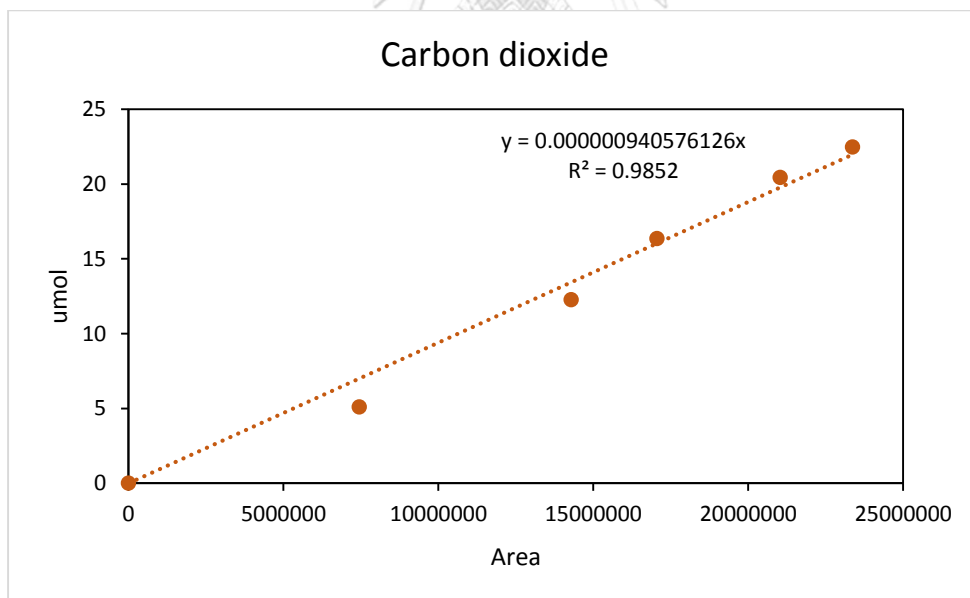


Figure C.1.1 The calibration of CO.

C.2 CO<sub>2</sub> calibrationFigure C.2.1 The calibration of CO<sub>2</sub>.

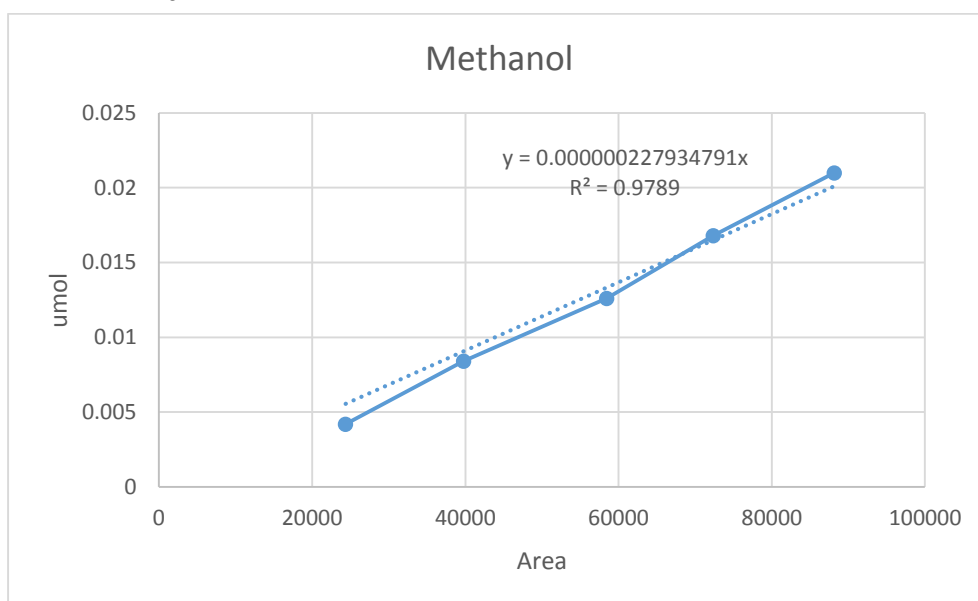
C.3 CH<sub>3</sub>OH calibration

Figure C.3.1 The calibration of methanol.



## APPENDIX.D X-RAY PHOTOELECTRON SPECTROSCOPY

## D.1 Chemical species of CZA catalyst.

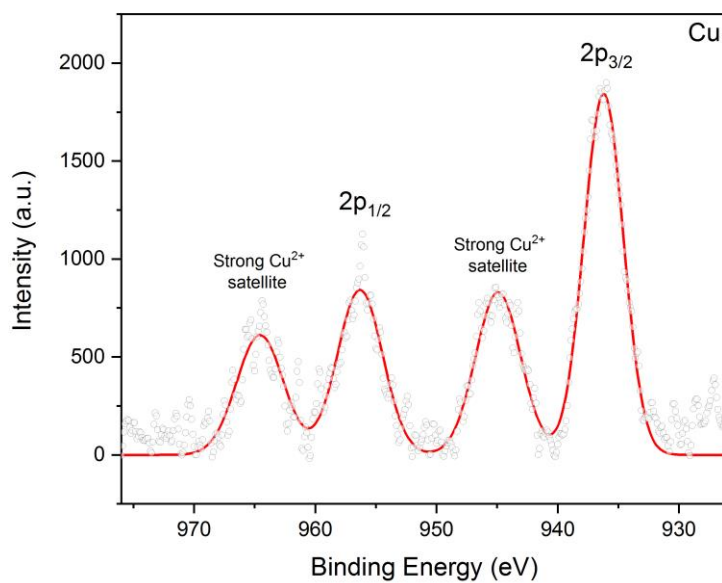


Figure D.1.1 XPS signals of Cu species.

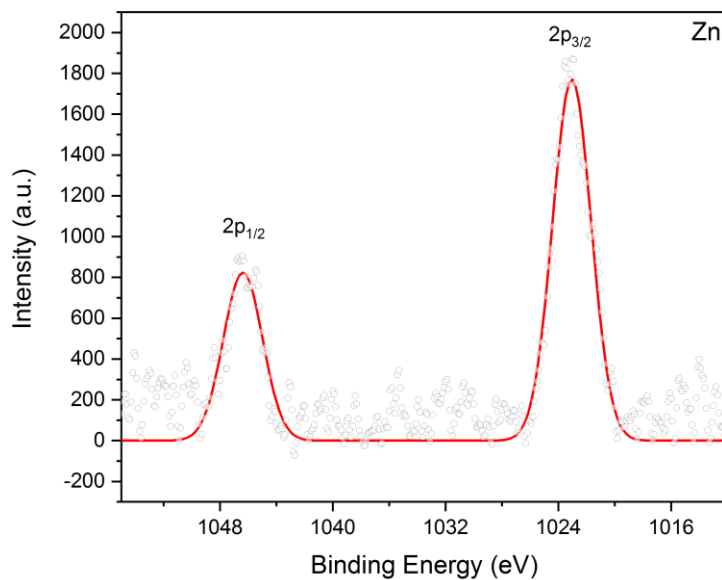


Figure D.1.2 XPS signals of Zn species.

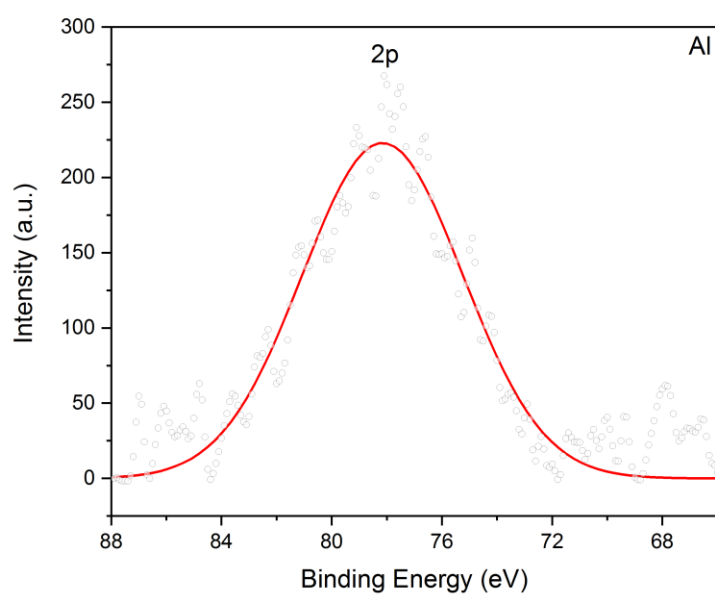


Figure D.1.3 XPS signals of Zn species.

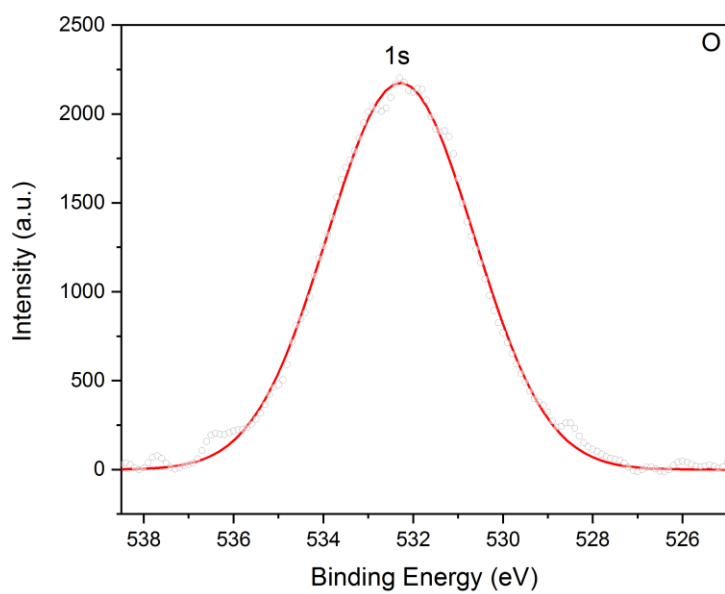


Figure D.1.4 XPS signals of O species.

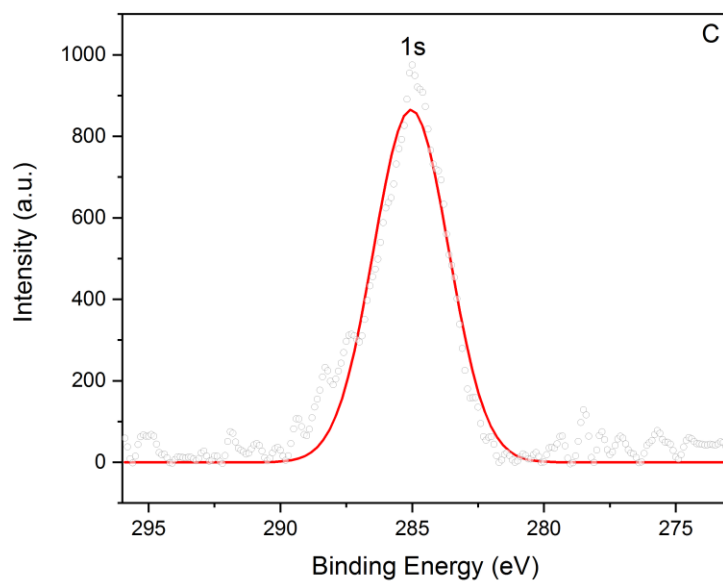


Figure D.1.5 XPS signals of C species.

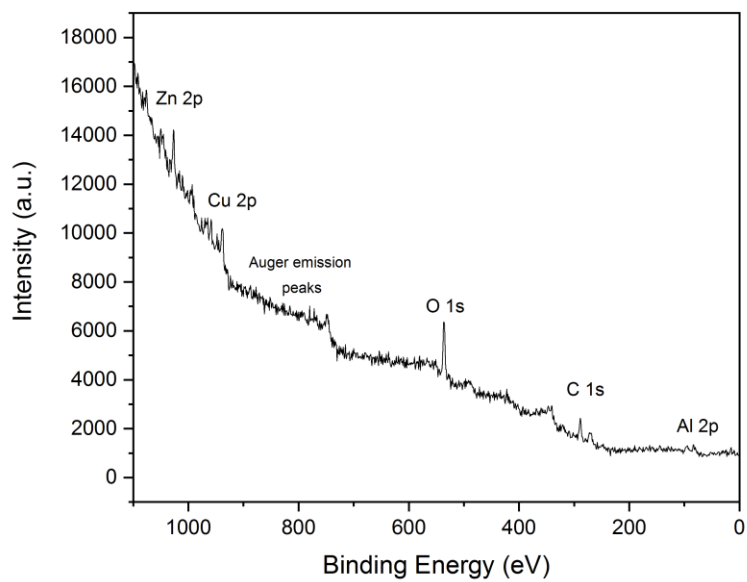


Figure D.1.6 XPS spectra of CZA catalyst.

## D.2 Chemical species of CZA-Mn catalyst

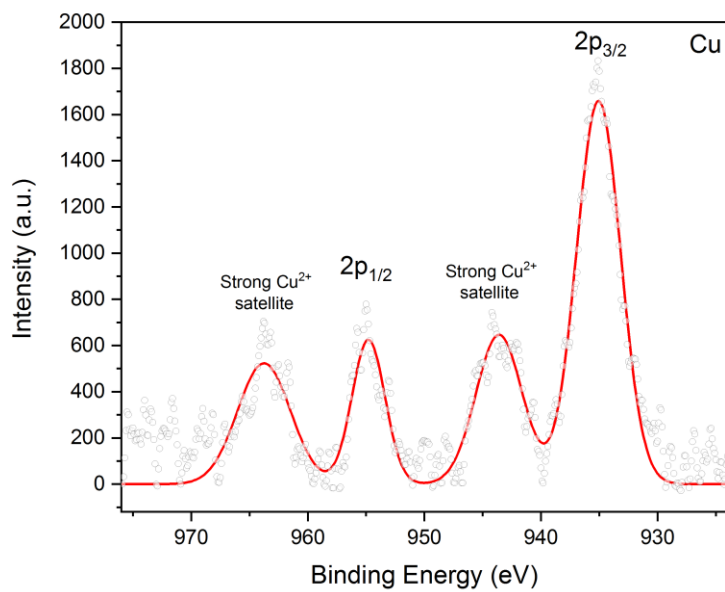


Figure D.2.1 XPS signals of Cu species.

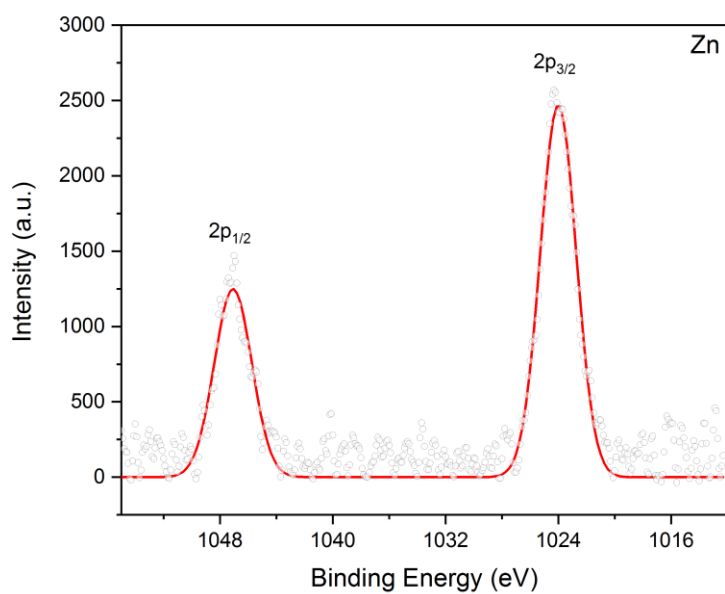


Figure D.2.2 XPS signals of Zn species.



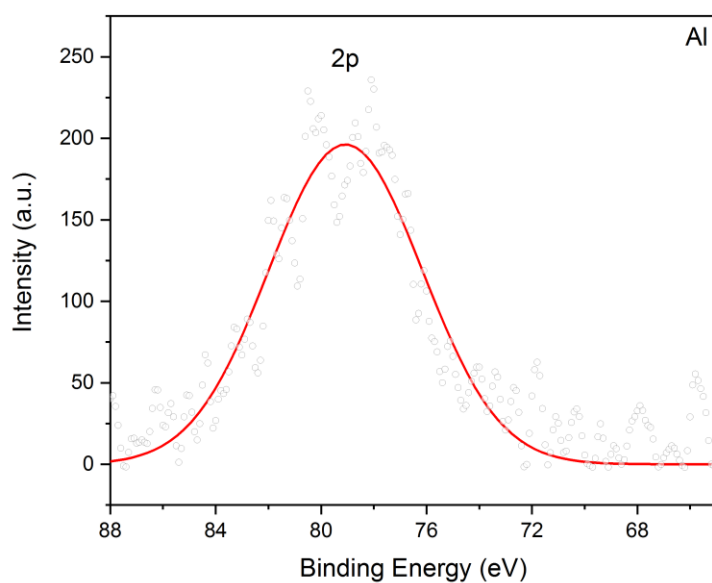


Figure D.2.3 XPS signals of Al species.

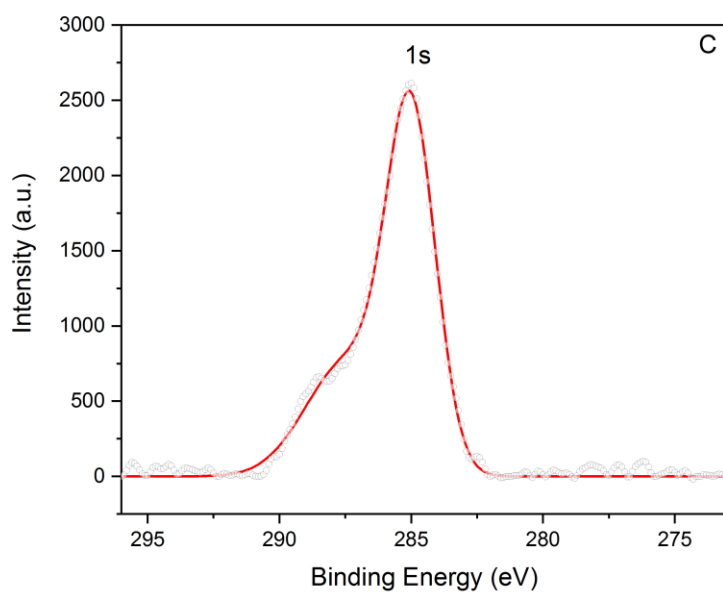


Figure D.2.4 XPS signals of C species.

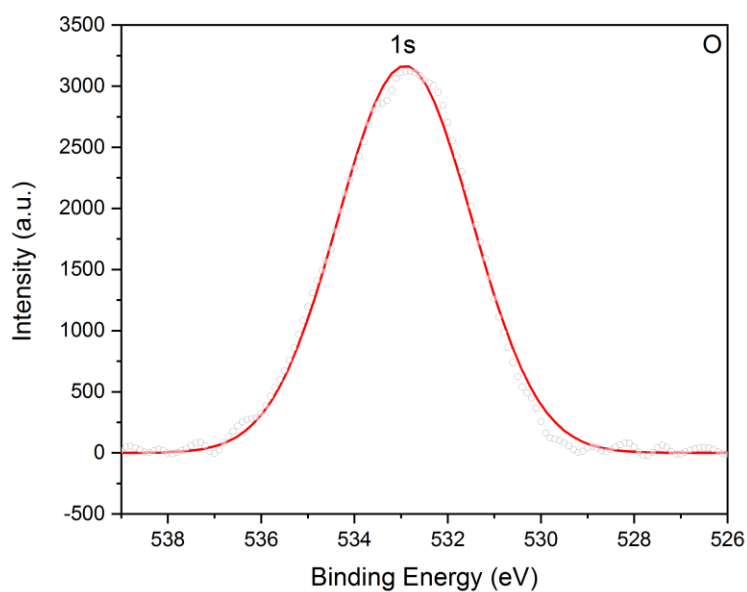


Figure D.2.5 XPS signals of O species.

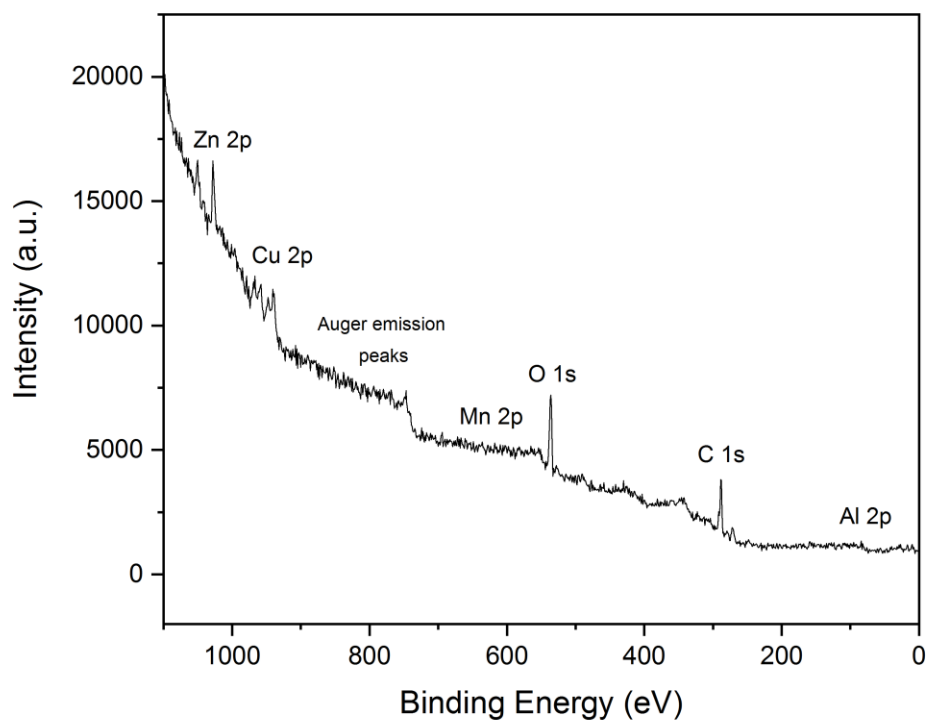


Figure D.2.6 XPS spectra of CZA-Mn catalyst.

## APPENDIX.E CALCULATING VOLUME CHEMISORBED

### E.1 Calculation volume chemisorbed in CO-Chemisorption

$$V_{ads}(cm^3) = \frac{V_{inj}}{m} \times \sum_{i=1}^n \left(1 - \frac{A_i}{A_f}\right)$$

Where:

$V_{inj}$  = volume injected,  $cm^3$

$m$  = mass of sample, g

$A_i$  = area of peak i

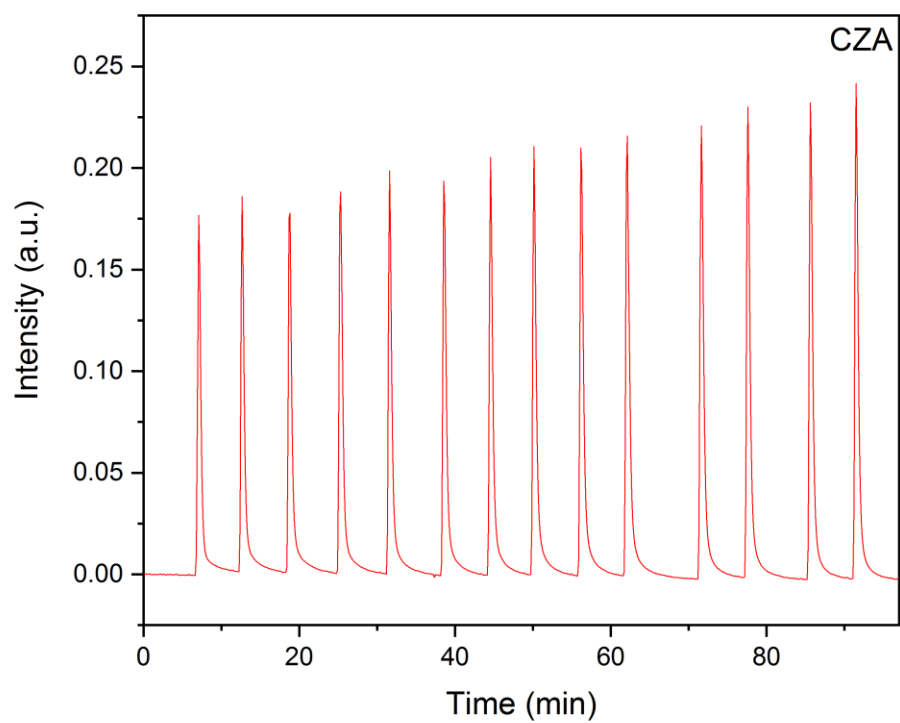
$A_f$  = area of last peak

**Table E.1.1** Area of each peak of CZA catalyst adsorbed CO gas.

Peak Number	Area
1	0.09662
2	0.10361
3	0.11014
4	0.1125
5	0.11562
6	0.1172
7	0.12026
8	0.12523
9	0.13045
10	0.13692
11	0.13357
12	0.13954
13	0.13798
14	0.13944

**Table E.1.2** Area of each peak of CZA-Mn catalyst adsorbed CO gas.

Peak Number	Area
1	0.06016
2	0.08415
3	0.07404
4	0.11134
5	0.13252
6	0.11918
7	0.12673

**Figure E.1.1** CO-Chemisorption of CZA catalyst.

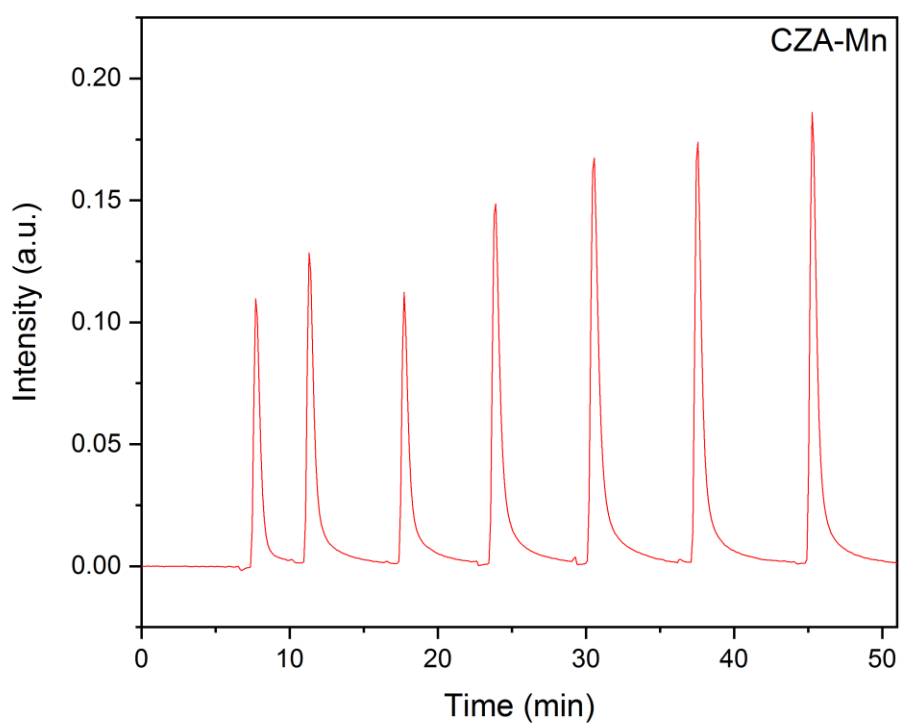
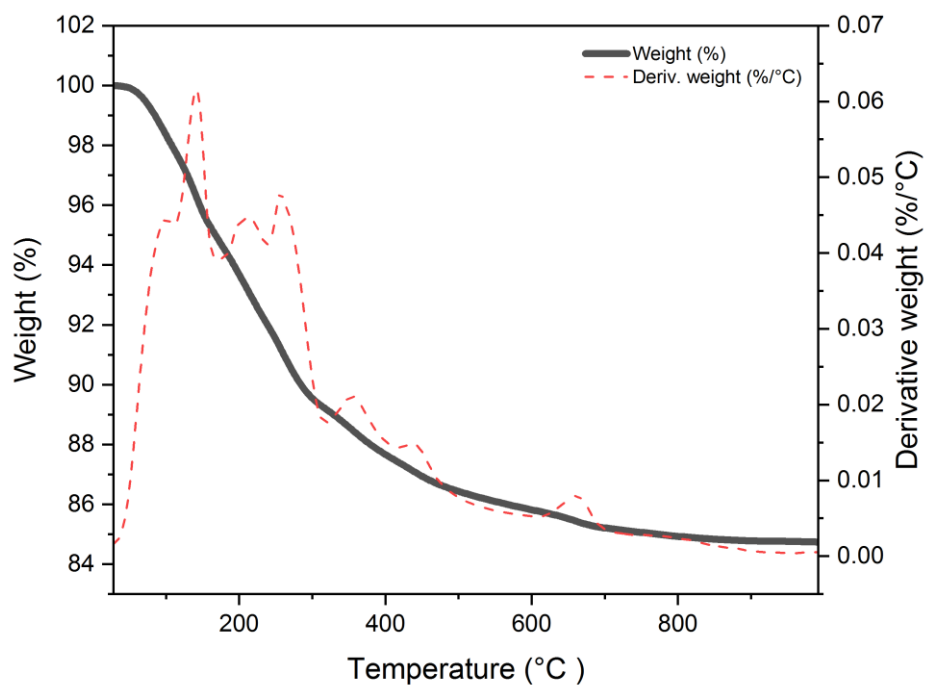
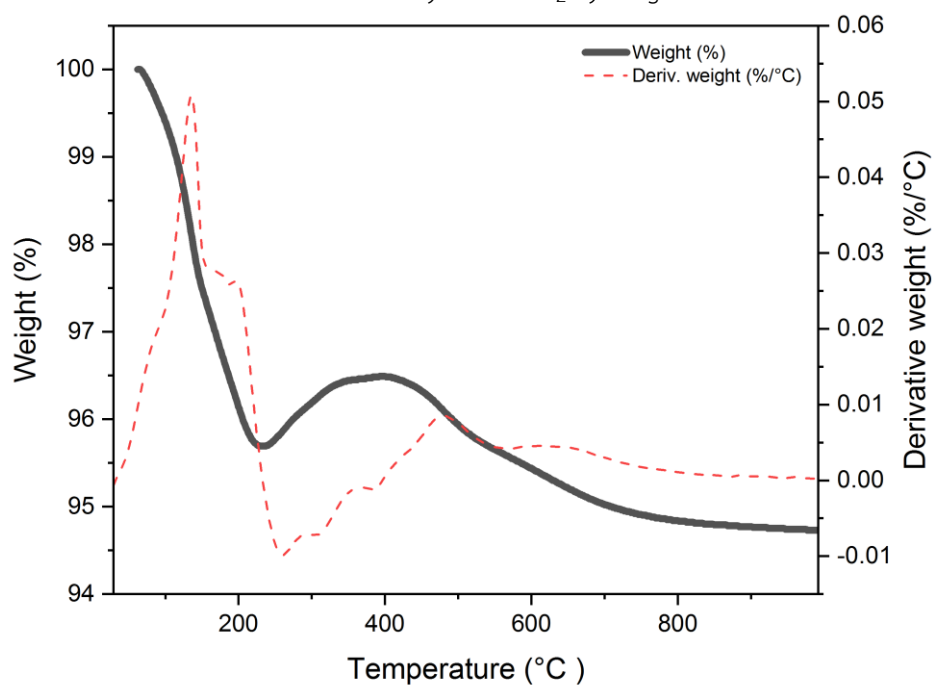


Figure E.1.2 CO-Chemisorption of CZA-Mn catalyst.



## APPENDIX.F THERMGRAVIMETRIC ANALYSIS

F.1 TGA curves for CO<sub>2</sub> hydrogenation.Figure F.1.1 TGA curve of the CZA catalyst for CO<sub>2</sub> hydrogenation.Figure F.1.2 TGA curve of the CZA-Mn catalyst for CO<sub>2</sub> hydrogenation.

F.2 TGA curves for CO hydrogenation.

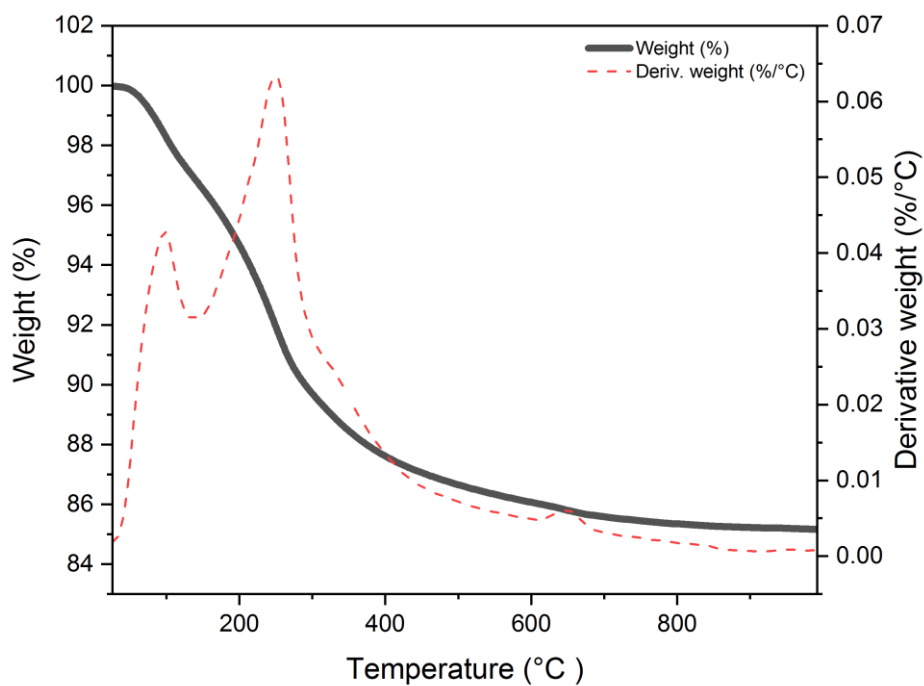


Figure F.2.1 TGA curve of the CZA catalyst for CO hydrogenation.

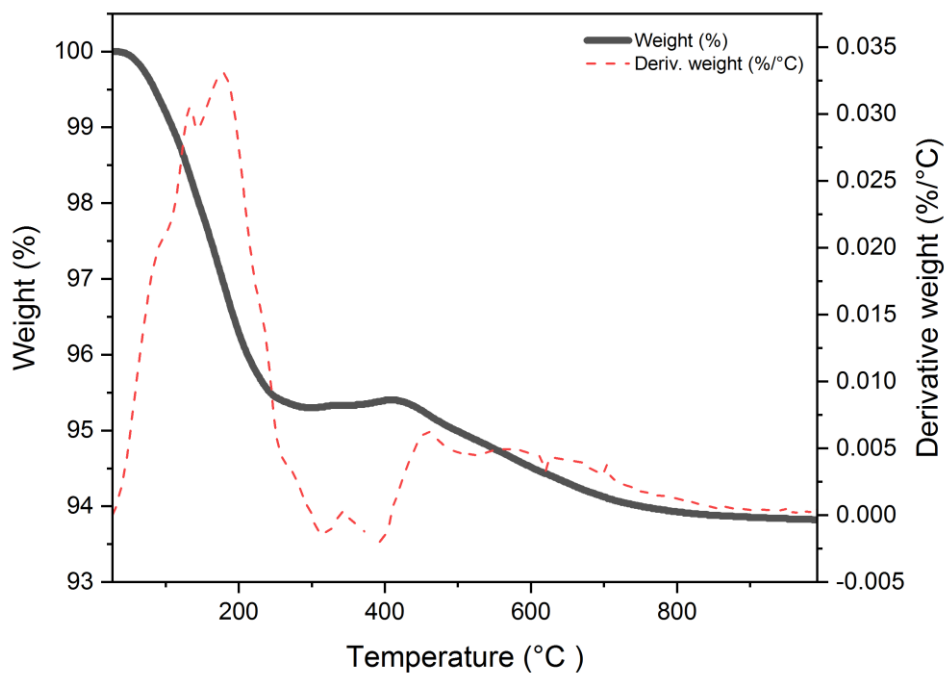


Figure F.2.2 TGA curve of the CZA-Mn catalyst for CO hydrogenation.

F.3 TGA curves for CO/CO<sub>2</sub> hydrogenation.

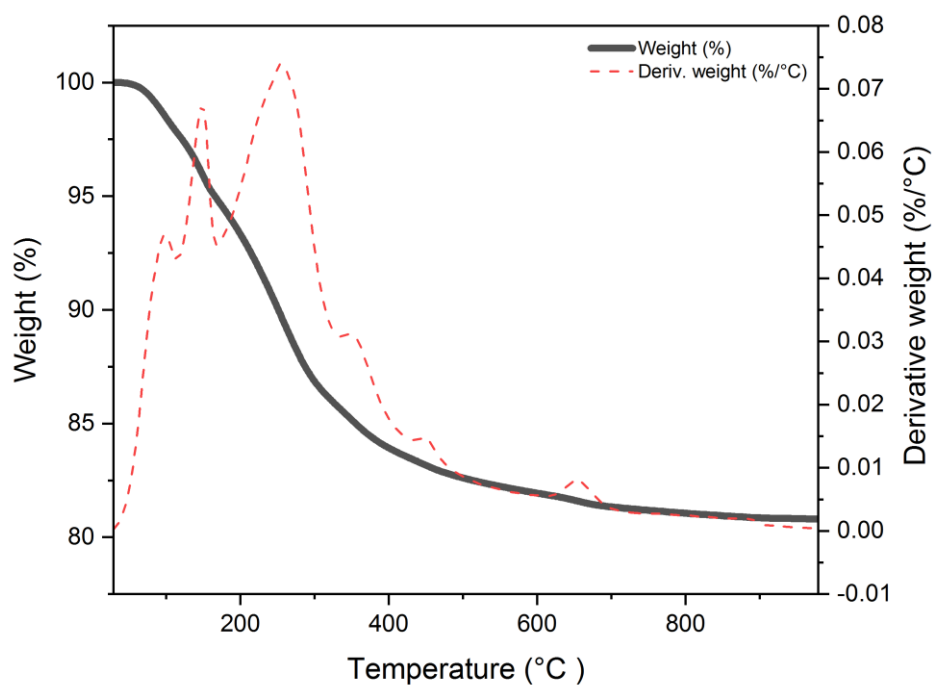


Figure F.3.1 TGA curve of the CZA catalyst for CO/CO<sub>2</sub> hydrogenation.

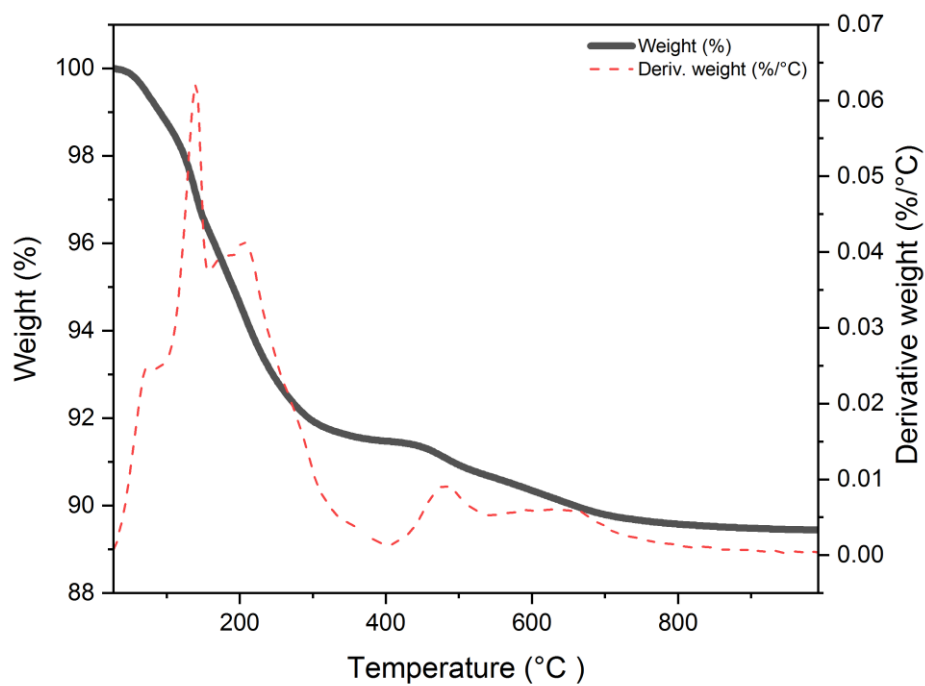


Figure F.3.2 TGA curve of the CZA-Mn catalyst for CO/CO<sub>2</sub> hydrogenation.



## APPENDIX.G DISCUSSION OF SIMULATION RESULTS

### G.1 Effect of CO<sub>2</sub> utilization in reforming of methane and methanol synthesis.

This study studied the operating condition of the reactor for methane steam reforming, bi-reforming, CO and CO/CO<sub>2</sub> hydrogenation from relevant researches as a guideline for a process simulation with experimental results obtained through the simulation process using Aspen Plus V.9. by using RKS-BM model for monitoring composition and energy consumption value.

For methane steam reforming reaction and bi-reforming. Refer to literature of [30] as shown **Table G.1.1**. This experimental was defined ratio of H<sub>2</sub>O to CH<sub>4</sub> is 4:1 and CH<sub>4</sub> feed rate is 0.0002719 mol/min. but the obtained results must be used to further comparison. Thus, mole flow rates of the components in feed stream was defined to 100 mol/min by maintaining ratio of H<sub>2</sub>O to CH<sub>4</sub> as shown in **Table G.1.2**.

**Table G.1.1** Mole flow rates of the components in feed stream and product stream on methane steam reforming.

		FEED	PRODUCT
Mole Flows	mol/min	0.0013595	0.0018979
CH <sub>4</sub>	mol/min	0.0002719	0.0000027
WATER	mol/min	0.0010876	0.0006281
CO	mol/min	0	0.0000789
H <sub>2</sub>	mol/min	0	0.0009979
CO <sub>2</sub>	mol/min	0	0.0001903

**Table G.1.2** Mole flow rates of the components in feed stream and product stream on methane steam reforming. (Assume total flow rate of feed steam to be 100 mol/min)

		FEED	PRODUCT
Mole Flows	mol/min	100	139.60
CH <sub>4</sub>	mol/min	20	0.20
WATER	mol/min	80	46.34
CO	mol/min	0	5.94
H <sub>2</sub>	mol/min	0	73.26
CO <sub>2</sub>	mol/min	0	13.86

**Table G.1.3** The product yield of methane steam reforming from simulation vs. experimental.

	%YIELD		%ERROR
	ASPEN	EXPERIMENT	
CO	29	30	3.33
H <sub>2</sub>	367	331	10.88
CO <sub>2</sub>	70	69	1.45

From **Table G.1.3**, it showed that product from pilot experiment comparing with actual experiment, product value can be calculated by equation (11).

$$\%Y_i = \frac{i(mol)}{CH_{4,in}(mol)} \times 100 \quad (11)$$

It was found that CO<sub>2</sub> and CO production were nearly the same but hydrogen production has error/ tolerance of obtained results. RStoic reactor had to be checked reliability because only mass balance could run in RStoic. Therefore, RPlug reactor for literature of [33] was applied. Due to reforming reactions were reversible reaction which the rate of reaction depended on operating condition and substance concentration. For the reaction prediction, the factors which concerned were kinetic information and chemical balance for RPlug by adjusting kinetic information with simulation by using Langmuir-Hinshelwood-Hougen-Watson equation as shown in **Table G.1.4**. It was found that two types of reactor provided nearly the same value. Therefore, Rstoi reactor was acceptable.

**Table G.1.4** Mole flow rates of the components in feed stream and product stream on methane steam reforming from RStoic vs RPlug.

		RStoic		RPlug	
		FEED	PRODUCT	FEED	PRODUCT
Mole Flows	mol/min	100	139.60	100	139.84
CH <sub>4</sub>	mol/min	20	0.20	20	0.08
WATER	mol/min	80	46.34	80	48.92
CO	mol/min	0	5.94	0	8.76
H <sub>2</sub>	mol/min	0	73.26	0	70.91
CO <sub>2</sub>	mol/min	0	13.86	0	11.16

**Table G.1.5** Mole flow rates of the components in feed stream and product stream on bi-reforming.

		FEED	PRODUCT
Mole Flows	mol/min	100	195.14
CH <sub>4</sub>	mol/min	51	3.43
WATER	mol/min	33	1.29
CO	mol/min	0	63.42
H <sub>2</sub>	mol/min	0	126.85
CO <sub>2</sub>	mol/min	16	0.14

**Table G.1.5** have shown the simulation results for bi-reforming, refer to literature of [31] comparing with value from RStoic reaction from **Table G.1.2** and **Table G.1.5** have found that production ratio between hydrogen and CO from methane steam reforming is more than from bi-reforming by increasing to 6 time. On the other hand, the total amount of CO and hydrogen production produced from methane steam reforming is less than bi-reforming and then considering the energy consumption for 2 processes have shown in **Table G.1.6** and **Table G.1.7**.

**Table G.1.6** Total energy consumption and the energy consumption per mole of main products on methane steam reforming.

		ENERGY CONSUMPTION		
Total	174.17	kW		
CO	29.32	kW/mol.min <sup>-1</sup>	1759.26	KJ/mol
H <sub>2</sub>	2.38	kW/mol.min <sup>-1</sup>	142.64	KJ/mol

**Table G.1.7** Total energy consumption and the energy consumption per mole of main products on bi-reforming.

	ENERGY CONSUMPTION			
Total	293.06	kW		
CO	4.62	kW/mol.min <sup>-1</sup>	277.24	KJ/mol
H <sub>2</sub>	2.31	kW/mol.min <sup>-1</sup>	138.62	KJ/mol

According to **Table G.1.6** and **Table G.1.7**, the overall energy consumption for 2 processes is positive. It is concluded that reforming reaction is endothermic process. For consideration of using energy for 1 mol hydrogen production. It was found that the energy consumption for 2 processes was nearly the same. On the other hand, for CO production, it was found that energy using for methane steam reforming is more than for 1 mol CO production. Due to chemical reaction consideration, CO produced from methane steam reforming is reacted with water, water gas shift reaction is occurred. It is found overall energy consumption for bi-reforming is more than methane steam reforming because of using CO<sub>2</sub> as co-reactant which conformed to the total amount of CO and hydrogen production from bi-reforming.

**Table G.1.8** Mole flow rates of the components in feed stream and product stream on CO hydrogenation and CO/CO<sub>2</sub> hydrogenation.

CO HYDROGENATION		FEED	PRODUCT	CO/CO <sub>2</sub> HYDROGENATION		FEED	PRODUCT
Mole Flows	mol/min	210249.9	178513.4	Mole Flows	mol/min	210250	100970
CO	mol/min	16529.4	661.2	CO	mol/min	13083.3	523.3
H <sub>2</sub>	mol/min	193720.5	161984	H <sub>2</sub>	mol/min	153333.3	1973.3
CO <sub>2</sub>	mol/min	0	0	CO <sub>2</sub>	mol/min	43833.3	1753.3
CH <sub>3</sub> OH	mol/min	0	15868.2	CH <sub>3</sub> OH	mol/min	0	54640
WATER	mol/min	0	0	WATER	mol/min	0	42080

**Table G.1.9** Total energy consumption and the energy consumption per mole of main products on CO hydrogenation and CO/CO<sub>2</sub> hydrogenation.

ENERGY CONSUMPTION				
CO HYDROGENATION				
Total	-2511.16	kW		
MeOH	-0.15825	kW/mol.min <sup>-1</sup>	-9.49506	KJ/mol
CO/CO <sub>2</sub> HYDROGENATION				
Total	-41301.9	kW		
MeOH	-0.75589	kW/mol.min <sup>-1</sup>	-45.3535	KJ/mol

For methanol synthesis of [32] literature. **Table G.1.8** showed using CO<sub>2</sub> as co-reactant provided higher methanol production by increasing to 3.4 time of methanol

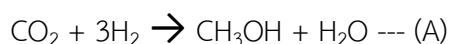
production from CO hydrogenation because methanol production for CO<sub>2</sub>-H<sub>2</sub> reaction is more than from CO-H<sub>2</sub> reaction. From **Table G.1.9** have found that negative overall energy consumption refer that methanol synthesis is exothermic process and overall energy consumption for using CO<sub>2</sub> as co-reactant and energy consumption using for 1 mol methanol production have to be higher.



## APPENDIX.H CALCULATION OF THE HEAT REQUIREMENT FOR THE REACTOR.

H.1 Calculate the heat requirement for the reactor.

**Example:** The methanol synthesis from CO<sub>2</sub> hydrogenation reaction with 250°C and atmospheric pressure:



The only other reaction to be considered is the reverse water-gas shift reaction:



The reactants are supplied and products are obtained as shown in **Table H.1.1** and heat is supplied to the reactor so that the products reach a temperature of 250°C (523.15 K). Assuming the temperature of reactants to be room temperature at 27°C (300.15 K).

**Table H.1.1** Mole flow rates of the components in feed stream and product stream on CO<sub>2</sub> hydrogenation (CZA catalyst).

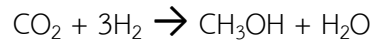
		FEED	PRODUCT
Mole Flows	mol/min	3.98x10 <sup>-5</sup>	3.98x10 <sup>-5</sup>
CO <sub>2</sub>	mol/min	7.97x10 <sup>-6</sup>	7.79x10 <sup>-6</sup>
H <sub>2</sub>	mol/min	2.39x10 <sup>-5</sup>	2.37x10 <sup>-5</sup>
CH <sub>3</sub> OH	mol/min	0	3.60x10 <sup>-10</sup>
H <sub>2</sub> O	mol/min	0	1.78x10 <sup>-7</sup>
CO	mol/min	0	1.77x10 <sup>-7</sup>
N <sub>2</sub>	mol/min	7.97x10 <sup>-6</sup>	7.97x10 <sup>-6</sup>

### Solution :

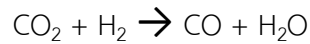
Standard heat of reaction at 298.15 K from Table: Standard Enthalpies and Gibbs Energies of Formation at 298.15 K are







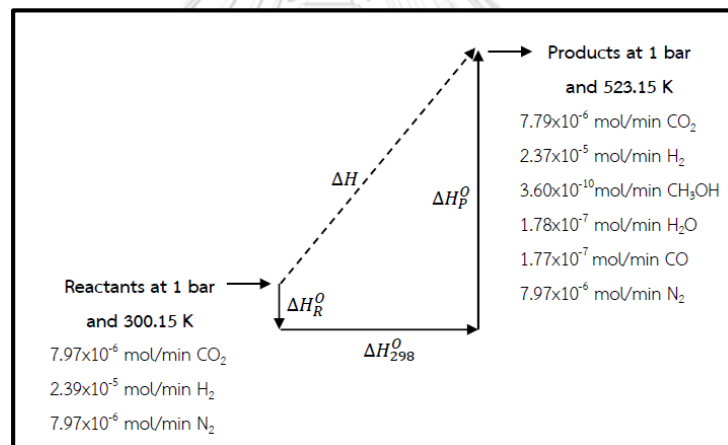
$$\Delta H_{298}^0 = (-200,660 \text{ J}) + (-241,818 \text{ J}) - (-393,509 \text{ J}) = -48,969 \text{ J}$$



$$\Delta H_{298}^0 = (-110,525 \text{ J}) + (-241,818 \text{ J}) - (-393,509 \text{ J}) = 41,166 \text{ J}$$

We now devise a path, for purposes of calculation, to proceed from reactants at 27°C (300.15 K) to products at 250°C (523.15 K). Because data are available for the standard heats of reaction at 25°C (298.15 K), the most convenient path is the one which includes the reactions at 25°C (298.15 K). This is shown schematically in the accompanying diagram. The dashed line represents the actual path for which the enthalpy change is  $\Delta H$ . Because this enthalpy change is independent of path,

$$\Delta H = \Delta H_R^0 + \Delta H_{298}^0 + \Delta H_P^0$$



For the calculation of  $\Delta H_{298}^0$ , reaction (A) and (B) must both be taken into account. Because  $3.60 \times 10^{-10}$  mol reacts by (A) and  $1.77 \times 10^{-7}$  mol reacts by (B),

$$\Delta H_{298}^0 = (3.60 \times 10^{-10})(-48,969) + (1.77 \times 10^{-7})(41,166) = 7.27 \times 10^{-3} \text{ J}$$

The enthalpy change of the reactants from 300.15 K to 298.15 K is

$$\Delta H_R^0 = (\sum_i n_i (C_{p_i}^0)_H)(298.15 - 300.15)$$

Where the values of  $(C_{p_i}^0)_H/R$  are

$$\frac{(C_{p_i}^0)_H}{R} = A + BT + CT^2 + DT^2 \quad ; T \text{ (kelvins)}$$

For constants in equation shown in **Table H.2**. From Table: Heat Capacities of Gases in the Ideal-Gas State.

**Table H.1.2** Heat capacities of gases in the ideal-gas state.

Chemical species	A	$10^3 B$	$10^6 C$	$10^{-5} D$
CH <sub>3</sub> OH	2.211	12.216	-3.450	-
H <sub>2</sub> O	3.470	1.450	-	0.121
CO <sub>2</sub>	6.311	6.311	-	-0.906
H <sub>2</sub>	3.249	0.422	-	0.083
CO	3.376	0.557	--0.906	-0.031
N <sub>2</sub>	3.280	0.593	-	0.040

$$\begin{aligned} \text{CO}_2 & : \int_{300.15}^{298.15} (6.311 + 6.311T + -0.906T^{-2})dT = -11.078 \\ \text{H}_2 & : \int_{300.15}^{298.15} (3.249 + 0.422T + 0.083T^{-2})dT = -6.936 \\ \text{N}_2 & : \int_{300.15}^{298.15} (3.280 + 0.593T + 0.040T^{-2})dT = -7.004 \end{aligned}$$

Whence,

$$\begin{aligned} \Delta H_R^0 & = (8.314)[(7.97 \times 10^{-6})(-11.078) + (2.39 \times 10^{-5})(-6.936) + (7.97 \times 10^{-6})(-7.004)] \\ & = -2.576 \times 10^{-3} \text{ J} \end{aligned}$$

The enthalpy change of the products as they are heated from 298.15 K to 523.15 K is calculated similarly:

$$\Delta H_P^0 = (\sum_i n_i (C_{p_i}^0)_H)(523.15 - 298.15)$$

Where  $(C_{p_i}^0)_H/R$  values are

$$\begin{aligned} \text{CO}_2 & : \int_{298.15}^{523.15} (6.311 + 6.311T + -0.906T^{-2})dT = 1363.660 \\ \text{H}_2 & : \int_{298.15}^{523.15} (3.249 + 0.422T + 0.083T^{-2})dT = 781.989 \\ \text{CH}_3\text{OH} & : \int_{298.15}^{523.15} (2.211 + 12.216T + -3.25T^{-2})dT = 1492.011 \\ \text{H}_2\text{O} & : \int_{298.15}^{523.15} (3.470 + 1.450T + 0.121T^{-2})dT = 932.179 \end{aligned}$$

$$\begin{aligned} \text{CO} & : \int_{298.15}^{523.15} (3.376 + 0.557T + -0.031T^{-2})dT = 806.593 \\ \text{N}_2 & : \int_{298.15}^{523.15} (3.280 + 0.593T + 0.040T^{-2})dT = 798.561 \end{aligned}$$

Whence,

$$\begin{aligned} \Delta H_p^0 & = (8.314)[(7.79 \times 10^{-6})(1363.660) + (2.37 \times 10^{-5})(781.989) + (3.60 \times 10^{-10})(1492.011) + \\ & \quad (1.78 \times 10^{-7})(932.179) + (1.77 \times 10^{-7})(806.593) + (7.97 \times 10^{-6})(798.561)] \\ & = 0.298 \text{ J} \end{aligned}$$

Therefore,

$$\Delta H = 7.27 \times 10^{-3} + -2.576 \times 10^{-3} + 0.298 = 0.302569 \text{ J} = 5.042 \times 10^{-6} \text{ kW}$$

For calculate the energy consumption for 1 mol methanol production is

$$\frac{5.042 \times 10^{-6} \frac{\text{kJ}}{\text{s}} \times 60 \frac{\text{s}}{\text{min}}}{3.60 \times 10^{-10} \frac{\text{mol}}{\text{min}}} = 8.33 \times 10^5 \text{ kJ/mol}_{\text{CH}_3\text{OH}}$$

**Table H.1.3** Mole flow rates of the components in feed stream and product stream on CO<sub>2</sub> hydrogenation (CZA-Mn catalyst).

		FEED	PRODUCT
Mole Flows	mol/min	4.03x10 <sup>-5</sup>	4.03x10 <sup>-5</sup>
CO <sub>2</sub>	mol/min	8.05x10 <sup>-6</sup>	7.73x10 <sup>-6</sup>
H <sub>2</sub>	mol/min	2.42x10 <sup>-5</sup>	2.39x10 <sup>-5</sup>
CH <sub>3</sub> OH	mol/min	0	6.73x10 <sup>-10</sup>
H <sub>2</sub> O	mol/min	0	3.18x10 <sup>-7</sup>
CO	mol/min	0	3.17x10 <sup>-7</sup>
N <sub>2</sub>	mol/min	8.05x10 <sup>-6</sup>	8.05x10 <sup>-6</sup>

**Table H.1.4** Mole flow rates of the components in feed stream and product stream on CO hydrogenation (CZA catalyst).

		FEED	PRODUCT
Mole Flows	mol/min	$4.11 \times 10^{-5}$	$4.11 \times 10^{-5}$
CO <sub>2</sub>	mol/min	0	0
H <sub>2</sub>	mol/min	$2.19 \times 10^{-5}$	$2.19 \times 10^{-5}$
CH <sub>3</sub> OH	mol/min	0	$3.48 \times 10^{-9}$
H <sub>2</sub> O	mol/min	0	0
CO	mol/min	$1.10 \times 10^{-5}$	$1.10 \times 10^{-5}$
N <sub>2</sub>	mol/min	$8.21 \times 10^{-6}$	$8.21 \times 10^{-6}$

**Table H.1.5** Mole flow rates of the components in feed stream and product stream on CO hydrogenation (CZA-Mn catalyst).

		FEED	PRODUCT
Mole Flows	mol/min	$4.07 \times 10^{-5}$	$4.07 \times 10^{-5}$
CO <sub>2</sub>	mol/min	0	0
H <sub>2</sub>	mol/min	$2.17 \times 10^{-5}$	$2.17 \times 10^{-5}$
CH <sub>3</sub> OH	mol/min	0	$5.17 \times 10^{-9}$
H <sub>2</sub> O	mol/min	0	0
CO	mol/min	$1.09 \times 10^{-5}$	$1.09 \times 10^{-5}$
N <sub>2</sub>	mol/min	$8.14 \times 10^{-6}$	$8.14 \times 10^{-6}$

**Table H.1.6** Mole flow rates of the components in feed stream and product stream on CO/CO<sub>2</sub> hydrogenation (CZA catalyst).

		FEED	PRODUCT
Mole Flows	mol/min	$3.85 \times 10^{-5}$	$3.85 \times 10^{-5}$
CO <sub>2</sub>	mol/min	$7.71 \times 10^{-6}$	$7.60 \times 10^{-6}$
H <sub>2</sub>	mol/min	$1.54 \times 10^{-5}$	$1.53 \times 10^{-5}$
CH <sub>3</sub> OH	mol/min	0	$9.94 \times 10^{-10}$
H <sub>2</sub> O	mol/min	0	$1.12 \times 10^{-7}$
CO	mol/min	$7.71 \times 10^{-6}$	$7.82 \times 10^{-6}$
N <sub>2</sub>	mol/min	$7.71 \times 10^{-6}$	$7.71 \times 10^{-6}$

**Table H.1.7** Mole flow rates of the components in feed stream and product stream on CO/CO<sub>2</sub> hydrogenation (CZA-Mn catalyst).

		FEED	PRODUCT
Mole Flows	mol/min	$3.86 \times 10^{-5}$	$3.86 \times 10^{-5}$
CO <sub>2</sub>	mol/min	$7.73 \times 10^{-6}$	$7.68 \times 10^{-6}$
H <sub>2</sub>	mol/min	$1.55 \times 10^{-5}$	$1.54 \times 10^{-5}$
CH <sub>3</sub> OH	mol/min	0	$1.06 \times 10^{-9}$
H <sub>2</sub> O	mol/min	0	$4.30 \times 10^{-8}$
CO	mol/min	$7.73 \times 10^{-6}$	$7.77 \times 10^{-6}$
N <sub>2</sub>	mol/min	$7.73 \times 10^{-6}$	$7.73 \times 10^{-6}$

## REFERENCES

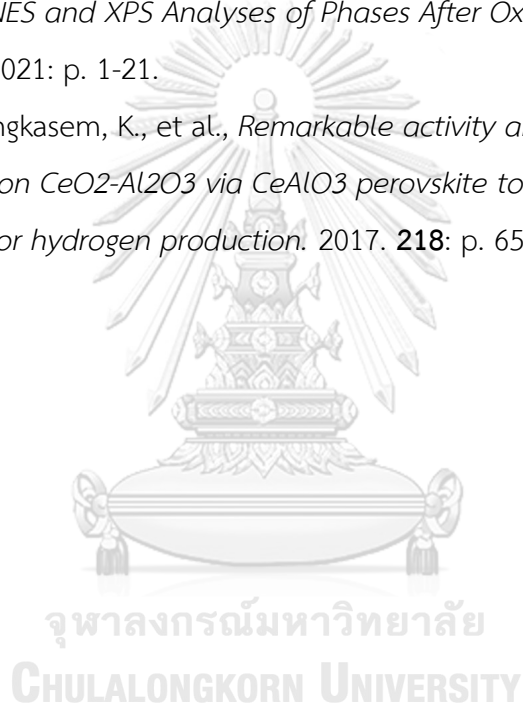
1. Sadeghinia, M., et al., *Effect of In<sub>2</sub>O<sub>3</sub> on the structural properties and catalytic performance of the CuO/ZnO/Al<sub>2</sub>O<sub>3</sub> catalyst in CO<sub>2</sub> and CO hydrogenation to methanol*. 2020. **484**: p. 110776.
2. Siang, T.J., et al., *Combined steam and CO<sub>2</sub> reforming of methane for syngas production over carbon-resistant boron-promoted Ni/SBA-15 catalysts*. 2018. **262**: p. 122-132.
3. Meshkini, F., M. Taghizadeh, and M.J.F. Bahmani, *Investigating the effect of metal oxide additives on the properties of Cu/ZnO/Al<sub>2</sub>O<sub>3</sub> catalysts in methanol synthesis from syngas using factorial experimental design*. 2010. **89**(1): p. 170-175.
4. ResearchGate. *World methanol demand according to use*. 2015; Available from: [https://www.researchgate.net/figure/World-methanol-demand-according-to-use-46\\_fig5\\_286085181](https://www.researchgate.net/figure/World-methanol-demand-according-to-use-46_fig5_286085181).
5. ResearchGate. *Catalyst Component and their Function*. 2009; Available from: [https://www.researchgate.net/figure/Fig-22-Catalyst-Component-and-their-Function\\_fig2\\_330957244](https://www.researchgate.net/figure/Fig-22-Catalyst-Component-and-their-Function_fig2_330957244).
6. Chemie, L. *Lab chemicals*. Available from: <https://www.lobachemie.com/laboratory-chemicals/laboratory-chemicals.aspx>.
7. Sigma-Aldrich. *substance*. Available from: <https://www.sigmaaldrich.com/catalog/search>.
8. Lei, H., Z. Hou, and J.J.F. Xie, *Hydrogenation of CO<sub>2</sub> to CH<sub>3</sub>OH over CuO/ZnO/Al<sub>2</sub>O<sub>3</sub> catalysts prepared via a solvent-free routine*. 2016. **164**: p. 191-198.
9. Danjun, W., et al., *Preparation of Cu/ZnO/Al<sub>2</sub>O<sub>3</sub> catalyst for CO<sub>2</sub> hydrogenation to methanol by CO<sub>2</sub> assisted aging*. 2011. **32**(9-10): p. 1452-1456.
10. Ren, H., et al., *Methanol synthesis from CO<sub>2</sub> hydrogenation over Cu/γ-Al<sub>2</sub>O<sub>3</sub> catalysts modified by ZnO, ZrO<sub>2</sub> and MgO*. 2015. **28**: p. 261-267.
11. Zhang, Y., et al., *Catalytic performance of spray-dried Cu/ZnO/Al<sub>2</sub>O<sub>3</sub>/ZrO<sub>2</sub>*

- catalysts for slurry methanol synthesis from CO<sub>2</sub> hydrogenation*. 2016. **15**: p. 72-82.
12. Hou, X.-X., et al., *Improved methanol synthesis from CO<sub>2</sub> hydrogenation over CuZnAlZr catalysts with precursor pre-activation by formaldehyde*. 2019. **379**: p. 147-153.
  13. Ren, S., et al., *Enhanced catalytic performance of Zr modified CuO/ZnO/Al<sub>2</sub>O<sub>3</sub> catalyst for methanol and DME synthesis via CO<sub>2</sub> hydrogenation*. 2020. **36**: p. 82-95.
  14. Lo, I.-C. and H.-S.J.J.o.t.T.I.o.C.E. Wu, *Methanol formation from carbon dioxide hydrogenation using Cu/ZnO/Al<sub>2</sub>O<sub>3</sub> catalyst*. 2019. **98**: p. 124-131.
  15. Liu, Z.-j., et al., *Synthesis and Catalytic Performance of Graphene Modified CuO-ZnO-Al<sub>2</sub>O<sub>3</sub> for CO<sub>2</sub> Hydrogenation to Methanol*. 2014.
  16. Tasfy, S., et al., *Methanol production via CO<sub>2</sub> hydrogenation reaction: effect of catalyst support*. 2017. **14**(1-6): p. 410-421.
  17. Allam, D., et al., *Operating Conditions and Composition Effect on the Hydrogenation of Carbon Dioxide Performed over CuO/ZnO/Al<sub>2</sub>O<sub>3</sub> Catalysts*. 2019. **14**(3): p. 604-613.
  18. Anton, J., et al., *The effect of sodium on the structure–activity relationships of cobalt-modified Cu/ZnO/Al<sub>2</sub>O<sub>3</sub> catalysts applied in the hydrogenation of carbon monoxide to higher alcohols*. 2016. **335**: p. 175-186.
  19. Anton, J., et al., *Structure–activity relationships of Co-modified Cu/ZnO/Al<sub>2</sub>O<sub>3</sub> catalysts applied in the synthesis of higher alcohols from synthesis gas*. 2015. **505**: p. 326-333.
  20. Liu, Y., et al., *CO hydrogenation to higher alcohols over Cu/Zn/Al catalysts without alkalis or Fischer–Tropsch elements: The effect of triethanolamine content*. 2016. **76**: p. 29-32.
  21. Heracleous, E., et al., *Investigation of K-promoted Cu-Zn-Al, Cu-X-Al and Cu-Zn-X (X= Cr, Mn) catalysts for carbon monoxide hydrogenation to higher alcohols*. 2013. **455**: p. 145-154.
  22. Liu, Y.-J., et al., *Higher alcohols synthesis via CO hydrogenation on Cu/Zn/Al/Zr catalysts without alkalis and F–T elements*. 2016. **144**: p. 186-190.

23. Samei, E., M. Taghizadeh, and M.J.F.p.t. Bahmani, *Enhancement of stability and activity of Cu/ZnO/Al<sub>2</sub>O<sub>3</sub> catalysts by colloidal silica and metal oxides additives for methanol synthesis from a CO<sub>2</sub>-rich feed*. 2012. **96**: p. 128-133.
24. Yang, R., et al., *A new method of low-temperature methanol synthesis on Cu/ZnO/Al<sub>2</sub>O<sub>3</sub> catalysts from CO/CO<sub>2</sub>/H<sub>2</sub>*. 2008. **87**(4-5): p. 443-450.
25. Zhang, F., et al., *Effect of Al-containing precursors on Cu/ZnO/Al<sub>2</sub>O<sub>3</sub> catalyst for methanol production*. 2018. **178**: p. 148-155.
26. Sadeghinia, M., A.N.K. Ghaziani, and M.J.M.C. Rezaei, *Component ratio dependent Cu/Zn/Al structure sensitive catalyst in CO<sub>2</sub>/CO hydrogenation to methanol*. 2018. **456**: p. 38-48.
27. Dasireddy, V.D. and B.J.R.E. Likozar, *The role of copper oxidation state in Cu/ZnO/Al<sub>2</sub>O<sub>3</sub> catalysts in CO<sub>2</sub> hydrogenation and methanol productivity*. 2019. **140**: p. 452-460.
28. Baltes, C., S. Vukojević, and F.J.J.o.c. Schüth, *Correlations between synthesis, precursor, and catalyst structure and activity of a large set of CuO/ZnO/Al<sub>2</sub>O<sub>3</sub> catalysts for methanol synthesis*. 2008. **258**(2): p. 334-344.
29. Pongpanumaporn, K., *Effects of CuO/ZnO/Al<sub>2</sub>O<sub>3</sub> catalyst modification using Zr, Mn and Si for methanol synthesis via CO<sub>2</sub> hydrogenation*. 2019, Chulalongkorn University.
30. Nazari, M. and S.M.J.I.J.o.H.E. Alavi, *An investigation of the simultaneous presence of Cu and Zn in different Ni/Al<sub>2</sub>O<sub>3</sub> catalyst loads using Taguchi design of experiment in steam reforming of methane*. 2020. **45**(1): p. 691-702.
31. Kumar, N., et al., *Bi-reforming of methane on Ni-based pyrochlore catalyst*. 2016. **517**: p. 211-216.
32. Luyben, W.L.J.I. and e.c. research, *Design and control of a methanol reactor/column process*. 2010. **49**(13): p. 6150-6163.
33. Amran, U., A. Ahmad, and M.R.J.C.E.T. Othman, *Kinetic based simulation of methane steam reforming and water gas shift for hydrogen production using aspen plus*. 2017. **56**: p. 1681-1686.
34. M. Marino, S. *ASPEN PLUS: LANGMUIR KINETICS (LHHW)*. 2012; Available from: <http://scuolatech.altervista.org/>.



35. Xaba, B., A. Mahomed, and H.J.J.o.E.C.E. Friedrich, *The effect of CO<sub>2</sub> and H<sub>2</sub> adsorption strength and capacity on the performance of Ga and Zr modified Cu-Zn catalysts for CO<sub>2</sub> hydrogenation to methanol*. 2021. **9**(1): p. 104834.
36. Wang, J.-G., et al., *Synthesis of ultralong MnO/C coaxial nanowires as freestanding anodes for high-performance lithium ion batteries*. 2015. **3**(26): p. 13699-13705.
37. Pori, M., et al., *Photo-Chemically-Deposited and Industrial Cu/ZnO/Al<sub>2</sub>O<sub>3</sub> Catalyst Material Surface Structures During CO<sub>2</sub> Hydrogenation to Methanol: EXAFS, XANES and XPS Analyses of Phases After Oxidation, Reduction, and Reaction*. 2021: p. 1-21.
38. Kamonsuangkasem, K., et al., *Remarkable activity and stability of Ni catalyst supported on CeO<sub>2</sub>-Al<sub>2</sub>O<sub>3</sub> via CeAlO<sub>3</sub> perovskite towards glycerol steam reforming for hydrogen production*. 2017. **218**: p. 650-663.





จุฬาลงกรณ์มหาวิทยาลัย  
**CHULALONGKORN UNIVERSITY**

## VITA

**NAME** Papawin Tunyasitikon

**DATE OF BIRTH** 6 September 1996

**PLACE OF BIRTH** Rayong

**INSTITUTIONS ATTENDED** Chemical Engineering, King Mongkut's University of Technology Thonburi, Bangkok, Thailand.

**HOME ADDRESS** 999/14 Sukhumvit Rd., Choeng Noen, Muang, Rayong 21000.

